The Journal of Supercomputing (2026) 82:770
https://doi.org/10.1007/s11227-026-08872-0

A hybrid snake and grey wolf optimizer for load frequency control in photovoltaic thermal power system

Eda Özkul[1] · **Özge Tezel**[1] · **Özay Can**[2]

Received: 29 January 2025 / Accepted: 4 September 2026
© The Author(s), under exclusive licence to Springer Science+Business Media, LLC, part of Springer Nature 2026

Abstract

Metaheuristic algorithms are widely employed to solve complex and high-dimensional real-world optimization problems. However, standalone algorithms often suffer from drawbacks such as premature convergence, stagnation in local optima, insufficient exploration of the search space, and unstable solution quality. To address these limitations, this study proposes a novel hybrid optimization algorithm, called SOGWO, by combining the leadership-guided search mechanism of the grey wolf optimizer (GWO) with the strategic update mechanisms of the snake optimizer (SO). The proposed hybrid structure aims to enhance exploration capability, maintain population diversity, and improve the balance between exploration and exploitation. Firstly, SOGWO is tested on 23 classical benchmark, 12 CEC-2022 test functions and compared with 13 well-known and recent algorithms to demonstrate its superiority. The experimental results demonstrate that SOGWO successfully combines the advantages of both constituent algorithms and consistently produces high-quality solutions. Statistical analyses indicate that SOGWO ranks second for the 10-dimensional problems and achieves the best overall performance for the 20-dimensional problems. To further assess its practical applicability, SOGWO is employed to optimize proportional–integral (PI) controller parameters for the load frequency control (LFC) problem in a two-area photovoltaic–thermal power system. The obtained results confirm the effectiveness of the proposed algorithm in solving a real-world engineering optimization problem and improving control performance. Moreover, the proposed SOGWO incurs a significant computational cost due to its population-based structure and applicability to large-scale problems, indicating that SOGWO has the potential to be suitable for high-performance computing (HPC), parallel, and distributed architectures. Consequently, the proposed algorithm can be suggested as a reliable and effective method for the solution of HPC and real-life engineering applications.

Keywords Optimization · Hybrid algorithm · Load frequency control · Photovoltaic thermal power system

Extended author information available on the last page of the article

Published online: 08 October 2026

1 Introduction

The effective operation of interconnected power systems is possible by providing a balance between the power produced and the power consumed. During operation, undesirable oscillations occur in system frequency and tie-line power change due to load demand or other factors. Load frequency control (LFC) is a control system used to eliminate these unwanted oscillations or to keep them within the specified values.

Due to the environmental problems caused by traditional energy sources, the integration of renewable energy sources (RES) into the electricity grid is increasing day by day. Photovoltaic (PV) systems are among the most preferred RES due to their advantages, such as low maintenance cost and compatibility with the grid. However, the power value that can be obtained from PV systems shows discontinuity due to climatic conditions. This discontinuity causes an imbalance between production and consumption. Therefore, it is necessary to perform the LFC process as shown in Fig. 1.

Proportional-integral-derivative (PID) controllers are used in the LFC process due to their simple structure and lower calculation processing requirements during the design phase [1–6]. When the studies on LFC are examined, it is observed that the determination of the controller parameters plays a major role in achieving successful results. In this context, various evolutionary algorithms, such as, firefly algorithm (FA) [1], hybrid shuffled frog leaping algorithm, teaching–learning based optimization (hybrid SFLA-TLBO) [7], equilibrium optimization algorithm (EOA) [8], grey wolf optimization (GWO) [9], hybrid gravitational-firefly (hGFA) [10], differential evolution-artificial electric field algorithm (DE-AEFA) [11], Jaya algorithm [12, 13], sine–cosine algorithm (SCA) [14, 15], lightning flash algorithm (LFA)

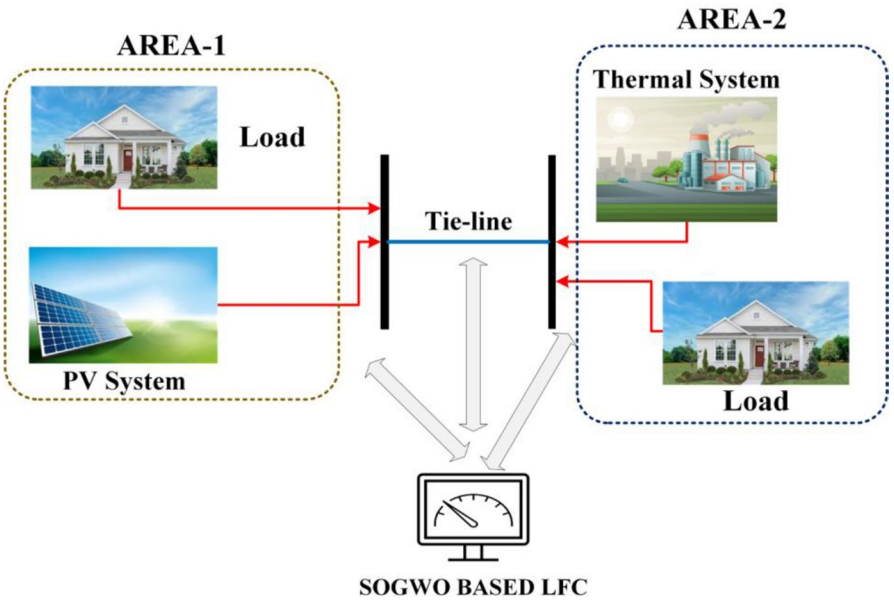


Fig. 1 The schematic diagram of two-area power system

[16], and gravitational search algorithm (GSA) [17] have been used to tune the controller parameters.

Additionally, different optimization algorithms, such as mine blast algorithm (MBA) [18], salp swarm algorithm (SSA) [19], hybrid moth flame optimization-generalized Hopfield neural network (MFO-GHNN) [20], whale optimization algorithm (WOA) [21], crow search algorithm (CSA) [22, 23], marine predator algorithm (MPA) [24], and Tribe-DE optimization algorithm [25] have been used to determine different kinds of controller gain, including fuzzy, cascade, fractional order.

In recent years, metaheuristic algorithms inspired by nature have become widely used in solving complex optimization problems. Their ability to easily adapt to different problem structures and extensively explore the solution space without getting stuck in local regions has made them a powerful alternative in many fields. However, No-Free-Lunch (NFL) theorem suggested by Wolpert and Macready [26], states that no optimization algorithm can be superior to others across all problem types. In essence, a single algorithm may not provide the universally best solution for all problem types. Therefore, the success of an algorithm may depend on the problem structure and, accordingly, may exhibit different characteristics in the search space. For this reason, while the search capabilities of existing algorithms are enhanced with different strategies, especially for solving complex and high-dimensional optimization problems, hybrid approaches that combine the strengths of different algorithms are also being developed.

Metaheuristic algorithms aim to strike an effective balance between global search and local search capabilities. However, in some cases, algorithms may focus more on one of these two components. This can lead to problems such as premature convergence, getting stuck in local optimum, or insufficient population diversity. Hybrid models can achieve a more balanced optimization process by leveraging one algorithm's exploration capacity to complement the other's exploitation capability. Based on the degree of interaction between the component algorithms, hybrid methods are divided into two categories: high-level and low-level. In high-level hybrid approaches, the individual identities of the original algorithms are preserved, while in low-level combinations, the individual components or functions of the algorithms may change [27]. In this context, a considerable number of algorithms have emerged over the past few years.

Gaidhane and Nigam [28] enhanced GWO by hybridizing it with upgrading strategy of employer bees from artificial bee colony (ABC) algorithm. Jafari et al. [29] combined elephant herding optimization (EHO) with cultural algorithm (CA), where the belief space defined by CA to improve standard EHO. Teng et al. [30] introduced a hybrid GWO by integrating via tent chaotic map initialization, a nonlinear control parameter, and PSO-based position update mechanism to enhance its convergence behavior. An improved GWO integrated with the aquila optimizer was proposed by Ma et al. [31] to enhance the exploration–exploitation trade-off and reduce premature convergence. Çetinbaş et al. [32] described the hWSO–ARO algorithm that merge the exploitation capabilities of the white shark optimizer (WSO) and artificial rabbits optimization (ARO) algorithms for photovoltaic parameter extraction. Tu et al. [33] augmented the grey wolf optimizer by integrating the exploitation mechanism of Harris hawks optimization (HHO), Latin hypercube sampling

for population initialization, nonlinear convergence control, local perturbations, and extended exploration strategies to improve the optimization capability of GWO. Zhang et al. [34] enhanced the grey wolf optimizer by utilizing the cluster and foraging behavior of artificial fish swarm algorithm (AFSA) to balance exploration and exploitation components and prevent premature convergence. Biswas et al. [35] incorporated exploration capability of coati optimization algorithm with the exploitation strength of differential evolution to improve optimization performance across complex search spaces. Al Afghani Edsa and Sunat [36] proposed a hybrid method that integrates Chernobyl disaster optimizer (CDO) with GWO to overcome getting stuck in local optima. Singh et al. [37] proposed a hybrid model by combining SCA with exploitation strategy of gazelle optimization algorithm (GOA) and Brownian motion and Lévy flight mechanisms to enhance both exploration and exploitation of SCA. Alawadi et al. [38] presented the SHIODEG algorithm by merging success-history intelligent optimizer (SHIO) with differential evolution (DE) and a Gaussian transformation to perform more effective optimization process. Ferradji and Seghir [39] merged the GWO and SSA by dividing population into two groups with different update strategies.

Building on these developments, studies investigating the effectiveness of hybrid algorithms that combine the complementary capabilities of different metaheuristic search mechanisms on LFC problems have increased significantly in recent years. Yameen et al. [40] combined grasshopper optimization algorithm (GOA) and particle swarm optimization (PSO) so that the complementary search characteristics of the two algorithms could be utilized for PID parameter optimization in renewable-integrated LFC systems. Similarly, Odelu et al. [41] developed a chaotic chimp–mountain gazelle optimizer (CCMGO) by integrating chaotic maps with the chimp optimization algorithm and mountain gazelle optimizer to enhance exploration and reduce the risk of premature convergence when tuning PID, cascaded PD-PID, fractional-order PID, and TID controllers in a renewable-source shipboard microgrid. Their results further demonstrated the importance of an appropriate balance between exploration and exploitation in complex LFC problems, with the CCMGO-optimized TID controller achieving the best performance among the investigated controller structures. The development of hybrid optimization methods has also been accompanied by the use of more advanced control structures beyond conventional PID controllers. Abdulaziz et al. [42] proposed an AI-enhanced LFC strategy for multi-area power systems based on a self-tuning PIDF controller, artificial neural network-based nonlinear model predictive control (ANN-based NMPC), and hybrid cat-pikas optimization. This approach illustrates a recent shift from solely optimizing fixed controller parameters toward combining metaheuristic optimization with adaptive and predictive control mechanisms for more complex multi-area frequency regulation problems. In a similar direction, Prusty et al. [43] developed a hybrid genetic algorithm–gorilla troops optimizer (GA-GTO) framework for optimizing model predictive control in marine microgrids.

Snake optimizer (SO) [44] is a metaheuristic algorithm developed by drawing inspiration from the mating, fighting, and foraging behaviors of snakes to solve complex optimization problems. Although SO yields effective results, it has limitations such as slow convergence, insufficient population diversity, and getting stuck

in local optima [45]. In this regard, various improvements and hybridization studies applied to the algorithm have been reported in the literature to enhance the optimization capabilities of the SO algorithm. Al-Shourbaji et al. [46] presented a combination of reptile search algorithm-snake optimizer (RSA-SO) to address feature selection problems. Another study is conducted by Yao et al. [47] that introduces a novel opposition-based learning strategy and new dynamic update mechanisms to enhance its global optimization capability. Samiayya et al. [48] presented a hybrid snake whale optimization algorithm integrated snake optimizer and enhanced whale optimization for optimal cluster head selection in wireless sensor network. Zheng et al. [49] developed an enhanced snake optimizer by using Sobol-based initialization, nonlinear inverse-tangent control of exploration–exploitation, and learning strategies to maintain diversity and avoid local optima, applied it to numerical optimization, feature selection, and engineering optimization. Yang et al. [50] introduced four improvement strategies, including good point set initialization, a new exploration and exploitation mechanism, differential evolution strategy, and Lévy flight strategy, to enhance its convergence speed and global search ability.

A review of studies on snake optimization reveals that, rather than extensive hybridization with different population-based algorithms, improvement strategies such as opposition-based learning, Levy flight, or adaptive parameter tuning predominate as methods to enhance the algorithm's performance. Although these strategies focus on increasing the algorithm's exploration capacity or reducing early convergence, studies in which hybridization SO with other metaheuristics is performed in a systematic and balanced manner are limited. As the NFL theorem states, no optimization algorithm can consistently deliver superior performance across all problem types. Therefore, hybrid approaches that leverage the complementary search behaviors of different algorithms play a crucial role in mitigating the limitations of a single algorithm, creating a more balanced exploration-exploration process, and achieving effective performance. In light of this motivation, this study proposes a hybrid algorithm called SOGWO, which integrates the powerful characteristics of SO and GWO algorithms to enhance global search capability and preserve population diversity. In the proposed algorithm, the SO and GWO algorithms maintain their fundamental characteristics while collaborating through robust interaction mechanisms. Key contribution of this study is the design of a leadership-oriented, high-level hybrid metaheuristic algorithm by integrating GWO's hierarchical leadership concept into SO's male–female social structure to improve the search behavior of the SO algorithm. The hierarchical leadership-based population update mechanism of the GWO serves as guiding reference points that provide global information to the search process of the SO algorithm. This high-level hybridization structure ensures a more balanced and generalizable optimization behavior by conducting the exploration and exploitation processes through different mechanisms, without altering the internal structure of the algorithms and while preserving their strengths. The main highlights of this paper can be summarized as follows:

- A hybrid snake-grey wolf optimizer (SOGWO) is proposed by incorporating the exploration capability of GWO and exploitation ability of SO.

- SOGWO effectively balances global exploration and local exploitation by systematically combining the leadership mechanism of GWO with the mating and foraging behavior of SO.
- Extensive experiments are conducted on 23 benchmark test function and CEC-2022 test suite for dimensions 10 and 20 to highlight the effectiveness and robustness of SOGWO. The SOGWO has been compared with 13 well-known and recent algorithms to prove its effectiveness and superiority against other algorithms.
- The proposed SOGWO is compared with several state-of-the-art optimization algorithms and CEC-2022 winner algorithm.
- Quantitative, qualitative, and statistical analyses are performed to highlight the optimization capabilities of the SOGWO and to provide insights into its search behavior.
- The Combined Compromise Solution (CoCoSo) method is employed for multi-criteria decision-making to systematically rank and compare SOGWO with competing algorithms.
- The SOGWO has been evaluated on load frequency control in PV-thermal power system.

The remainder of this paper is organized as follows: Sect. 2 details the proposed SOGWO. Performance evaluation of SOGWO is discussed in Sect. 3. Section 4 presents the PV-thermal power system model. In Sect. 5, optimization problem of load frequency controller is discussed. Simulation studies and results are given in Sect. 6. Finally, Sect. 7 draws the main conclusions.

2 Hybrid snake and grey wolf optimizer

Snake and grey wolf optimizers are swarm-based meta-heuristic algorithms. The combination of these algorithms, called SOGWO, is proposed to enhance the exploration and exploitation stages, gain the ability of avoidance trapping into the local optima, and get high-quality solutions for complex optimization problems.

2.1 Snake optimizer

The snake optimizer (SO) is a swarm-based meta-heuristic algorithm proposed by Hashim and Hussien [44]. The algorithm models the mating behavior of snakes. When adequate food and low temperature are provided, each snake will fight with each other to mate with the best partner. As in other meta-heuristic algorithms, the initial population is randomly generated in the SO algorithm as follows.

$$X_{ij} = lb_j + r \cdot \left(ub_j - lb_j\right), \begin{matrix} i = 1,2,\ldots,N \\ j = 1,2,\ldots,D \end{matrix} \tag{1}$$

where X_{ij} represents the position of snake i in the dimension j, lb_j and ub_j are the lower and upper bounds of the search space, respectively. r is a random number

uniformly distributed in the range of [0,1], N is the population size and D refers to the dimension of the problem.

In the SO algorithm, the population is divided into two groups as male and female using Eqs. (2) and (3).

$$N_m \approx N/2 \tag{2}$$

$$N_f = N - N_m \tag{3}$$

where N_m is the number of male snakes and N_f is the number of female snakes. Then, the best solutions of male ($X_{best,m}$) and female ($X_{best,f}$) populations and the position of food (X_{food}) are determined. Temperature and food quality are defined as in the equations below.

$$Temp = e^{\frac{-t}{T}} \tag{4}$$

$$Q = c_1 \cdot e^{\frac{t-T}{T}} \tag{5}$$

where t refers to current iteration, T refers to maximum number of iterations and c_1 is a constant which equals 0.5.

When there is not enough food, depending on a threshold, the snakes explore the search space.

If $Q < Threshold = 0.25$, the snakes search globally and update their current position to a random position. The mathematical model of the exploration behavior of male and female snakes is as follows.

- The exploration phase of the male snakes:

$$X_{i,m}^{(t+1)} = X_{rand,m}^{(t)} \pm c_2 \cdot A_m \cdot ((ub - lb) \cdot r + lb) \tag{6}$$

where $X_{i,m}$ refers to the position of ith male snake, $X_{rand,m}$ refers to a random male snake, r is a random number in the range of [0,1]. $\pm$ refers to flag operator that takes either -1 or $+1$, and it is used to randomly scan all possible directions in the given search space. A_m is the male ability to get the food and can be calculated as:

$$A_m = e^{\frac{-f_{rand,m}}{f_{i,m}}} \tag{7}$$

where $f_{rand,m}$ is the fitness of $X_{rand,m}$ and $f_{i,m}$ is the fitness of ith male snake. c_2 equals to 0.05.

- The exploration phase of the female snakes:

$$X_{i,f}^{(t+1)} = X_{rand,f}^{(t)} \pm c_2 \cdot A_f \cdot ((ub - lb) \cdot r + lb) \tag{8}$$

where $X_{i,f}$ refers to the position of ith female snake, $X_{rand,f}$ refers to a random female snake, r is a random number in the range of [0,1]. A_f is the female ability to get the food and can be calculated as:

$$A_f = e^{\frac{-f_{rand,f}}{f_{i,f}}} \tag{9}$$

where $f_{rand,f}$ is the fitness of $X_{rand,f}$ and $f_{i,f}$ is the fitness of ith female snake.

If there is enough food ($Q < Threshold = 0.25$), the snakes move into the exploitation phase at this stage and try to find the best solution according to the fighting or mating mode, depending on the temperature.

If $Temp > 0.6$ (hot), snakes only move towards food. In this case, the position of snakes (male or female) is updated by Eq. (10).

$$X_{ij}^{(t+1)} = X_{food} \pm c_3 \cdot Temp \cdot r \cdot \left(X_{food} - X_{ij}^{(t)} \right) \tag{10}$$

where X_{ij} is the position of ith snake in the dimension j. X_{food} is the position of the best snake and c_3 is a constant that equals to 2.

If $Temp < 0.6$ (cold), snakes are either in fighting or mating mode.

- Fighting mode:

In the fighting mode, the male snakes update their position as follows:

$$X_{i,m}^{(t+1)} = X_{i,m}^{(t)} + c_3 \cdot F_m \cdot r \cdot \left(Q \cdot X_{best,f} - X_{i,m}^{(t)} \right) \tag{11}$$

where $X_{i,m}$ is the position of ith male snake and $X_{best,f}$ is the position of best female snake. F_m refers to fighting ability of male snakes and can be calculated as follows:

$$F_m = e^{\frac{-f_{best,f}}{f_i}} \tag{12}$$

where $f_{best,f}$ refers to the fitness value of the best female snake and f_i is the fitness value of ith snake.

In the fight mode, the female snakes update their position as follows:

$$X_{i,f}^{(t+1)} = X_{i,f}^{(t)} + c_3 \cdot F_f \cdot r \cdot \left(Q \cdot X_{best,m} - X_{i,f}^{(t)} \right) \tag{13}$$

where $X_{i,f}$ is the position of ith female snake and $X_{best,m}$ is the position of best male snake. F_f refers to fighting ability of female snakes and can be calculated as follows:

$$F_f = e^{\frac{-f_{best,m}}{f_i}} \tag{14}$$

where $f_{best,m}$ refers to the fitness value of the best male snake and f_i is the fitness value of ith snake.

- Mating mode:

In the mating mode, the male and female snakes update their positions as follows.

$$X_{i,m}^{(t+1)} = X_{i,m}^{(t)} + c_3 \cdot M_m \cdot r \cdot \left(Q \cdot X_{i,f}^{(t)} - X_{i,m}^{(t)} \right) \tag{15}$$

$$X_{i,f}^{(t+1)} = X_{i,f}^{(t)} + c_3 \cdot M_f \cdot r \cdot \left(Q \cdot X_{i,m}^{(t)} - X_{i,f}^{(t)} \right) \tag{16}$$

where $X_{i,m}$ is the position of ith male snake, $X_{i,f}$ is the position of ith female snake, M_m and M_f are the mating ability of male and female snakes, respectively. They can be calculated as follows:

$$M_m = e^{\frac{-f_{i,f}}{f_{i,m}}} \tag{17}$$

$$M_f = e^{\frac{-f_{i,m}}{f_{i,f}}} \tag{18}$$

If the egg hatch, select the worst male and the worst female snakes and replace them to the new positions randomly in the search space using Eq. (1).

2.2 Grey wolf optimizer

The grey wolf optimizer (GWO) [51] is a meta-heuristic optimization algorithm inspired by the social hierarchy and hunting behavior of grey wolves. It models the hunting and social behavior of grey wolves in five stages: social hierarchy, encircling, hunting, attacking and searching prey. In the algorithm, as in nature, grey wolves are classified into alpha, beta, delta, and omega. To mathematically model the social hierarchy of grey wolves, the optimal solution is considered as alpha (α). The second and third best solutions are denoted as beta (β) and delta (δ), respectively. The remaining candidate solutions are assumed to be omega (ω). In the algorithm, hunting is performed by α, β and δ wolves, while ω wolves follow these three dominant wolves. The encircling behavior of grey wolves is mathematically modeled as follows.

$$D = \left| C \cdot X_g^{(t)} - X^{(t)} \right| \tag{19}$$

$$X^{(t+1)} = X_g^{(t)} - A \cdot D \tag{20}$$

where t is the current iteration, X_g is the position of the best three wolves, X is the position of the omega wolves. A and C are random parameters calculated as follows:

$$A = 2 \cdot a^{(t)} \cdot r_1 - a^{(t)} \tag{21}$$

$$C = 2 \cdot r_2 \tag{22}$$

where r_1 and r_2 are the random number defined in the range of $[0, 1]$, a is linearly decreased from 2 to 0 over the course of iterations and calculated as follows.

$$a^{(t)} = 2 - \frac{2 \cdot t}{T} \tag{23}$$

In the algorithm, since it is assumed that alpha, beta and delta have the best information about potential prey, the best three solutions are recorded. Then, based on the position of best wolves, the position of other wolves including omegas are updated as follows.

$$X_{i1}^{(t)} = X_{\alpha}^{(t)} - A_{i1} \cdot \left| C_{i1} \cdot X_{\alpha}^{(t)} - X_{i}^{(t)} \right| \tag{24}$$

$$X_{i2}^{(t)} = X_{\beta}^{(t)} - A_{i2} \cdot \left| C_{i2} \cdot X_{\beta}^{(t)} - X_{i}^{(t)} \right| \tag{25}$$

$$X_{i3}^{(t)} = X_{\delta}^{(t)} - A_{i3} \cdot \left| C_{i3} \cdot X_{\delta}^{(t)} - X_{i}^{(t)} \right| \tag{26}$$

$$X_{i}^{(t+1)} = \frac{X_{i1}^{(t)} + X_{i2}^{(t)} + X_{i3}^{(t)}}{3} \tag{27}$$

where X_{α}, X_{β} and X_{δ} are the first three best solutions at iteration t and $X_{i}^{(t+1)}$ refers to the positions of the wolf at the iteration $(t + 1)$.

When the prey stops moving, the grey wolves attack the prey and finish the hunting. Mathematically, α is linearly decreased from 2 to 0. Therefore, A is gradually decreased. When $|A| < 1$, wolves tend to converge towards the prey. When $|A| > 1$, wolves tend to diverge from the prey.

2.3 Proposed hybrid snake and grey wolf optimizer (SOGWO)

This study proposes an approach called SOGWO that combines the strengths of the SO and GWO algorithms. To develop an effective hybrid metaheuristic algorithm, the search strategies, population interaction mechanisms, and information sharing of the selected algorithms must be complementary. Therefore, the proposed algorithm has been developed not as a random combination of the SO and GWO algorithms but based on the complementary features of SO's adaptive population structure and GWO's hierarchical leadership mechanism.

The SO algorithm models the mating and foraging behaviors of male and female snake populations to perform optimization, which allows for the simultaneous execution of interactions between individuals and different search strategies. It dynamically manages the exploration and exploitation processes based on various environmental factors such as temperature and food quality. However, the literature has shown that in the later stages of the optimization process, the SO algorithm tends to reduce population diversity, information sharing between individuals remains limited, and it gets stuck in local solutions in complex optimization problems. One of the main reasons for this is that the individual update mechanisms in SO rely primarily on interactions among subpopulations, and there is no strong leadership

mechanism to guide the population. Consequently, the algorithm requires a supportive leadership characteristic that will enhance its global search capability.

The GWO algorithm, which constitutes another component of the hybrid structure, exhibits leadership-based search behavior. In GWO, the search process relies not only on the best solution but also on the guidance of three elite individuals defined as alpha, beta, and delta. This hierarchical leadership structure reduces the concentration of individuals around a single solution by sharing information obtained from high-quality solutions with other agents. This enables balanced guidance among individuals, thereby improving both global search capability and solution quality.

The primary motivation behind the proposed SOGWO is to facilitate effective information sharing among individuals in the population by holistically utilizing the hierarchical leadership mechanism of GWO and the male–female based population structure of SO. In this context, the hybrid SOGWO preserves the basic search behaviors of its two component algorithms, supporting SO's population interaction structure with GWO's multiple leadership mechanism, increasing population diversity, and avoiding stagnation in local optima.

The fundamental principle of the proposed SOGWO method is not to replace the operators of the GWO and SO algorithms, but rather to restructure the information flow between the two mechanisms. In this context, GWO is used as the first stage, guiding the existing population towards elite solutions, while SO performs second-stage improvement on the intermediate solutions obtained from this guidance. To avoid repeating the mathematical operators defined in the underlying algorithms and to maintain consistency, the basic update equations for GWO and SO are used as presented in Eqs. (24)–(27) and Eqs. (6)–(18), respectively. The computational steps for the proposed SOGWO are presented below in the following order.

2.3.1 Initialization

Considering the lower and upper limits of the search space, an initial population consisting of N individuals, $X = \{X_1, X_2, \ldots, X_N\}$, is randomly generated. While preserving the original structure of the search space, the population is divided into two subpopulations, male and female, which are denoted as X_m and X_f respectively. Therefore, the entire population is defined in the following form.

$$X = X_m \cup X_f \tag{28}$$

2.3.2 Population evaluation and determination of elite solutions

The fitness values of the snakes in each subpopulation are evaluated, and the best three individuals in each group are selected as the leader solutions. Accordingly, the top three individuals in the male subpopulation are identified as X_{m_α}, X_{m_β} and X_{m_δ} while the top three individuals in the female subpopulation are identified as X_{f_α}, X_{f_β} and X_{f_δ}.

Leader solutions for the male population are represented by $L_m = \left\{ X_{m_\alpha}, X_{m_\beta}, X_{m_\delta} \right\}$ while leader solutions for the female population are denoted as $L_f = \left\{ X_{f_\alpha}, X_{f_\beta}, X_{f_\delta} \right\}$. Furthermore, by evaluating both subpopulations together, the best individual within the entire population is determined as the global best solution, X_{food}. Thus, proposed SOGWO utilizes both gender-specific leadership information and the global solution in subsequent update processes. Therefore, these elite snakes play a guiding role in swarm behavior, serving as reference points for updating the positions of other search agents.

2.3.3 GWO-based guidance

The leader solutions for the male and female populations determined in the previous step are used as reference points in the GWO-based guidance phase. In this phase, the male and female subpopulations are updated independently through the GWO position update mechanism defined in Eqs. (24)–(27). Accordingly, the intermediate male and female populations obtained from the GWO phase are denoted by $X_m^{(t,G)}$ and $X_f^{(t,G)}$, respectively, and are expressed as follows:

$$\begin{aligned} X_m^{(t,G)} &= G_m\left(X_m^{(t)}, X_{m_\alpha}^{(t)}, X_{m_\beta}^{(t)}, X_{m_\delta}^{(t)}\right) \\ X_f^{(t,G)} &= G_f\left(X_f^{(t)}, X_{f_\alpha}^{(t)}, X_{f_\beta}^{(t)}, X_{f_\delta}^{(t)}\right) \end{aligned} \tag{29}$$

Here, $X_m^{(t,G)}$ and $X_f^{(t,G)}$ represent the male and female intermediate populations obtained after the GWO-based update in the iteration t, respectively. $G_m(\cdot)$ and $G_f(\cdot)$ refer to the GWO-based position update operators applied to the male and female subpopulations. These operators generate new intermediate positions using the current positions of the respective subpopulation and the α, β and δ leader solutions determined in the previous step. The $X_m^{(t,G)}$ and $X_f^{(t,G)}$ intermediate populations are evaluated together to determine the best individual $\left(X_{food}^{(t,G)}\right)$ obtained during the GWO phase. This solution represents the food source transferred from the GWO phase to the SO phase and is used as a reference in subsequent SO position updates. Thus, the new solutions generated in the GWO phase do not remain merely as intermediate results but directly form the input to the SO mechanism, thereby facilitating intra-iteration information transfer between the two search mechanisms. Moreover, this enables more informed movement within the search space, allowing the snakes to explore different regions simultaneously and reducing the risk of premature convergence.

2.3.4 SO-based improvement

Following the GWO-based guidance phase, the population applies the optimization approach of the standard SO. The SO operates on intermediate solutions guided by GWO, rather than on a newly created population independently. The SO phase can be described as follows:

$$\begin{aligned} X_m^{(t+1)} &= S_m\left(X_m^{(t,G)}, X_{food}^{(t,G)}\right) \\ X_f^{(t+1)} &= S_f\left(X_f^{(t,G)}, X_{food}^{(t,G)}\right) \end{aligned} \tag{30}$$

where $S_m(\cdot)$ ve $S_f(\cdot)$ depict SO-based update operators applied to the male and female populations, respectively. The overall transformation of both populations in SOGWO can be illustrated as follows:

$$\begin{aligned} X_m^{(t+1)} &= S_m\left(G_m\left(X_m^{(t)}\right)\right) \\ X_f^{(t+1)} &= S_f\left(G_f\left(X_f^{(t)}\right)\right) \end{aligned} \tag{31}$$

In this process, snakes mate based on temperature and food quality; otherwise, they forage for food or feed on available food. Individuals in both the female and male populations search for food in their surroundings if the environment is cold and food is scarce. This behavior is modeled by Eqs. (6) and (8) for male and female snakes. If the temperature is high and food is available, they focus on consuming the food and update their positions via Eq. (10). However, if the temperature is cold and food exists, the mating process occurs. During the mating process, there are two states: mating mode and fighting mode. In fighting mode, each male fights to obtain the best female by using Eq. (11), while each female tries to choose the best male by using Eq. (13). In mating mode, each pair mate depending on the availability of food and snakes determine their new positions according to Eqs. (15) and (16). If mating occurs during the search space, female snakes may lay their eggs, and new snakes may hatch from them in random locations of the solution space.

2.3.5 Population update and termination

Considering the sequential information transfer between GWO and SO, the general structure of the proposed SOGWO can be summarized as follows:

$$\left(X_m^{(t)}, X_f^{(t)}\right) \rightarrow GWO \rightarrow \left(X_m^{(t,G)}, X_f^{(t,G)}\right) \rightarrow SO \rightarrow \left(X_m^{(t+1)}, X_f^{(t+1)}\right) \tag{32}$$

The male and female populations derived from the SO are defined as $X_m^{(t+1)}$ and $X_f^{(t+1)}$, respectively, and constitute the populations for the next iteration. This process is repeated until the maximum number of iterations, T, is reached, and the best solution obtained at the end of the optimization process is assumed as the final solution of the SOGWO.

In the proposed hybrid structure, GWO is responsible for identifying promising regions in the search space and guiding individuals to these regions, the mating and foraging mechanisms of SO enables an intensive local search around promising solutions. This establishes an effective balance between exploration and exploitation, improving the algorithm's convergence rate, consistency, and solution quality,

reducing the probability of the trapping into a local optimum, and maintaining the population diversity.

The SOGWO, which forms a multi-layered hybrid structure, has a strong parallel processing capabilities because it simultaneously evaluates male and female populations, independently identifies elite individuals in each population, and performs position updates in parallel. This characteristic enables the SOGWO to operate efficiently on multi-core processors, GPU architectures, and distributed computing systems. Thus, SOGWO establishes a scalable framework for HPC and supercomputer environments.

Figure 2 shows the flowchart of the SOGWO and the pseudo code of the proposed method is given in Algorithm 1.

Algorithm 1 Pseudocode of the Proposed SOGWO

Set the parameters c_1, c_2, c_3
Initialize male and female snake populations $\left(X_m, X_f\right)$
Evaluate the snake population and determine the best solution $\left(X_{food}\right)$
while termination condition is not met **do**
    Select the three best male snakes $\left(X_{m_\alpha}, X_{m_\beta}, X_{m_\delta}\right)$
    Select the three best female snakes $\left(X_{f_\alpha}, X_{f_\beta}, X_{f_\delta}\right)$
    Update male and female populations using the GWO strategy by using Eqs. (24)-(27)
    Evaluate solutions and update $\left(X_{food}\right)$
    Calculate $Temp$ by using Eq. (4)
    Calculate Q by using Eq. (5)
    if $(Q < 0.25)$ **then**
        Perform exploration by Eqs. (6)-(9)
    else
        if $(Temp < 0.6)$ **then**
            Perform exploitation by Eq. (10)
        else
            if $(rand < 0.6)$ **then**
                Perform fighting mode Eqs. (11)-(14)
            else
                Perform mating mode Eqs. (15)-(18)
                Identify the snakes with the worst fitness values and update by using Eq. (1)
            end if
        end if
    end if
    Evaluate solutions and update the best solution $\left(X_{food}\right)$
end while
return the best solution

2.4 Computational complexity analysis of SOGWO

The computational complexity of a meta-heuristic algorithm is a key parameter for evaluating its effectiveness and efficiency. Complexity analysis is a theoretical framework that facilitates the estimation of the execution time and memory requirements of an algorithm, considering the problem size. Although the proposed SOGWO provides performance gains by combining the strengths of the SO and GWO algorithms, it may also introduce additional computational overhead.

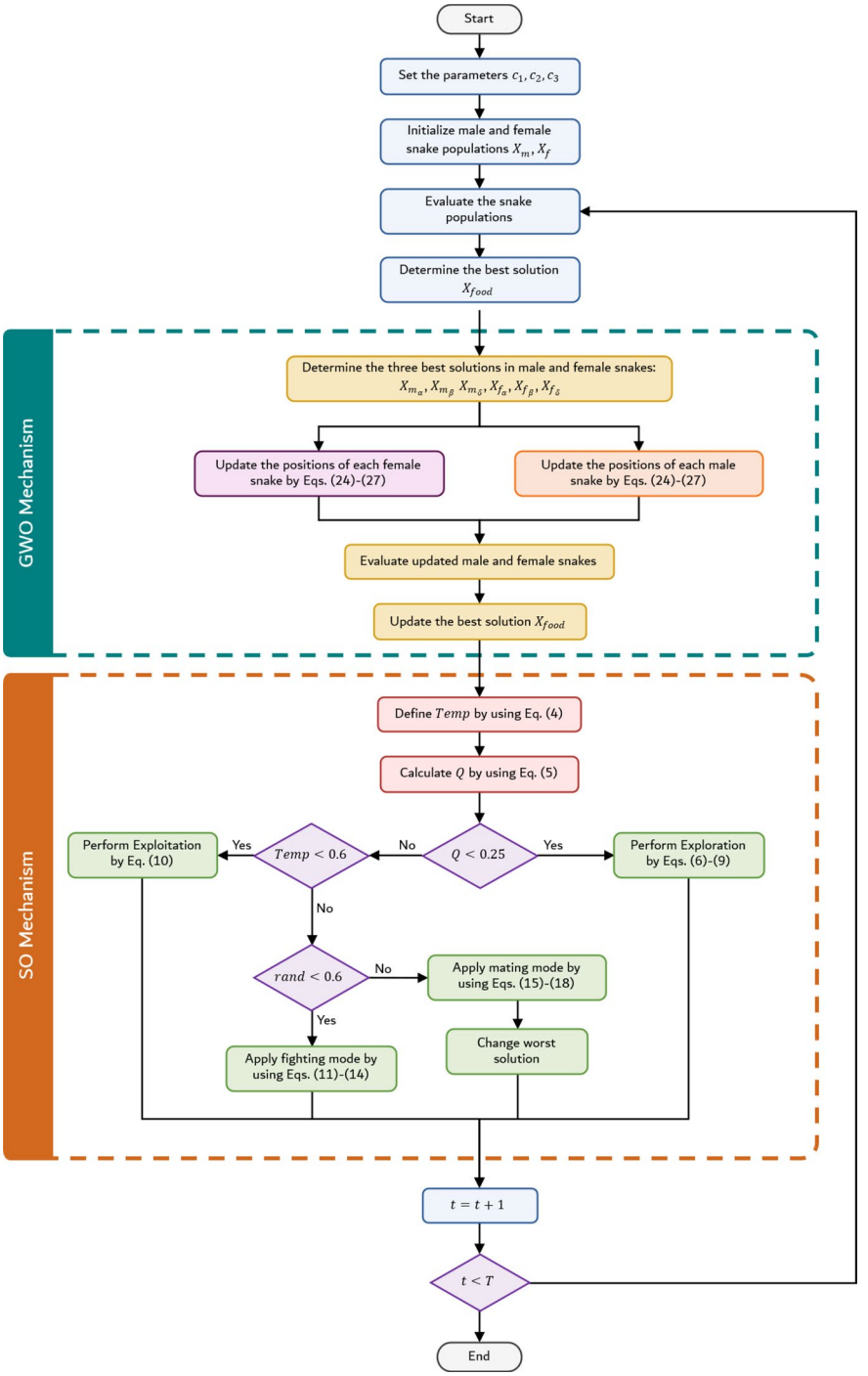


Fig. 2 The flowchart of the SOGWO

Therefore, this section contains both time and space complexity analyses to evaluate whether this enhancement occurs at a reasonable computational cost by utilizing Big-O notation.

2.4.1 Time complexity

Time complexity is defined as the rate at which the number of operations performed by an algorithm increases as the problem size grows. The computational cost of the SOGWO is influenced by four primary components: problem definition, initialization, fitness evaluation, and solution update.

- *Problem definition*: Since the operations in the problem definition phase are independent of the problem size and require a fixed number of operations, the time complexity is $\mathcal{O}(1)$.
- *Initialization*: Population initialization involves generating D-dimensional solution vectors for N individuals. Therefore, the time complexity of this stage is expressed as $\mathcal{O}(N \times D)$.
- *Fitness evaluation*: In each iteration (T), N candidate solutions are evaluated depending on the problem dimension (D). The calculation of the fitness for each solution requires an additional cost of C. Therefore, the total time complexity of evaluation is $\mathcal{O}(T \times N \times D \times C)$.
- *Solution update*: In this phase, new candidate solutions are generated improving the current population. Firstly, position updates are performed based on the elite individuals from the GWO. Subsequently, a fundamental search characteristic of the SO algorithm is selected and applied to each search agent. Hence, the time complexity for this stage can be expressed as follows:

$$\mathcal{O}(SO) + \mathcal{O}(GWO) = \mathcal{O}(T \times N \times D) + \mathcal{O}(T \times N \times D) = \mathcal{O}(2 \times T \times N \times D)$$

Since constant numbers are neglected in Big-O notation, the time complexity of solution update simplified to $\mathcal{O}(T \cdot N \cdot D)$.

Considering all components, the overall time complexity of SOGWO is obtained as follows:

$$\begin{aligned}\mathcal{O}_{time}(SOGWO) =& \mathcal{O}(1) + \mathcal{O}(N \times D) + \mathcal{O}(T \times N \times D \times C) + \mathcal{O}(T \times N \times D) \\ =& \mathcal{O}(T \times N \times D)\end{aligned}$$

2.4.2 Space complexity

Space complexity refers to how the total memory consumption of an algorithm varies depending on the problem size during its execution. Consequently, the algorithm's memory requirement exhibits a linear increase in proportion to the population size and the problem size. The space complexity can be outlined as follows.

Table 1 Description of unimodal benchmark functions

Function	D	*Range*	f_{min}
$F1(x) = \sum_{i=1}^{D} x_i^2$	30	$[-100, 100]$	0
$F2(x) = \sum_{i=1}^{D} \lvert x_i \rvert + \prod_{i=1}^{D} \lvert x_i \rvert$	30	$[-10, 10]$	0
$F3(x) = \sum_{i=1}^{D} \left(\sum_{j-1}^{i} x_j \right)^2$	30	$[-100, 100]$	0
$F4(x) = \max_i \{ \lvert x_i \rvert, 1 \le i \le D \}$	30	$[-100, 100]$	0
$F5(x) = \sum_{i=1}^{D-1} \left[100 \left(x_{i+1} - x_i^2 \right)^2 + \left(x_i - 1 \right)^2 \right]$	30	$[-30, 30]$	0
$F6(x) = \sum_{i=1}^{D} \left(x_i + 0.5 \right)^2$	30	$[-100, 100]$	0
$F7(x) = \sum_{i=1}^{D} i x_i^4 + \text{random}[0,1)$	30	$[-1.28, 1.28]$	0

$$\mathcal{O}_{space}(SOGWO) = \mathcal{O}(N \times D)$$

3 Experimental results and analysis

In this section, various experimental studies are presented on well-established optimization problems in the literature to comprehensively evaluate the performance of the proposed SOGWO. The findings are discussed in detail through comparative analyses and various performance metrics, and the algorithm's convergence behavior, stability, and overall effectiveness are evaluated.

3.1 Description of benchmark test suites

This subsection provides a detailed description of the standard benchmark functions and the CEC-2022 test suite for experimental evaluation. These function sets include test problems of varying difficulty levels and diverse characteristics. This allows for the evaluation of algorithm performance on a broader and more reliable testing platform.

3.1.1 Standard benchmark functions

In this study, standard benchmark functions of varying difficulty are utilized to assess the performance of the proposed SOGWO. These benchmark functions can be divided into three groups: unimodal, multimodal, and fixed-dimension multimodal. Each group facilitates the analysis of exploration and exploitation capabilities of the algorithms from different perspectives, comparing their effectiveness on diverse problem landscapes. The unimodal benchmark functions F1-F7 displayed in Table 1 have only one global optimum and highlight the exploitation capabilities of algorithms. The multimodal test functions F8-F13 have more than one local optimum and only one global optimum and are depicted in Table 2. It is noteworthy

Table 2 Description of multimodal benchmark functions

Function	D	*Range*	f_{min}
$F8(x) = \sum_{i=1}^{D} - x_i \sin\left(\sqrt{\lvert x_i \rvert}\right)$	30	$[-500, 500]$	$-418.9829 \times D$
$F9(x) = \sum_{i=1}^{D} \left[x_i^2 - 10\cos\left(2\pi x_i\right) + 10\right]$	30	$[-5.12, 5.12]$	0
$F10(x) = -20\exp\left(-0.2\sqrt{\frac{1}{D}\sum_{i=1}^{D} x_i^2}\right) - \exp\left(\frac{1}{D}\sum_{i=1}^{D}\cos\left(2\pi x_i\right)\right) + 20 + e$	30	$[-32, 32]$	0
$F11(x) = \frac{1}{4000}\sum_{i=1}^{D} x_i^2 - \prod_{i=1}^{D}\cos\left(\frac{x_i}{\sqrt{i}}\right) + 1$	30	$[-600, 600]$	0
$F12(x) = \frac{\pi}{D}\left\{10\sin\left(\pi y_1\right) + \sum_{i=1}^{D-1}\left(y_i - 1\right)^2\left[1 + 10\sin^2\left(\pi y_{i+1}\right)\right] + \left(y_{\mathrm{D}} - 1\right)^2\right\} + \sum_{i=1}^{D} u\left(x_i, 10, 100, 4\right)$ $y_i = 1 + \frac{x_i + 1}{4}$, $u\left(x_i, a, k, m\right) = \begin{cases} k\left(x_i - a\right)^m, & x_i > a \\ 0, & -a < x_i < a \\ k\left(-x_i - a\right)^m, & x_i < -a \end{cases}$	30	$[-50, 50]$	0
$F13(x) = 0.1\left\{\sin^2\left(3\pi x_1\right) + \sum_{i=1}^{D}\left(x_i - 1\right)^2\left[1 + \sin^2\left(3\pi x_i + 1\right)\right] + \left(x_D - 1\right)^2\left[1 + \sin^2\left(2\pi x_D\right)\right]\right\} + \sum_{i=1}^{D} u\left(x_i, 5, 100, 4\right)$	30	$[-50, 50]$	0

that optimization algorithms have the possibility of trapping into a local optimum in multimodal test functions, thereby demonstrating their exploration capability. The fixed-dimension multimodal functions F14-F23 reported in Table 3 contain many local optima and depict the balance that algorithms strike between exploration and exploitation.

3.1.2 CEC-2022 test suite

The standard test functions provide a valuable testing environment for analyzing the basic optimization capabilities of an algorithm. However, these functions may not accurately demonstrate the algorithm's effectiveness in addressing complex optimization problems. The CEC-2022 test suite is chosen because it represents problems of varying dimensions and levels of complexity, thereby enabling the evaluation of the proposed algorithm's exploration and exploitation capabilities under different optimization scenarios. Thus, an extended suite of tests is performed on the CEC-2022 benchmark set, which incorporates more challenging problem characteristics, to reveal the robustness and solution quality of the SOGWO. The CEC-2022 test suite encompasses twelve test functions, which are denoted as C1–C12, namely unimodal, basic, hybrid, and composition. Table 4 details the CEC-2022 test functions designed to evaluate the exploration and exploitation abilities. Moreover, CEC-2022 enables the assessment of the generalization and stability characteristics of algorithms.

Table 3 Description of fixed-dimension multimodal benchmark functions

Function	D	Range	f_{min}
$F14(x)=\left(\frac{1}{500}+\sum_{j=1}^{25}\frac{1}{j+\sum_{i=1}^{2}(x_i-a_{ij})^6}\right)^{-1}$	2	$[-65,65]$	1
$F15(x)=\sum_{i=1}^{11}\left[a_i-\frac{x_1(b_i^2+b_ix_2)}{b_i^2+b_ix_3+x_4}\right]^2$	2	$[-5,5]$	0.00030
$F16(x)=4x_1^2-2.1x_1^4+\frac{1}{3}x_1^6+x_1x_2-4x_2^2+4x_2^4$	2	$[-5,5]$	-1.0316
$F17(x)=\left(x_2-\frac{5.1}{4\pi^2}x_1^2+\frac{5}{\pi}x_1-6\right)^2+10\left(1-\frac{1}{8\pi}\right)\cos x_1+10$	2	$[-5,5]$	0.398
$F18(x)=\left[1+(x_1+x_2+1)^2(19-14x_1+3x_1^2-14x_2+6x_1x_2+3x_2^2)\right]\times\left[30+(2x_1-3x_2)^2\times(18-32x_1+12x_1^2+48x_2-36x_1x_2+27x_2^2)\right]$	2	$[-2,2]$	3
$F19(x)=-\sum_{i=1}^{4}c_i\exp\left(-\sum_{j=1}^{3}a_{ij}(x_j-p_{ij})^2\right)$	3	$[1,3]$	-3.86
$F20(x)=-\sum_{i=1}^{4}c_i\exp\left(-\sum_{j=1}^{6}a_{ij}(x_j-p_{ij})^2\right)$	6	$[0,1]$	-3.32
$F21(x)=-\sum_{i=1}^{5}\left[(X-a_i)(X-a_i)^T+c_i\right]^{-1}$	4	$[0,10]$	-10.1532
$F22(x)=-\sum_{i=1}^{7}\left[(X-a_i)(X-a_i)^T+c_i\right]^{-1}$	4	$[0,10]$	-10.4028
$F23(x)=-\sum_{i=1}^{10}\left[(X-a_i)(X-a_i)^T+c_i\right]^{-1}$	4	$[0,10]$	-10.5363

Table 4 Description of CEC-2022 test suite

Class	No	Functions	F_i^*	Range
Unimodal Function	C1	Shifted and full Rotated Zakharov Function	300	[− 100,100]
Basic Functions	C2	Shifted and full Rotated Rosenbrock's Function	400	[− 100,100]
	C3	Shifted and full Rotated Expanded Schaffer's $f6$ Function	600	[− 100,100]
	C4	Shifted and full Rotated Non-Continuous Rastrigin's Function	800	[− 100,100]
	C5	Shifted and full Rotated Levy Function	900	[− 100,100]
Hybrid Functions	C6	Hybrid Function 1 (N=3)	1800	[− 100,100]
	C7	Hybrid Function 2 (N=6)	2000	[− 100,100]
	C8	Hybrid Function 3 (N=5)	2200	[− 100,100]
Composition Functions	C9	Composition Function 1 (N=5)	2300	[− 100,100]
	C10	Composition Function 2 (N=4)	2400	[− 100,100]
	C11	Composition Function 3 (N=5)	2600	[− 100,100]
	C12	Composition Function 4 (N=6)	2700	[− 100,100]

3.2 Experimental setup

The performance of SOGWO is evaluated by using mean, error margin (EM), standard deviation (Std), and standard error of mean (SEM) values obtained over 30 independent runs. The reason for using these metrics is to provide a comprehensive assessment of the algorithm's effectiveness, robustness, stability, convergence, and reliability.

In the experimental study, the competing algorithms are terminated either when the maximum number of function evaluations is reached, or when the best solution obtained approaches the known optimal value with an accuracy of 10^{-12}. The function error is calculated according to $f\left(X_{best}\right) - f(X^*)$, where the X_{best} denotes the solution obtained by the algorithm, and X^* states the global optimum for the regarding test function. The maximum number of function evaluations is set by $MaxFes = D \times 1000$ for all test suites, where D is the problem dimension. Additionally, the population size is set to 30, and the simulation results are reported based on 30 independent runs. To guarantee a fair comparison, all competing algorithms are conducted under the same conditions.

SOGWO compared with many other well-known and state-of-the-art optimization algorithms like snake optimizer (SO) [44], grey wolf optimizer (GWO) [51], particle swarm optimization (PSO) [52], artificial bee colony algorithm (ABC) [53], equilibrium optimizer (EO) [54], salp swarm algorithm (SSA) [55], whale optimization algorithm (WOA) [56], sine–cosine algorithm (SCA) [57], Chernobyl disaster optimizer (CDO) [58], red-billed blue magpie optimizer (RBMO) [59], hybrid success-history intelligent optimization algorithm (SHIODEG) [38], Rüppell's fox optimizer (RFO) [60], salp swarm–Kepler optimization algorithm (SSAKOA) [61]. Parameter configurations of the competing algorithms are listed in Table 5 are defined according to the recommendations in the original papers. Moreover, all

Table 5 Parameter configurations of the competing algorithms

Algorithm	Parameter and description	Value
SOGWO	Threshold value $\left(Threshold_1\right)$	0.25
	Threshold value $\left(Threshold_2\right)$	0.6
	Constant $\left(c_1\right)$	0.5
	Constant $\left(c_2\right)$	0.05
	Constant $\left(c_3\right)$	2
	Convergence parameter (a)	Linearly decreases from 2 to 0
SO	Threshold value $\left(Threshold_1\right)$	0.25
	Threshold value $\left(Threshold_2\right)$	0.6
	Constant $\left(c_1\right)$	0.5
	Constant $\left(c_2\right)$	0.05
	Constant $\left(c_3\right)$	2
GWO	Convergence parameter (a)	Linearly decreases from 2 to 0
PSO	Cognitive coefficient $\left(c_1\right)$	2
	Social coefficient $\left(c_2\right)$	2
	Inertia weight (w)	$[0.2, 0.9]$
	Velocity bounds	$v_{max} = 0.2(ub - lb), v_{min} = -v_{max}$
ABC	Limit parameter	$0.6 \times D \times N$
	ϕ	Uniform random in $[-1, 1]$
EO	Magnitude of exploration $\left(a_1\right)$	2
	Magnitude of exploration $\left(a_2\right)$	1
	V	1
	Generation probability (GP)	0.5
SSA	Exploration–exploitation coefficient $\left(c_1\right)$	Linearly decreases from 2 to 0
WOA	Converge constant $\left(a_1\right)$	Linearly decreases from 2 to 0
	Converge constant $\left(a_2\right)$	Linearly decreases from -1 to -2
	Spiral factor (b)	1
SCA	Movement direction $\left(r_1\right)$	Linearly decreases from 2 to 0
	r_2	Uniform random in $[0, 2\pi]$
	r_3	Uniform random in $[0, 2]$
	r_4	Uniform random in $[0, 1]$
CDO	Walking speed of human $\left(WS_h\right)$	Linearly decreases from 3 to 0
	Speed of gamma $\left(S_\gamma\right)$	Rand $(1, 300000)$
	Speed of beta $\left(S_\beta\right)$	Rand $(1, 270000)$
	Speed of alpha $\left(S_\alpha\right)$	Rand $(1, 16000)$
RBMO	p	$[2, 5]$
	q	$[10, N]$
	CF	$[0, 1]$
	ε	0.5
SHIODEG	DE scaling factor (F)	0.5
	Crossover probability (CR):	0.9
	a	1.5

Table 5 (continued)

Algorithm	Parameter and description	Value
RFO	Walk rate update (β)	0.000001
	Positive constants (e_0, e_1)	1, 3
	Positive constants (c_0, c_1)	2, 2
	Positive constants (a_0, a_1)	
SSAKOA	T	3
	Initial value of the gravitational constant.(μ_0)	0.1
	Predefined constant (γ)	15
	Exploration–exploitation coefficient (c_1)	Linearly decreases from 2 to 0

algorithms were implemented in MATLAB R2022b and performed on Intel Core i5-10,400 CPU 2.90 GHz processor with 8 GB of RAM.

3.3 Quantitative analysis

In this subsection, the performance of the SOGWO is quantitatively investigated on standard benchmark functions and CEC-2022 test suite. The robustness and reliability of the SOGWO are assessed using metrics such as the mean, the margin of error (ErrorM), the standard deviation (Std), and the standard error of the mean (SEM).

3.3.1 Performance evaluation with standard benchmark functions

The optimization capability of the proposed SOGWO is first evaluated on standard test functions. Unimodal test functions are employed to assess the exploitation capability of SOGWO. Table 6 reports the experimental results obtained on unimodal test functions.

As indicated by the findings presented in Table 6, SOGWO demonstrates superior performance in functions F1, F2, F3, and F4. However, SOGWO produces results quite close to the optimum for functions F5, F6, and F7, while the SO, CDO, and SSAKOA algorithms produce more successful results, respectively. Furthermore, considering the overall performance ranking, it can be stated that the proposed algorithm possesses a strong local search capability. Moreover, the low standard deviation (Std) and standard error of the mean (SEM) emphasize stability and consistency of the SOGWO. Consequently, the SOGWO exhibits strong exploitation ability and rapidly converges to the optimal value.

Table 7 summarizes a comparative analysis of the results from experiments conducted on multimodal test functions to evaluate the exploration capability of the SOGWO. Upon examining the results in Table 7, the proposed algorithm exhibits outperforming performance in functions F8, F10, and F12. In contrast, for the functions F9, F11, and F12, the WOA, GWO, and SSAKOA algorithms, respectively, produce superior results. Nevertheless, the proposed SOGWO ensures first position in the overall ranking due to its effective performance on multimodal test functions.

Table 6 Comparison of optimization results of unimodal benchmark functions (F1-F7)

Function	Metric	SOGWO	SO	GWO	PSO	ABC	EO	SSA	WOA	SCA	CDO	RBMO	SHIODEG	RFO	SSAKOA
*F*1	Mean	8.660E−13	5.787E−09	8.343E−09	3.508E−07	5.849E+01	2.521E−04	1.342E+04	8.013E−09	2.350E−03	8.865E−09	1.726E−02	9.337E−09	8.466E+03	1.424E−08
	ErrorM	8.660E−13	5.787E−09	8.343E−09	3.508E−07	5.849E+01	2.521E−04	1.342E+04	8.013E−09	2.350E−03	8.865E−09	1.726E−02	9.337E−09	8.466E+03	1.424E−08
	Std	1.055E−13	2.321E−09	8.723E−10	9.579E−07	3.218E+01	1.834E−04	2.599E+03	1.417E−09	5.419E−03	8.344E−10	7.722E−02	4.791E−10	2.570E+03	2.910E−09
	SEM	1.926E−14	4.237E−10	1.593E−10	1.749E−07	5.875E+00	3.349E−05	4.744E+02	2.587E−10	9.894E−04	1.523E−10	1.410E−02	8.748E−11	4.691E+02	5.314E−10
	Rank	1	2	4	8	12	9	14	3	10	5	11	6	13	7
*F*2	Mean	9.113E−13	8.176E−09	9.239E−09	3.000E+00	2.800E−02	3.240E−03	1.560E+02	8.368E−09	4.775E−08	9.099E−09	4.105E−02	9.790E−09	3.804E+01	8.475E−03
	ErrorM	9.113E−13	8.176E−09	9.239E−09	3.000E+00	2.800E−02	3.240E−03	1.560E+02	8.368E−09	4.775E−08	9.099E−09	4.105E−02	9.790E−09	3.804E+01	8.475E−03
	Std	6.661E−14	1.180E−09	5.066E−10	4.661E+00	1.104E−02	1.863E−03	4.130E+02	1.707E−09	6.534E−08	5.278E−10	1.217E−01	1.412E−10	6.823E+00	1.725E−02
	SEM	1.216E−14	2.155E−10	9.249E−11	8.509E−01	2.015E−03	3.402E−04	7.540E+01	3.117E−10	1.193E−08	9.637E−11	2.221E−02	2.578E−11	1.246E+00	3.149E−03
	Rank	1	2	5	12	10	8	14	3	7	4	11	6	13	9
*F*3	Mean	6.331E−13	6.507E−09	9.005E−09	2.588E+03	3.672E+04	6.137E+02	5.762E+04	2.042E+04	2.916E+03	7.430E−09	1.335E+02	8.552E−09	1.051E+04	1.084E+02
	ErrorM	6.331E−13	6.507E−09	9.005E−09	2.588E+03	3.672E+04	6.137E+02	5.762E+04	2.042E+04	2.916E+03	7.430E−09	1.335E+02	8.552E−09	1.051E+04	1.084E+02
	Std	2.085E−13	2.363E−09	6.599E−10	3.881E+03	4.248E+03	5.490E+02	4.013E+04	9.879E+03	2.663E+03	1.369E−09	9.732E+01	1.452E−09	4.136E+03	6.200E+01
	SEM	3.807E−14	4.315E−10	1.205E−10	7.085E+02	7.757E+02	1.002E+02	7.327E+03	1.804E+03	4.862E+02	2.500E−10	1.777E+01	2.650E−10	7.551E+02	1.132E+01
	Rank	1	2	5	9	13	8	14	12	10	3	7	4	11	6
*F*4	Mean	8.666E−13	7.940E−09	9.290E−09	3.831E+00	6.718E+01	4.810E−01	4.299E+01	4.081E+01	1.442E+01	9.100E−09	4.360E+00	3.617E−03	2.666E+01	1.992E+00
	ErrorM	8.666E−13	7.940E−09	9.290E−09	3.831E+00	6.718E+01	4.810E−01	4.299E+01	4.081E+01	1.442E+01	9.100E−09	4.360E+00	3.617E−03	2.666E+01	1.992E+00
	Std	8.598E−14	1.358E−09	4.860E−10	1.105E+00	5.083E+00	2.740E−01	5.269E+00	2.806E+01	1.009E+01	6.873E−10	1.999E+00	4.534E−03	4.900E+00	1.554E+00
	SEM	1.570E−14	2.480E−10	8.873E−11	2.017E−01	9.281E−01	5.002E−02	9.619E−01	5.123E+00	1.843E+00	1.255E−10	3.650E−01	8.278E−04	8.946E−01	2.838E−01
	Rank	1	2	4	8	14	6	13	12	10	3	9	5	11	7
*F*5	Mean	1.448E+01	1.002E+01	2.690E+01	2.925E+02	2.155E+06	2.863E+01	1.203E+07	2.720E+01	1.266E+02	2.727E+01	1.585E+02	2.788E+01	5.102E+06	5.568E+01
	ErrorM	1.448E+01	1.002E+01	2.690E+01	2.925E+02	2.155E+06	2.863E+01	1.203E+07	2.720E+01	1.266E+02	2.727E+01	1.585E+02	2.788E+01	5.102E+06	5.568E+01
	Std	1.107E+01	1.079E+01	8.396E−01	7.649E+02	8.192E+05	2.434E−01	5.928E+06	5.984E−01	2.553E+02	2.612E−01	1.169E+02	8.992E−01	4.442E+06	4.053E+01
	SEM	2.021E+00	1.971E+00	1.533E−01	1.397E+02	1.496E+05	4.444E−02	1.082E+06	1.092E−01	4.662E+01	4.768E−02	2.134E+01	1.642E−01	8.111E+05	7.400E+00
	Rank	2	1	3	11	12	7	14	4	9	5	10	6	13	8

Table 6 (continued)

Function	Metric	SOGWO	SO	GWO	PSO	ABC	EO	SSA	WOA	SCA	CDO	RBMO	SHIODEG	RFO	SSAKOA
$F6$	Mean	3.108E−02	1.161E−01	9.818E−01	1.809E−06	5.635E+01	2.066E+00	1.265E+04	1.118E−01	4.481E+00	7.500E+00	1.482E−03	2.876E+00	8.338E+03	1.515E−08
	ErrorM	3.108E−02	1.161E−01	9.818E−01	1.809E−06	5.635E+01	2.066E+00	1.265E+04	1.118E−01	4.481E+00	7.500E+00	1.482E−03	2.876E+00	8.338E+03	1.515E−08
	Std	8.084E−02	1.062E−01	5.142E−01	7.074E−06	2.785E+01	3.918E−01	3.181E+03	1.480E−01	3.929E−01	0.000E+00	2.289E−03	6.041E−01	3.022E+03	3.005E−09
	SEM	1.476E−02	1.938E−02	9.389E−02	1.292E−06	5.085E+00	7.153E−02	5.807E+02	2.702E−02	7.173E−02	0.000E+00	4.179E−04	1.103E−01	5.518E+02	5.487E−10
	Rank	4	6	7	2	12	8	14	5	10	11	3	9	13	1
$F7$	Mean	2.005E−04	1.002E−04	6.918E−04	1.133E−01	1.141E+00	1.701E−02	6.800E+00	1.632E−03	3.114E−02	9.430E−05	3.545E−02	3.933E−03	2.306E+00	4.383E−02
	ErrorM	2.005E−04	1.002E−04	6.918E−04	1.133E−01	1.141E+00	1.701E−02	6.800E+00	1.632E−03	3.114E−02	9.430E−05	3.545E−02	3.933E−03	2.306E+00	4.383E−02
	Std	1.265E−04	8.898E−05	3.379E−04	4.892E−01	3.635E−01	1.016E−02	4.459E+00	1.797E−03	2.963E−02	7.355E−05	1.767E−02	2.236E−03	1.798E+00	1.422E−02
	SEM	2.310E−05	1.625E−05	6.170E−05	8.932E−02	6.636E−02	1.856E−03	8.141E−01	3.280E−04	5.409E−03	1.343E−05	3.226E−03	4.082E−04	3.283E−01	2.597E−03
	Rank	3	2	4	11	12	7	14	5	8	1	9	6	13	10
$w/t/l$		~	5/0/2	7/0/0	6/0/1	7/0/0	7/0/0	7/0/0	7/0/0	7/0/0	6/0/1	6/0/1	7/0/0	7/0/0	6/0/1
Mean Rank		1.86	2.43	4.57	8.71	12.14	7.57	13.86	6.29	9.14	4.57	8.57	6.00	12.43	6.86
Overall Rank		1	2	3.5	10	12	8	14	6	11	3.5	9	5	13	7

Table 7 Comparison of optimization results of multimodal benchmark functions (F8-F13)

Function	Metric	SOGWO	SO	GWO	PSO	ABC	EO	SSA	WOA	SCA	CDO	RBMO	SHIODEG	RFO	SSAKOA
*F*8	Mean	-1.257E+04	-1.256E+04	-6.017E+03	-8.759E+03	-5.069E+03	-4.933E+03	-6.006E+03	-1.081E+04	-3.938E+03	-4.151E+03	-8.755E+03	-5.618E+03	-4.439E+03	-8.861E+03
	ErrorM	4.461E+00	7.979E+00	6.553E+03	3.811E+03	7.501E+03	7.636E+03	6.563E+03	1.758E+03	8.632E+03	8.419E+03	3.814E+03	6.952E+03	8.130E+03	3.708E+03
	Std	3.469E+00	1.453E+01	9.374E+02	5.251E+02	2.888E+02	7.875E+02	2.074E+02	1.891E+03	2.845E+02	3.213E+02	7.082E+02	9.004E+02	6.089E+02	7.992E+02
	SEM	6.333E−01	2.653E+00	1.711E+02	9.587E+01	5.273E+01	1.438E+02	3.787E+01	3.453E+02	5.194E+01	5.865E+01	1.293E+02	1.644E+02	1.112E+02	1.459E+02
	Rank	1	2	7	5	10	11	8	3	14	13	6	9	12	4
*F*9	Mean	1.087E+00	7.472E−05	1.266E+00	5.294E+01	2.357E+02	2.416E+00	2.806E+02	7.722E−09	1.390E+01	1.393E+02	5.192E+01	2.916E+01	1.782E+02	4.318E+01
	ErrorM	1.087E+00	7.472E−05	1.266E+00	5.294E+01	2.357E+02	2.416E+00	2.806E+02	7.722E−09	1.390E+01	1.393E+02	5.192E+01	2.916E+01	1.782E+02	4.318E+01
	Std	5.704E+00	1.627E−05	6.936E+00	1.562E+01	1.199E+01	6.263E+00	2.408E+01	2.267E−09	2.357E+01	1.002E+02	2.100E+01	1.199E+01	2.910E+01	1.141E+01
	SEM	1.041E+00	2.971E−06	1.266E+00	2.852E+00	2.188E+00	1.143E+00	4.396E+00	4.140E−10	4.304E+00	1.829E+01	3.834E+00	2.188E+00	5.314E+00	2.082E+00
	Rank	3	2	4	10	13	5	14	1	6	11	9	7	12	8
*F*10	Mean	9.324E−13	8.024E−09	9.067E−09	4.322E−01	4.550E+00	4.425E−03	1.624E+01	8.723E−09	1.620E+01	9.399E−09	1.932E+00	9.926E−09	1.452E+01	5.766E+00
	ErrorM	9.324E−13	8.024E−09	9.067E−09	4.322E−01	4.550E+00	4.425E−03	1.624E+01	8.723E−09	1.620E+01	9.399E−09	1.932E+00	9.926E−09	1.452E+01	5.766E+00
	Std	6.068E−14	1.514E−09	5.389E−10	6.985E−01	6.739E−01	1.735E−03	8.853E−01	1.298E−09	7.175E+00	4.769E−10	8.486E−01	6.173E−11	1.057E+00	7.832E+00
	SEM	1.108E−14	2.765E−10	9.839E−11	1.275E−01	1.230E−01	3.168E−04	1.616E−01	2.370E−10	1.310E+00	8.708E−11	1.549E−01	1.127E−11	1.929E−01	1.430E+00
	Rank	1	2	4	8	10	7	14	3	13	5	9	6	12	11
*F*11	Mean	8.531E−04	3.641E−02	7.706E−04	1.350E−02	1.534E+00	3.210E−03	1.148E+02	6.717E−03	1.536E−01	2.099E−03	2.713E−02	1.033E−02	6.557E+01	6.979E−03
	ErrorM	8.531E−04	3.641E−02	7.706E−04	1.350E−02	1.534E+00	3.210E−03	1.148E+02	6.717E−03	1.536E−01	2.099E−03	2.713E−02	1.033E−02	6.557E+01	6.979E−03
	Std	3.484E−03	6.272E−02	3.017E−03	1.837E−02	3.359E−01	6.410E−03	2.690E+01	2.628E−02	2.047E−01	4.192E−03	2.956E−02	2.085E−02	2.183E+01	8.653E−03
	SEM	6.360E−04	1.145E−02	5.508E−04	3.354E−03	6.132E−02	1.170E−03	4.912E+00	4.797E−03	3.738E−02	7.653E−04	5.396E−03	3.806E−03	3.985E+00	1.580E−03
	Rank	2	10	1	8	12	4	14	5	11	3	9	7	13	6
*F*12	Mean	2.681E−04	1.503E−02	6.288E−02	5.529E−02	3.675E+06	1.171E−01	6.343E+06	9.542E−03	3.338E+01	1.294E+00	1.050E+00	3.035E−01	7.074E+05	4.437E−01
	ErrorM	2.681E−04	1.503E−02	6.288E−02	5.529E−02	3.675E+06	1.171E−01	6.343E+06	9.542E−03	3.338E+01	1.294E+00	1.050E+00	3.035E−01	7.074E+05	4.437E−01
	Std	1.332E−03	3.793E−02	9.745E−02	8.493E−02	2.730E+06	4.724E−02	5.407E+06	7.393E−03	1.749E+02	2.699E−01	1.525E+00	2.618E−01	1.007E+06	5.491E−01
	SEM	2.431E−04	6.925E−03	1.779E−02	1.551E−02	4.984E+05	8.625E−03	9.872E+05	1.350E−03	3.193E+01	4.927E−02	2.784E−01	4.780E−02	1.838E+05	1.003E−01
	Rank	1	3	5	4	13	6	14	2	11	10	9	7	12	8

Table 7 (continued)

Function	Metric	SOGWO	SO	GWO	PSO	ABC	EO	SSA	WOA	SCA	CDO	RBMO	SHIODEG	RFO	SSAKOA
$F13$	Mean	2.644E−03	1.023E−02	6.639E−01	7.765E−02	1.055E+07	1.178E+00	2.802E+07	2.896E−01	2.186E+03	4.070E−01	2.034E+00	1.902E+00	8.459E+06	2.642E−03
	ErrorM	2.644E−03	1.023E−02	6.639E−01	7.765E−02	1.055E+07	1.178E+00	2.802E+07	2.896E−01	2.186E+03	4.070E−01	2.034E+00	1.902E+00	8.459E+06	2.642E−03
	Std	5.518E−03	1.143E−02	2.756E−01	2.980E−01	6.120E+06	2.362E−01	2.021E+07	2.045E−01	1.195E+04	6.721E−02	4.749E+00	3.199E−01	1.217E+07	4.686E−03
	SEM	1.007E−03	2.086E−03	5.032E−02	5.440E−02	1.117E+06	4.312E−02	3.690E+06	3.734E−02	2.182E+03	1.227E−02	8.671E−01	5.840E−02	2.222E+06	8.555E−04
	Rank	2	3	7	4	13	8	14	5	11	6	10	9	12	1
$w/t/l$		~	5/0/1	5/0/1	6/0/0	6/0/0	6/0/0	6/0/0	5/0/1	6/0/0	6/0/0	6/0/0	6/0/0	6/0/0	5/0/1
Mean Rank		1.67	3.67	4.67	6.50	11.83	6.83	13.00	3.17	11.00	8.00	8.67	7.50	12.17	6.33
Overall Rank		1	3	4	6	12	7	14	2	11	9	10	8	13	5

This outcome underscores that SOGWO is consistent and competitive not only in specific problems but also in multimodal functions with different characteristics, while effectively identifying promising regions. Additionally, SOGWO maintains relatively stable performance with minimal standard deviation (Std), and standard error of the mean (SEM). Hence, it can be concluded that the proposed method displays notable exploration efficacy.

The SOGWO is executed on fixed-dimensional multimodal functions to analyze the balance it strikes between exploration and exploitation. Table 8 depicts the comparison results for the fixed-dimensional multimodal functions. As per results in Table 8, SOGWO attains the best results on functions F20, F21, and F22 with a lower standard deviation (Std), and standard error of the mean (SEM). Conversely, some competing algorithms deliver better solutions for the rest of the fixed-dimensional multimodal functions. Despite the performance differences observed in some functions, the proposed algorithm remains in the leading position in the overall ranking. Furthermore, the proposed algorithm is highly competitive with respect to standard deviation (Std), and standard error of the mean (SEM), reflecting both consistent solution quality and strong statistical reliability. As such, it can be stated that SOGWO offers robust and balanced optimization ability across fixed-dimension multimodal functions with diverse characteristics.

To sum up, SOGWO has competitive performance on standard benchmark functions. Due to its strong exploitation capability, it rapidly converges on unimodal functions. In addition, it yields successful results in terms of local optima avoidance and global search capability. Thus, SOGWO performs a balanced exploration–exploitation mechanism across different problem types, ranks among the top-performing methods in the overall evaluation, and proves to be a reliable and effective approach.

3.3.2 Performance evaluation with CEC-2022 test suite

To further demonstrate the performance of the proposed SOGWO, the challenging and complex test functions called CEC-2022 are utilized. Experimental studies are conducted at $D = 10$ and $D = 20$ dimensions to investigate the algorithm's performance at varying problem dimensions. The results obtained for $D = 10$ in the CEC-2022 test functions for SOGWO and the comparison methods are detailed in Table 9.

The outcomes presented in Table 9 demonstrate that SOGWO outperforms all competitive optimizers on C4, C5, and C8. The SOGWO shares the leader position with the SSAKOA algorithm for the C1 test function. The findings indicate that the SSAKOA algorithm demonstrates a substantial advantage on functions C3, C10, C11, and C12, while the proposed SOGWO method exhibits a performance that is highly competitive with this algorithm. The results of the ranking analyses made for CEC-2022 ($D = 10$) clearly state that the SSAKOA algorithm is the best with a score of 2.13, while the proposed SOGWO is second with an average rank value of 2.5. Overall evaluation of the results of all test functions concludes that the

Table 8 Comparison of optimization results of fixed-dimension multimodal benchmark functions (F14-F23)

Function	Metric	SOGWO	SO	GWO	PSO	ABC	EO	SSA	WOA	SCA	CDO	RBMO	SHIODEG	RFO	SSAKOA
*F*14	Mean	2.721E+00	2.642E+00	8.577E+00	2.696E+00	2.369E+00	1.361E+01	3.429E+00	6.623E+00	3.639E+00	1.501E+01	1.924E+00	8.993E+00	8.285E+00	2.037E+00
	ErrorM	1.721E+00	1.642E+00	7.577E+00	1.696E+00	1.369E+00	1.261E+01	2.429E+00	5.623E+00	2.639E+00	1.401E+01	9.235E−01	7.993E+00	7.285E+00	1.037E+00
	Std	3.245E+00	3.261E+00	4.617E+00	3.399E+00	1.536E+00	6.707E+00	2.908E+00	5.174E+00	2.955E+00	4.634E+00	1.101E+00	4.577E+00	5.575E+00	1.079E+00
	SEM	5.925E−01	5.953E−01	8.430E−01	6.205E−01	2.804E−01	1.225E+00	5.310E−01	9.446E−01	5.395E−01	8.460E−01	2.010E−01	8.356E−01	1.018E+00	1.971E−01
	Rank	6	4	11	5	3	13	7	9	8	14	1	12	10	2
*F*15	Mean	1.295E−03	1.923E−03	7.182E−03	2.765E−03	1.491E−03	9.451E−03	3.321E−03	1.351E−03	1.277E−03	4.985E−04	3.222E−03	7.230E−03	5.045E−03	1.179E−03
	ErrorM	9.950E−04	1.623E−03	6.882E−03	2.465E−03	1.191E−03	9.151E−03	3.021E−03	1.051E−03	9.770E−04	1.985E−04	2.922E−03	6.930E−03	4.745E−03	8.787E−04
	Std	3.611E−03	4.376E−03	9.521E−03	5.978E−03	4.371E−04	7.889E−03	4.352E−03	2.128E−03	4.711E−04	1.303E−04	6.843E−03	9.491E−03	8.154E−03	3.661E−04
	SEM	6.592E−04	7.989E−04	1.738E−03	1.092E−03	7.980E−05	1.440E−03	7.945E−04	3.885E−04	8.601E−05	2.379E−05	1.249E−03	1.733E−03	1.489E−03	6.683E−05
	Rank	4	7	12	8	6	14	10	5	3	1	9	13	11	2
*F*16	Mean	-1.032E+00	-9.772E−01	-1.032E+00	-1.032E+00	-1.029E+00	-9.127E−01	-1.032E+00	-1.032E+00	-1.031E+00	-1.001E+00	-1.032E+00	-1.032E+00	-1.032E+00	-1.032E+00
	ErrorM	2.840E−05	5.438E−02	4.130E−05	2.850E−05	2.562E−03	1.189E−01	1.668E−05	2.610E−05	5.470E−04	3.030E−02	2.850E−05	9.587E−06	2.850E−05	2.850E−05
	Std	1.682E−07	2.071E−01	3.710E−04	0.000E+00	2.546E−03	1.057E−01	2.396E−04	5.711E−06	5.490E−04	6.681E−03	0.000E+00	2.073E−05	0.000E+00	0.000E+00
	SEM	3.070E−08	3.781E−02	6.774E−05	0.000E+00	4.648E−04	1.930E−02	4.375E−05	1.043E−06	1.002E−04	1.220E−03	0.000E+00	3.784E−06	0.000E+00	0.000E+00
	Rank	4	13	9	6.5	11	14	2	3	10	12	6.5	1	6.5	6.5
*F*17	Mean	3.977E−01	3.979E−01	3.980E−01	3.979E−01	3.997E−01	6.861E−01	3.980E−01	4.019E−01	4.095E−01	4.015E−01	3.979E−01	3.990E−01	3.979E−01	3.979E−01
	ErrorM	1.124E−04	1.126E−04	4.764E−05	1.126E−04	1.661E−03	2.881E−01	2.608E−05	3.932E−03	1.148E−02	3.503E−03	1.126E−04	9.861E−04	1.126E−04	1.126E−04
	Std	4.973E−08	1.694E−16	8.000E−05	1.694E−16	2.179E−03	3.384E−01	2.802E−04	6.220E−03	9.705E−03	3.861E−03	1.694E−16	8.279E−04	1.694E−16	1.694E−16
	SEM	9.079E−09	3.092E−17	1.461E−05	3.092E−17	3.978E−04	6.178E−02	5.116E−05	1.136E−03	1.772E−03	7.050E−04	3.092E−17	1.511E−04	3.092E−17	3.092E−17
	Rank	3	6	2	6	10	14	1	12	13	11	6	9	6	6
*F*18	Mean	4.800E+00	7.500E+00	7.454E+00	3.000E+00	3.117E+00	1.036E+01	3.000E+00	4.882E+00	3.007E+00	5.427E+01	3.000E+00	1.020E+01	5.700E+00	3.000E+00
	ErrorM	1.800E+00	4.500E+00	4.454E+00	0.000E+00	1.174E−01	7.355E+00	1.015E−05	1.882E+00	7.402E−03	5.127E+01	0.000E+00	7.202E+00	2.700E+00	0.000E+00
	Std	6.850E+00	1.023E+01	1.735E+01	0.000E+00	1.450E−01	1.201E+01	5.103E−05	7.139E+00	1.251E−02	3.349E+01	0.000E+00	2.120E+01	1.479E+01	0.000E+00
	SEM	1.251E+00	1.869E+00	3.167E+00	0.000E+00	2.647E−02	2.193E+00	9.318E−06	1.303E+00	2.283E−03	6.115E+00	0.000E+00	3.870E+00	2.700E+00	0.000E+00
	Rank	7	11	10	2	6	13	4	8	5	14	2	12	9	2

Table 8 (continued)

Function	Metric	SOGWO	SO	GWO	PSO	ABC	EO	SSA	WOA	SCA	CDO	RBMO	SHIODEG	RFO	SSAKOA
*F*19	Mean	-3.863E+00	-3.863E+00	-3.861E+00	-3.863E+00	-3.863E+00	-3.809E+00	-3.861E+00	-3.809E+00	-3.849E+00	-3.847E+00	-3.863E+00	-3.860E+00	-3.863E+00	-3.863E+00
	ErrorM	2.781E−03	2.782E−03	8.275E−04	2.782E−03	2.532E−03	5.071E−02	7.457E−04	5.137E−02	1.143E−02	1.285E−02	2.782E−03	1.088E−04	2.782E−03	2.733E−03
	Std	5.307E−08	1.355E−15	2.308E−03	1.355E−15	2.498E−04	6.450E−02	4.432E−03	7.753E−02	1.086E−02	9.018E−03	1.355E−15	2.656E−03	3.469E−07	1.842E−04
	SEM	9.689E−09	2.474E−16	4.214E−04	2.474E−16	4.560E−05	1.178E−02	8.091E−04	1.416E−02	1.983E−03	1.646E−03	2.474E−16	4.849E−04	6.333E−08	3.362E−05
	Rank	6	8.5	3	8.5	4	13	2	14	11	12	8.5	1	8.5	5
*F*20	Mean	-3.314E+00	-3.310E+00	-3.254E+00	-3.290E+00	-3.314E+00	-3.110E+00	-3.224E+00	-3.129E+00	-2.897E+00	-3.210E+00	-3.267E+00	-3.247E+00	-3.107E+00	-3.284E+00
	ErrorM	5.945E−03	1.024E−02	6.600E−02	2.972E−02	6.407E−03	2.096E−01	9.643E−02	1.911E−01	4.235E−01	1.099E−01	5.349E−02	7.294E−02	2.127E−01	3.642E−02
	Std	3.016E−02	3.617E−02	9.068E−02	6.195E−02	2.185E−02	1.329E−01	7.465E−02	2.304E−01	3.179E−01	6.599E−02	6.033E−02	7.682E−02	3.007E−01	5.565E−02
	SEM	5.506E−03	6.604E−03	1.656E−02	1.131E−02	3.989E−03	2.426E−02	1.363E−02	4.206E−02	5.805E−02	1.205E−02	1.101E−02	1.402E−02	5.490E−02	1.016E−02
	Rank	1	3	7	4	2	12	9	11	14	10	6	8	13	5
*F*21	Mean	-9.733E+00	-9.427E+00	-8.432E+00	-5.820E+00	-7.463E+00	-2.003E+00	-6.988E+00	-6.632E+00	-1.745E+00	-4.309E+00	-7.061E+00	-5.347E+00	-6.188E+00	-7.716E+00
	ErrorM	4.203E−01	7.261E−01	1.721E+00	4.333E+00	2.690E+00	8.150E+00	3.166E+00	3.521E+00	8.409E+00	5.844E+00	3.092E+00	4.806E+00	3.965E+00	2.437E+00
	Std	1.278E+00	1.097E+00	2.923E+00	3.464E+00	2.781E+00	1.572E+00	3.525E+00	2.797E+00	1.598E+00	1.095E+00	3.455E+00	2.969E+00	3.324E+00	2.744E+00
	SEM	2.333E−01	2.003E−01	5.337E−01	6.324E−01	5.078E−01	2.869E−01	6.436E−01	5.106E−01	2.918E−01	2.000E−01	6.307E−01	5.421E−01	6.069E−01	5.011E−01
	Rank	1	2	3	10	5	13	7	8	14	12	6	11	9	4
*F*22	Mean	-9.877E+00	-9.659E+00	-9.289E+00	-6.804E+00	-9.559E+00	-2.147E+00	-7.148E+00	-5.644E+00	-2.308E+00	-5.189E+00	-7.586E+00	-6.529E+00	-5.828E+00	-8.490E+00
	ErrorM	5.254E−01	7.442E−01	1.114E+00	3.599E+00	8.439E−01	8.256E+00	3.255E+00	4.759E+00	8.095E+00	5.214E+00	2.817E+00	3.874E+00	4.575E+00	1.912E+00
	Std	1.481E+00	1.483E+00	2.498E+00	3.708E+00	1.689E+00	9.587E−01	3.397E+00	2.327E+00	1.527E+00	1.610E+00	3.538E+00	3.098E+00	3.597E+00	2.832E+00
	SEM	2.705E−01	2.707E−01	4.560E−01	6.770E−01	3.083E−01	1.750E−01	6.203E−01	4.249E−01	2.787E−01	2.940E−01	6.460E−01	5.656E−01	6.567E−01	5.170E−01
	Rank	1	2	4	8	3	14	7	11	13	12	6	9	10	5
*F*23	Mean	-1.011E+01	-9.762E+00	-9.795E+00	-8.284E+00	-1.030E+01	-2.176E+00	-7.589E+00	-5.784E+00	-2.696E+00	-4.857E+00	-8.840E+00	-6.363E+00	-7.541E+00	-8.391E+00
	ErrorM	4.248E−01	7.746E−01	7.416E−01	2.252E+00	2.319E−01	8.361E+00	2.948E+00	4.753E+00	7.841E+00	5.679E+00	1.696E+00	4.174E+00	2.995E+00	2.145E+00
	Std	1.288E+00	1.242E+00	2.229E+00	3.533E+00	2.597E−01	9.638E−01	3.724E+00	2.596E+00	1.448E+00	1.295E+00	3.182E+00	3.233E+00	3.543E+00	3.124E+00
	SEM	2.352E−01	2.268E−01	4.069E−01	6.450E−01	4.742E−02	1.760E−01	6.799E−01	4.740E−01	2.643E−01	2.364E−01	5.809E−01	5.902E−01	6.469E−01	5.703E−01
	Rank	2	4	3	7	1	14	8	11	13	12	5	10	9	6
w/*t*/*l*		~	9/0/1	8/0/2	8/0/2	6/0/4	10/0/0	6/0/4	9/0/1	8/0/2	9/0/1	8/0/2	8/0/2	9/0/1	6/0/4

Table 8 (continued)

Function Metric	SOGWO	SO	GWO	PSO	ABC	EO	SSA	WOA	SCA	CDO	RBMO	SHIODEG	RFO	SSAKOA
Mean Rank	3.50	6.05	6.40	6.50	5.10	13.40	5.70	9.20	10.40	11.00	5.60	8.60	9.20	4.35
Overall Rank	1	6	7	8	3	14	5	10.5	12	13	4	9	10.5	2

Table 9 Comparison of optimization results of CEC-2022 test functions ($D = 10$)

Function	Metric	SOGWO	SO	GWO	PSO	ABC	EO	SSA	WOA	SCA	CDO	RBMO	SHIODEG	RFO	SSAKOA
*C*1	Mean	3.000E+02	3.000E+02	2.305E+03	6.858E+02	8.570E+03	5.348E+03	1.785E+04	1.524E+04	1.175E+03	8.389E+04	3.620E+02	3.998E+03	7.825E+03	3.000E+02
	ErrorM	0.000E+00	1.300E−05	2.005E+03	3.858E+02	8.270E+03	5.048E+03	1.755E+04	1.494E+04	8.754E+02	8.359E+04	6.199E+01	3.698E+03	7.525E+03	0.000E+00
	Std	0.000E+00	5.292E−05	2.200E+03	1.648E+03	2.286E+03	2.807E+03	6.620E+03	8.925E+03	7.402E+02	3.487E+05	7.415E+01	2.000E+03	5.288E+03	0.000E+00
	SEM	0.000E+00	9.663E−06	4.017E+02	3.009E+02	4.173E+02	5.125E+02	1.209E+03	1.629E+03	1.351E+02	6.366E+04	1.354E+01	3.652E+02	9.654E+02	0.000E+00
	Rank	1.5	3	7	5	11	9	13	12	6	14	4	8	10	1.5
*C*2	Mean	4.041E+02	4.024E+02	4.265E+02	4.227E+02	4.169E+02	4.135E+02	6.073E+02	4.343E+02	4.633E+02	8.483E+02	4.143E+02	4.407E+02	5.773E+02	4.073E+02
	ErrorM	4.106E+00	2.368E+00	2.651E+01	2.271E+01	1.691E+01	1.353E+01	2.073E+02	3.426E+01	6.330E+01	4.483E+02	1.435E+01	4.069E+01	1.773E+02	7.334E+00
	Std	3.805E+00	3.395E+00	2.109E+01	2.666E+01	3.152E+00	2.002E+01	1.057E+02	2.973E+01	2.228E+01	1.910E+01	2.110E+01	3.328E+01	2.012E+02	2.731E+00
	SEM	6.948E−01	6.199E−01	3.850E+00	4.868E+00	5.756E−01	3.655E+00	1.929E+01	5.428E+00	4.068E+00	3.488E+00	3.852E+00	6.075E+00	3.674E+01	4.986E−01
	Rank	2	1	8	7	6	4	13	9	11	14	5	10	12	3
*C*3	Mean	6.002E+02	6.027E+02	6.015E+02	6.001E+02	6.035E+02	6.007E+02	6.695E+02	6.319E+02	6.182E+02	6.349E+02	6.010E+02	6.146E+02	6.212E+02	6.000E+02
	ErrorM	1.932E−01	2.739E+00	1.478E+00	1.061E−01	3.482E+00	6.803E−01	6.953E+01	3.195E+01	1.821E+01	3.486E+01	1.005E+00	1.463E+01	2.122E+01	4.860E−02
	Std	5.331E−01	2.571E+00	1.879E+00	3.646E−01	1.005E+00	5.303E−01	1.466E+01	1.533E+01	3.921E+00	3.175E+00	1.378E+00	9.308E+00	8.296E+00	4.879E−02
	SEM	9.733E−02	4.694E−01	3.430E−01	6.656E−02	1.834E−01	9.683E−02	2.676E+00	2.799E+00	7.158E−01	5.796E−01	2.516E−01	1.699E+00	1.515E+00	8.907E−03
	Rank	3	7	6	2	8	4	14	12	10	13	5	9	11	1
*C*4	Mean	8.082E+02	8.211E+02	8.154E+02	8.131E+02	8.407E+02	8.350E+02	8.768E+02	8.357E+02	8.384E+02	8.446E+02	8.158E+02	8.223E+02	8.305E+02	8.126E+02
	ErrorM	8.159E+00	2.108E+01	1.545E+01	1.310E+01	4.073E+01	3.504E+01	7.682E+01	3.572E+01	3.837E+01	4.463E+01	1.581E+01	2.232E+01	3.054E+01	1.264E+01
	Std	3.204E+00	5.008E+00	4.952E+00	5.512E+00	4.853E+00	1.107E+01	1.515E+01	1.439E+01	5.954E+00	4.808E+00	5.415E+00	7.673E+00	1.092E+01	5.419E+00
	SEM	5.850E−01	9.144E−01	9.042E−01	1.006E+00	8.860E−01	2.022E+00	2.765E+00	2.628E+00	1.087E+00	8.778E−01	9.886E−01	1.401E+00	1.993E+00	9.894E−01
	Rank	1	6	4	3	12	9	14	10	11	13	5	7	8	2
*C*5	Mean	9.000E+02	9.590E+02	9.158E+02	9.003E+02	9.813E+02	9.043E+02	2.416E+03	1.322E+03	1.001E+03	1.374E+03	9.055E+02	1.057E+03	1.179E+03	9.002E+02
	ErrorM	3.880E−02	5.902E+01	1.577E+01	3.030E−01	8.126E+01	4.301E+00	1.516E+03	4.219E+02	1.015E+02	4.741E+02	5.519E+00	1.569E+02	2.788E+02	2.295E−01
	Std	5.088E−02	6.813E+01	3.382E+01	3.396E−01	3.049E+01	1.600E+01	7.418E+02	2.607E+02	4.612E+01	7.189E+01	8.756E+00	1.465E+02	1.957E+02	7.426E−01
	SEM	9.290E−03	1.244E+01	6.174E+00	6.201E−02	5.566E+00	2.922E+00	1.354E+02	4.759E+01	8.421E+00	1.312E+01	1.599E+00	2.674E+01	3.572E+01	1.356E−01
	Rank	1	7	6	3	8	4	14	12	9	13	5	10	11	2

Table 9 (continued)

Function	Metric	SOGWO	SO	GWO	PSO	ABC	EO	SSA	WOA	SCA	CDO	RBMO	SHIODEG	RFO	SSAKOA
*C*6	Mean	3.285E+03	2.848E+03	5.174E+03	5.066E+03	5.908E+04	1.073E+04	4.998E+03	4.283E+03	1.414E+06	9.211E+08	2.139E+03	4.758E+03	1.970E+03	3.432E+03
	ErrorM	1.485E+03	1.048E+03	3.374E+03	3.266E+03	5.728E+04	8.929E+03	3.198E+03	2.483E+03	1.412E+06	9.211E+08	3.386E+02	2.958E+03	1.695E+02	1.632E+03
	Std	1.846E+03	1.044E+03	2.443E+03	2.611E+03	4.785E+04	1.718E+04	1.903E+03	2.035E+03	1.484E+06	1.182E+09	8.194E+02	1.873E+03	2.526E+02	1.475E+03
	SEM	3.371E+02	1.905E+02	4.460E+02	4.767E+02	8.737E+03	3.137E+03	3.475E+02	3.716E+02	2.710E+05	2.158E+08	1.496E+02	3.419E+02	4.612E+01	2.693E+02
	Rank	4	3	10	9	12	11	8	6	13	14	2	7	1	5
*C*7	Mean	2.017E+03	2.037E+03	2.036E+03	2.015E+03	2.037E+03	2.030E+03	2.085E+03	2.068E+03	2.053E+03	2.141E+03	2.042E+03	2.060E+03	2.040E+03	2.019E+03
	ErrorM	1.672E+01	3.702E+01	3.577E+01	1.547E+01	3.663E+01	3.043E+01	8.496E+01	6.843E+01	5.338E+01	1.409E+02	4.150E+01	6.009E+01	4.037E+01	1.882E+01
	Std	9.790E+00	3.668E+01	1.783E+01	9.149E+00	4.203E+00	6.805E+00	2.390E+01	3.039E+01	7.854E+00	6.208E+00	3.667E+01	1.903E+01	1.928E+01	6.599E+00
	SEM	1.787E+00	6.697E+00	3.255E+00	1.670E+00	7.674E−01	1.242E+00	4.364E+00	5.548E+00	1.434E+00	1.133E+00	6.695E+00	3.474E+00	3.521E+00	1.205E+00
	Rank	2	7	5	1	6	4	13	12	10	14	9	11	8	3
*C*8	Mean	2.219E+03	2.220E+03	2.223E+03	2.236E+03	2.230E+03	2.237E+03	2.310E+03	2.234E+03	2.232E+03	2.233E+03	2.230E+03	2.230E+03	2.254E+03	2.221E+03
	ErrorM	1.926E+01	2.042E+01	2.347E+01	3.627E+01	3.015E+01	3.682E+01	1.102E+02	3.367E+01	3.177E+01	3.285E+01	2.991E+01	3.001E+01	5.368E+01	2.063E+01
	Std	2.463E+01	4.290E+00	5.535E+00	4.168E+01	2.526E+00	2.158E+01	6.414E+01	7.032E+00	3.217E+00	5.153E+00	2.270E+01	5.785E+00	5.392E+01	4.166E+00
	SEM	4.498E+00	7.833E−01	1.011E+00	7.610E+00	4.612E−01	3.940E+00	1.171E+01	1.284E+00	5.873E−01	9.408E−01	4.145E+00	1.056E+00	9.845E+00	7.606E−01
	Rank	1	2	4	11	7	12	14	10	8	9	5	6	13	3
*C*9	Mean	2.529E+03	2.529E+03	2.574E+03	2.556E+03	2.533E+03	2.529E+03	2.594E+03	2.565E+03	2.565E+03	2.658E+03	2.532E+03	2.580E+03	2.659E+03	2.529E+03
	ErrorM	2.293E+02	2.293E+02	2.742E+02	2.563E+02	2.331E+02	2.294E+02	2.938E+02	2.646E+02	2.648E+02	3.579E+02	2.319E+02	2.798E+02	3.587E+02	2.293E+02
	Std	9.250E−13	1.015E−01	3.253E+01	5.236E+01	1.206E+00	1.544E−01	6.818E+01	4.314E+01	1.728E+01	1.219E+00	7.121E+00	3.190E+01	6.265E+01	5.467E−05
	SEM	1.689E−13	1.853E−02	5.940E+00	9.559E+00	2.202E−01	2.818E−02	1.245E+01	7.877E+00	3.156E+00	2.225E−01	1.300E+00	5.824E+00	1.144E+01	9.981E−06
	Rank	2	2	10	7	6	4	12	8	9	13	5	11	14	2
*C*10	Mean	2.502E+03	2.611E+03	2.571E+03	2.597E+03	2.502E+03	2.605E+03	2.512E+03	2.617E+03	2.542E+03	2.830E+03	2.638E+03	2.515E+03	2.661E+03	2.500E+03
	ErrorM	1.020E+02	2.111E+02	1.709E+02	1.972E+02	1.021E+02	2.049E+02	1.118E+02	2.171E+02	1.424E+02	4.302E+02	2.377E+02	1.150E+02	2.606E+02	1.004E+02
	Std	1.404E+00	1.332E+02	6.139E+01	6.568E+01	1.235E+00	1.455E+02	4.618E+00	1.868E+02	5.630E+01	1.986E+02	2.548E+02	1.795E+01	1.729E+02	1.247E−01
	SEM	2.563E−01	2.432E+01	1.121E+01	1.199E+01	2.255E−01	2.656E+01	8.431E−01	3.410E+01	1.028E+01	3.625E+01	4.652E+01	3.277E+00	3.156E+01	2.277E−02
	Rank	2	10	7	8	3	9	4	11	6	14	12	5	13	1

Table 9 (continued)

Function	Metric	SOGWO	SO	GWO	PSO	ABC	EO	SSA	WOA	SCA	CDO	RBMO	SHIODEG	RFO	SSAKOA
$C11$	Mean	2.658E+03	2.665E+03	2.847E+03	2.830E+03	2.727E+03	2.764E+03	3.433E+03	2.851E+03	2.774E+03	3.325E+03	2.828E+03	2.882E+03	3.182E+03	2.630E+03
	ErrorM	5.840E+01	6.511E+01	2.471E+02	2.299E+02	1.272E+02	1.637E+02	8.333E+02	2.514E+02	1.742E+02	7.248E+02	2.277E+02	2.819E+02	5.819E+02	3.011E+01
	Std	1.100E+02	1.019E+02	1.801E+02	1.606E+02	1.880E+01	1.804E+02	3.556E+02	1.999E+02	9.548E+00	7.456E+01	1.782E+02	1.973E+02	3.726E+02	6.125E+01
	SEM	2.008E+01	1.861E+01	3.288E+01	2.933E+01	3.432E+00	3.294E+01	6.492E+01	3.650E+01	1.743E+00	1.361E+01	3.253E+01	3.601E+01	6.803E+01	1.118E+01
	Rank	2	3	9	8	4	5	14	10	6	13	7	11	12	1
$C12$	Mean	2.866E+03	2.871E+03	2.870E+03	2.879E+03	2.865E+03	2.864E+03	2.868E+03	2.884E+03	2.869E+03	3.071E+03	2.866E+03	2.869E+03	2.931E+03	2.862E+03
	ErrorM	1.663E+02	1.715E+02	1.698E+02	1.789E+02	1.655E+02	1.645E+02	1.678E+02	1.842E+02	1.693E+02	3.713E+02	1.661E+02	1.685E+02	2.314E+02	1.620E+02
	Std	5.863E+00	1.170E+01	1.101E+01	1.944E+01	7.671E−01	1.698E+00	2.622E+00	2.688E+01	1.302E+00	3.158E+01	2.757E+00	1.724E+00	3.198E+01	1.444E+00
	SEM	1.071E+00	2.136E+00	2.009E+00	3.550E+00	1.401E−01	3.099E−01	4.787E−01	4.907E+00	2.378E−01	5.766E+00	5.034E−01	3.147E−01	5.838E+00	2.635E−01
	Rank	5	10	9	11	3	2	6	12	8	14	4	7	13	1
$w/t/l$		~	9/1/2	12/0/0	10/0/2	11/0/1	11/0/1	12/0/0	12/0/0	12/0/0	12/0/0	10/0/2	12/0/0	11/0/1	6/2/4
Mean Rank		2.21	5.08	7.08	6.25	7.17	6.42	11.58	10.33	8.92	13.17	5.67	8.50	10.5	2.13
Overall Rank		2	3	7	5	8	6	13	11	10	14	4	9	12	1

performance of the SOGWO is similar to that of the top-ranked SSAKOA, and that it generally exhibits successful optimization capabilities.

The mean, ErrorM, Std, and SEM values that are produced by executing the results of 30 independent runs for $D = 20$ in the CEC-2022 test suite are listed in Table 10. The results summarized in Table 10 indicate that the SOGWO outperformed its competitors on the C1, C4, and C5 test functions, achieving the lowest Std and SEM values.

SOGWO, SO, and EO algorithms exhibited identical performance on the C9 test function. As a result of the tied-ranking procedure, each algorithm is assigned a rank value of 2 while jointly occupying the leading position. However, an overview of the standard deviation (Std) and standard error mean (SEM) values illustrates that the SOGWO tends to produce more stable results with less variation. This result confirms that the SOGWO not only produces high-quality solutions but also outperforms its competitors in terms of consistency. Even in test functions where the best results are not achieved, the proposed algorithm yielded results close to those of leading methods, thus demonstrating overall competitive and balanced performance. When the overall ranking results are examined, it is seen that the proposed algorithm ranks first by achieving the lowest average rank value. This demonstrates that the algorithm's potential is not limited to specific test functions, but rather that it consistently and fairly performs across the entire test suite. Consequently, it is emphasized that SOGWO strikes an effective balance between the exploration and exploitation processes and is able to maintain solution quality across various optimization problems.

3.3.3 Execution time analysis of SOGWO

The proposed SOGWO has a theoretical time complexity of $\mathcal{O}(T \times N \times D)$ as presented in Sect. 2.4. However, the theoretical complexity analysis alone does not directly reflect its actual execution time in practice. Therefore, this section analyzes the runtimes of SOGWO and its competitors to evaluate their computational efficiency in experiments. Regarding this, all competing algorithms are conducted under the same experimental conditions, using the same hardware and software configurations, the same population size, and termination criteria to ensure a fair comparison, and the average running times obtained from 30 independent runs for each function are reported in Tables 11, 12 and 13.

According to execution time analysis, it is observed that the runtime of the proposed SOGWO is relatively higher compared to the component algorithms. This result is expected due to the additional operations performed by the hybrid mechanism in each iteration. However, this increase in running time is limited, SOGWO exhibits comparable computational costs to many competing algorithms, and achieves lower running times than some algorithms. Consequently, SOGWO demonstrates competitive performance in terms of runtime, which reflects that it is an effective and balanced approach for complex problems across a wide range of practical domains, by providing high optimization performance with an acceptable computational cost.

Table 10 Comparison of optimization results of CEC-2022 test functions ($D = 20$)

Function	Metric	SOGWO	SO	GWO	PSO	ABC	EO	SSA	WOA	SCA	CDO	RBMO	SHIODEG	RFO	SSAKOA
*C*1	Mean	3.000E+02	3.000E+02	1.029E+04	5.808E+03	3.515E+04	1.540E+04	1.053E+05	3.420E+03	8.098E+03	2.303E+04	3.667E+03	1.777E+04	3.460E+04	2.151E+03
	ErrorM	0.000E+00	5.520E−04	9.994E+03	5.508E+03	3.485E+04	1.510E+04	1.050E+05	3.120E+03	7.798E+03	2.273E+04	3.367E+03	1.747E+04	3.430E+04	1.851E+03
	Std	0.000E+00	1.804E−03	3.328E+03	9.142E+03	4.581E+03	4.372E+03	1.445E+04	1.945E+03	1.752E+03	2.723E+02	3.455E+03	4.793E+03	1.108E+04	1.637E+03
	SEM	0.000E+00	3.293E−04	6.075E+02	1.669E+03	8.363E+02	7.982E+02	2.638E+03	3.551E+02	3.199E+02	4.972E+01	6.308E+02	8.752E+02	2.023E+03	2.989E+02
	Rank	1	2	8	6	13	9	14	4	7	11	5	10	12	3
*C*2	Mean	4.463E+02	4.423E+02	4.928E+02	4.801E+02	4.536E+02	4.589E+02	4.572E+03	4.860E+02	6.356E+02	1.981E+03	4.744E+02	6.433E+02	2.100E+03	4.549E+02
	ErrorM	4.628E+01	4.228E+01	9.277E+01	8.011E+01	5.362E+01	5.893E+01	4.172E+03	8.605E+01	2.356E+02	1.581E+03	7.437E+01	2.433E+02	1.700E+03	5.489E+01
	Std	1.892E+01	1.607E+01	3.493E+01	6.584E+01	2.119E+00	1.457E+01	1.534E+03	4.662E+01	5.196E+01	1.701E+01	3.283E+01	1.271E+02	1.226E+03	9.884E+00
	SEM	3.454E+00	2.935E+00	6.377E+00	1.202E+01	3.868E−01	2.660E+00	2.800E+02	8.512E+00	9.487E+00	3.106E+00	5.995E+00	2.321E+01	2.238E+02	1.805E+00
	Rank	2	1	9	7	3	5	14	8	10	12	6	11	13	4
*C*3	Mean	6.006E+02	6.097E+02	6.047E+02	6.018E+02	6.032E+02	6.003E+02	7.148E+02	6.654E+02	6.355E+02	6.536E+02	6.044E+02	6.376E+02	6.610E+02	6.015E+02
	ErrorM	5.815E−01	9.693E+00	4.656E+00	1.791E+00	3.197E+00	2.514E−01	1.148E+02	6.538E+01	3.552E+01	5.360E+01	4.393E+00	3.763E+01	6.097E+01	1.465E+00
	Std	6.710E−01	7.647E+00	3.783E+00	1.933E+00	7.848E−01	3.501E−01	1.108E+01	1.309E+01	5.475E+00	4.872E+00	3.638E+00	1.460E+01	1.126E+01	1.190E+00
	SEM	1.225E−01	1.396E+00	6.907E−01	3.530E−01	1.433E−01	6.392E−02	2.023E+00	2.389E+00	9.995E−01	8.895E−01	6.643E−01	2.665E+00	2.056E+00	2.173E−01
	Rank	2	8	7	4	5	1	14	13	9	11	6	10	12	3
*C*4	Mean	8.240E+02	8.593E+02	8.514E+02	8.352E+02	9.224E+02	8.778E+02	1.043E+03	9.273E+02	9.270E+02	9.320E+02	8.454E+02	8.808E+02	9.434E+02	8.407E+02
	ErrorM	2.399E+01	5.935E+01	5.140E+01	3.520E+01	1.224E+02	7.777E+01	2.426E+02	1.273E+02	1.270E+02	1.320E+02	4.542E+01	8.078E+01	1.434E+02	4.071E+01
	Std	9.373E+00	1.713E+01	1.863E+01	1.037E+01	9.824E+00	3.069E+01	2.799E+01	3.387E+01	1.035E+01	1.271E+01	1.353E+01	1.989E+01	2.200E+01	1.593E+01
	SEM	1.711E+00	3.128E+00	3.401E+00	1.893E+00	1.794E+00	5.603E+00	5.110E+00	6.184E+00	1.890E+00	2.321E+00	2.471E+00	3.631E+00	4.017E+00	2.908E+00
	Rank	1	6	5	2	9	7	14	11	10	12	4	8	13	3
*C*5	Mean	9.001E+02	1.227E+03	1.150E+03	9.452E+02	1.589E+03	9.961E+02	8.047E+03	3.177E+03	1.942E+03	2.975E+03	9.866E+02	2.513E+03	2.924E+03	9.257E+02
	ErrorM	1.015E−01	3.269E+02	2.502E+02	4.515E+01	6.890E+02	9.606E+01	7.147E+03	2.277E+03	1.042E+03	2.075E+03	8.662E+01	1.613E+03	2.024E+03	2.566E+01
	Std	1.071E−01	2.125E+02	1.992E+02	8.528E+01	1.296E+02	2.041E+02	1.410E+03	8.996E+02	3.985E+02	2.248E+02	8.526E+01	8.966E+02	6.157E+02	2.904E+01
	SEM	1.955E−02	3.880E+01	3.637E+01	1.557E+01	2.366E+01	3.726E+01	2.575E+02	1.642E+02	7.276E+01	4.103E+01	1.557E+01	1.637E+02	1.124E+02	5.303E+00
	Rank	1	7	6	3	8	5	14	13	9	12	4	10	11	2

Table 10 (continued)

Function	Metric	SOGWO	SO	GWO	PSO	ABC	EO	SSA	WOA	SCA	CDO	RBMO	SHIODEG	RFO	SSAKOA
*C*6	Mean	6.763E+03	8.506E+03	2.429E+06	1.496E+06	2.290E+06	4.315E+03	1.586E+08	1.489E+04	6.808E+07	4.921E+09	6.339E+03	1.645E+07	6.935E+08	7.847E+03
	ErrorM	4.963E+03	6.706E+03	2.428E+06	1.494E+06	2.289E+06	2.515E+03	1.586E+08	1.309E+04	6.808E+07	4.921E+09	4.539E+03	1.644E+07	6.935E+08	6.047E+03
	Std	5.319E+03	6.193E+03	7.777E+06	7.877E+06	9.263E+05	3.647E+03	2.168E+08	1.887E+04	3.827E+07	2.099E+09	6.469E+03	3.097E+07	1.006E+09	5.570E+03
	SEM	9.710E+02	1.131E+03	1.420E+06	1.438E+06	1.691E+05	6.658E+02	3.957E+07	3.446E+03	6.987E+06	3.833E+08	1.181E+03	5.654E+06	1.836E+08	1.017E+03
	Rank	3	5	9	7	8	1	12	6	11	14	2	10	13	4
*C*7	Mean	2.054E+03	2.089E+03	2.077E+03	2.062E+03	2.120E+03	2.072E+03	2.263E+03	2.183E+03	2.119E+03	2.304E+03	2.083E+03	2.153E+03	2.162E+03	2.052E+03
	ErrorM	5.428E+01	8.856E+01	7.737E+01	6.171E+01	1.199E+02	7.221E+01	2.630E+02	1.826E+02	1.185E+02	3.043E+02	8.287E+01	1.530E+02	1.619E+02	5.161E+01
	Std	1.577E+01	4.340E+01	2.544E+01	4.280E+01	1.585E+01	3.970E+01	4.535E+01	5.509E+01	1.888E+01	2.126E+01	3.422E+01	5.136E+01	6.752E+01	1.361E+01
	SEM	2.880E+00	7.924E+00	4.644E+00	7.814E+00	2.894E+00	7.248E+00	8.280E+00	1.006E+01	3.447E+00	3.881E+00	6.248E+00	9.376E+00	1.233E+01	2.485E+00
	Rank	2	7	5	3	9	4	13	12	8	14	6	10	11	1
*C*8	Mean	2.238E+03	2.235E+03	2.252E+03	2.273E+03	2.244E+03	2.242E+03	2.479E+03	2.270E+03	2.253E+03	2.242E+03	2.253E+03	2.292E+03	2.367E+03	2.227E+03
	ErrorM	3.761E+01	3.502E+01	5.205E+01	7.280E+01	4.413E+01	4.239E+01	2.794E+02	7.023E+01	5.321E+01	4.226E+01	5.305E+01	9.229E+01	1.673E+02	2.717E+01
	Std	4.122E+01	2.977E+01	4.830E+01	5.894E+01	3.279E+00	2.912E+01	1.099E+02	5.085E+01	7.248E+00	4.229E+00	4.568E+01	5.997E+01	1.409E+02	2.681E+00
	SEM	7.526E+00	5.435E+00	8.818E+00	1.076E+01	5.986E−01	5.317E+00	2.007E+01	9.284E+00	1.323E+00	7.721E−01	8.341E+00	1.095E+01	2.572E+01	4.895E−01
	Rank	3	2	7	11	6	5	14	10	9	4	8	12	13	1
*C*9	Mean	2.481E+03	2.481E+03	2.512E+03	2.543E+03	2.483E+03	2.481E+03	2.668E+03	2.497E+03	2.553E+03	3.443E+03	2.482E+03	2.598E+03	2.964E+03	2.481E+03
	ErrorM	1.808E+02	1.808E+02	2.123E+02	2.429E+02	1.829E+02	1.808E+02	3.685E+02	1.970E+02	2.531E+02	1.143E+03	1.817E+02	2.981E+02	6.636E+02	1.809E+02
	Std	3.051E−05	2.191E−04	1.977E+01	6.578E+01	6.063E−01	1.057E−02	3.320E+01	1.676E+01	2.027E+01	7.615E+01	2.090E+00	4.672E+01	3.504E+02	1.104E−01
	SEM	5.571E−06	4.000E−05	3.610E+00	1.201E+01	1.107E−01	1.930E−03	6.062E+00	3.061E+00	3.700E+00	1.390E+01	3.817E−01	8.529E+00	6.398E+01	2.015E−02
	Rank	2	2	8	9	6	2	12	7	10	14	5	11	13	4
*C*10	Mean	3.169E+03	3.650E+03	3.095E+03	3.177E+03	2.534E+03	3.122E+03	6.242E+03	4.245E+03	2.612E+03	5.829E+03	4.068E+03	3.601E+03	5.065E+03	2.606E+03
	ErrorM	7.688E+02	1.250E+03	6.952E+02	7.772E+02	1.345E+02	7.219E+02	3.842E+03	1.845E+03	2.117E+02	3.429E+03	1.668E+03	1.201E+03	2.665E+03	2.059E+02
	Std	5.517E+02	6.008E+02	5.918E+02	4.307E+02	1.454E+01	5.471E+02	2.837E+02	1.146E+03	5.130E+02	3.111E+02	7.127E+02	9.788E+02	1.367E+03	2.558E+02
	SEM	1.007E+02	1.097E+02	1.080E+02	7.863E+01	2.655E+00	9.989E+01	5.179E+01	2.092E+02	9.367E+01	5.681E+01	1.301E+02	1.787E+02	2.495E+02	4.670E+01
	Rank	6	9	4	7	1	5	14	11	3	13	10	8	12	2

Table 10 (continued)

Function	Metric	SOGWO	SO	GWO	PSO	ABC	EO	SSA	WOA	SCA	CDO	RBMO	SHIODEG	RFO	SSAKOA
$C11$	Mean	2.890E+03	2.884E+03	3.489E+03	3.525E+03	3.031E+03	2.921E+03	9.487E+03	3.037E+03	4.358E+03	8.458E+03	3.026E+03	4.626E+03	7.700E+03	2.909E+03
	ErrorM	2.902E+02	2.840E+02	8.890E+02	9.253E+02	4.312E+02	3.207E+02	6.887E+03	4.368E+02	1.758E+03	5.858E+03	4.256E+02	2.026E+03	5.100E+03	3.090E+02
	Std	8.401E+01	7.818E+01	3.378E+02	5.083E+02	2.127E+01	7.679E+01	8.731E+02	3.260E+02	4.055E+02	1.860E+01	1.410E+02	7.588E+02	1.078E+03	7.337E+01
	SEM	1.534E+01	1.427E+01	6.168E+01	9.280E+01	3.884E+00	1.402E+01	1.594E+02	5.952E+01	7.404E+01	3.396E+00	2.574E+01	1.385E+02	1.969E+02	1.339E+01
	Rank	2	1	8	9	6	4	14	7	10	13	5	11	12	3
$C12$	Mean	2.968E+03	3.011E+03	2.979E+03	3.032E+03	2.955E+03	2.960E+03	3.079E+03	3.014E+03	3.020E+03	3.484E+03	2.982E+03	3.026E+03	3.621E+03	2.948E+03
	ErrorM	2.677E+02	3.107E+02	2.788E+02	3.321E+02	2.551E+02	2.596E+02	3.795E+02	3.140E+02	3.198E+02	7.845E+02	2.821E+02	3.263E+02	9.208E+02	2.483E+02
	Std	1.317E+01	3.835E+01	2.678E+01	6.459E+01	3.644E+00	1.965E+01	4.350E+01	5.740E+01	2.018E+01	2.891E+01	3.426E+01	2.412E+01	2.743E+02	8.029E+00
	SEM	2.405E+00	7.002E+00	4.890E+00	1.179E+01	6.652E−01	3.587E+00	7.942E+00	1.048E+01	3.684E+00	5.279E+00	6.255E+00	4.403E+00	5.008E+01	1.466E+00
	Rank	4	7	5	11	2	3	12	8	9	13	6	10	14	1
$w/t/l$		~	8/1/3	11/0/1	12/0/0	10/0/2	7/1/4	12/0/0	12/0/0	11/0/1	12/0/0	11/0/1	12/0/0	12/0/0	8/0/4
Mean Rank		2.42	4.75	6.75	6.58	6.33	4.25	13.42	9.17	8.75	11.92	5.58	10.08	12.42	2.58
Overall Rank		1	4	8	7	6	3	14	10	9	12	5	11	13	2

Table 11 Computational times of SOGWO and its rivals across standard benchmark functions

Function	SOGWO	SO	GWO	PSO	ABC	EO	SSA	WOA	SCA	CDO	RBMO	SHIODEG	RFO	SSAKOA
*F*1	0.0396	0.0713	0.0209	0.7858	0.4699	0.0067	0.0971	0.0152	0.1312	0.0722	0.2395	0.9361	0.1921	0.2047
*F*2	0.0621	0.0825	0.0288	0.8327	0.4784	0.0091	0.1123	0.0207	0.1165	0.0813	0.3147	1.6478	0.2239	0.2050
*F*3	0.2050	0.1819	0.1211	1.0896	0.7032	0.0184	0.2850	0.2300	0.3256	0.2017	0.4497	5.9478	0.3919	0.3757
*F*4	0.1092	0.0837	0.0473	0.8383	0.4809	0.0076	0.0961	0.0547	0.1300	0.0904	0.2374	9.3038	0.1916	0.1912
*F*5	0.1813	0.1362	0.2052	0.8489	0.5037	0.0087	0.1235	0.0949	0.1527	0.2726	0.2516	9.8075	0.2179	0.2515
*F*6	0.2235	0.2064	0.2066	1.0015	0.5197	0.0107	0.1021	0.0554	0.1333	0.3111	0.2525	10.7233	0.1954	0.1992
*F*7	0.2836	0.2280	0.2935	0.9500	0.6223	0.0130	0.2241	0.1660	0.2433	0.3639	0.3648	10.7617	0.3170	0.3208
*F*8	0.2193	0.1674	0.2336	0.9620	0.5628	0.0100	0.1272	0.0834	0.1659	0.3089	0.2778	10.0604	0.2222	0.2351
*F*9	0.1792	0.1119	0.0440	0.8825	0.5307	0.0080	0.1319	0.0221	0.1504	0.2598	0.2651	10.0647	0.2165	0.2449
*F*10	0.0793	0.0959	0.0303	0.8722	0.5096	0.0078	0.1282	0.0272	0.1597	0.0905	0.2624	2.6572	0.2241	0.2384
*F*11	0.0832	0.1269	0.0443	0.8726	0.5130	0.0079	0.1319	0.0220	0.1562	0.1093	0.2641	5.6926	0.2269	0.2247
*F*12	0.5062	0.4566	0.5196	1.1341	0.9256	0.0246	0.4538	0.3904	0.4695	0.6017	0.5831	10.9483	0.5358	0.5433
*F*13	0.5113	0.4750	0.5431	1.2663	0.9636	0.0259	0.4171	0.3645	0.4867	0.6225	0.6157	10.4850	0.5705	0.5027
*F*14	0.0383	0.0364	0.0345	0.0924	0.0696	0.0033	0.0353	0.0346	0.0346	0.0358	0.0446	0.1075	0.0438	0.0426
*F*15	0.0137	0.0117	0.0106	0.1342	0.0685	0.0022	0.0105	0.0090	0.0093	0.0127	0.0298	0.1769	0.0262	0.0233
*F*16	0.0084	0.0070	0.0057	0.0683	0.0398	0.0016	0.0049	0.0047	0.0051	0.0062	0.0165	0.0524	0.0151	0.0127
*F*17	0.0077	0.0068	0.0052	0.0679	0.0387	0.0019	0.0050	0.0039	0.0045	0.0058	0.0164	0.0514	0.0142	0.0123
*F*18	0.0075	0.0056	0.0049	0.0558	0.0374	0.0020	0.0048	0.0038	0.0039	0.0058	0.0098	0.0534	0.0072	0.0106
*F*19	0.0151	0.0142	0.0131	0.1078	0.0595	0.0022	0.0122	0.0110	0.0113	0.0133	0.0269	0.1118	0.0243	0.0224
*F*20	0.0301	0.0258	0.0268	0.1912	0.1085	0.0031	0.0234	0.0200	0.0215	0.0289	0.0514	0.3982	0.0469	0.0410
*F*21	0.0244	0.0218	0.0208	0.1317	0.0787	0.0028	0.0207	0.0184	0.0186	0.0233	0.0396	0.1932	0.0367	0.0332
*F*22	0.0287	0.0263	0.0252	0.1359	0.0845	0.0034	0.0246	0.0223	0.0234	0.0270	0.0434	0.2034	0.0398	0.0372
*F*23	0.0352	0.0334	0.0317	0.1387	0.0896	0.0030	0.0309	0.0287	0.0290	0.0339	0.0506	0.2164	0.0460	0.0432

Table 12 Computational times of SOGWO and its rivals across CEC-2022 test functions ($D = 10$)

Function	SOGWO	SO	GWO	PSO	ABC	EO	SSA	WOA	SCA	CDO	RBMO	SHIODEG	RFO	SSAKOA
$C1$	0.1906	0.1241	0.2016	0.9633	0.8623	0.0153	0.1514	0.1115	0.1513	0.2489	0.0890	5.3028	0.3289	0.2622
$C2$	0.1793	0.1464	0.1757	1.3440	0.8382	0.0099	0.1477	0.1094	0.1484	0.2123	0.3379	5.3281	0.3144	0.2677
$C3$	0.2512	0.2133	0.2447	1.1391	0.9053	0.0126	0.2262	0.1772	0.2145	0.2867	0.4073	5.4614	0.3817	0.3518
$C4$	0.2002	0.1648	0.1999	1.3872	0.8517	0.0094	0.1691	0.1302	0.1681	0.2401	0.3948	5.3712	0.3366	0.2878
$C5$	0.2077	0.1738	0.2050	1.2139	0.8645	0.0104	0.1777	0.1377	0.1760	0.2468	0.2573	5.3983	0.3454	0.2829
$C6$	0.1861	0.1501	0.1829	1.3748	0.8633	0.0103	0.1526	0.1143	0.1550	0.2218	0.3754	5.3120	0.3215	0.2740
$C7$	0.2886	0.2495	0.2837	1.4799	0.9677	0.0151	0.2519	0.2129	0.2540	0.3197	0.4759	5.5217	0.4143	0.3733
$C8$	0.3169	0.2819	0.3159	1.5075	0.9985	0.0155	0.2840	0.2469	0.2866	0.3513	0.5099	5.5642	0.4479	0.4082
$C9$	0.2641	0.2279	0.2580	1.4442	0.9528	0.0132	0.2339	0.1944	0.2326	0.2983	0.4553	5.4860	0.3989	0.3558
$C10$	0.2524	0.2168	0.2481	1.4370	0.9454	0.0137	0.2229	0.1833	0.2224	0.2882	0.4436	5.4590	0.3902	0.3407
$C11$	0.3135	0.2740	0.3132	1.4374	1.0049	0.0152	0.2828	0.2427	0.2818	0.3488	0.3819	5.5667	0.4522	0.4028
$C12$	0.3232	0.2860	0.3162	1.5304	1.0294	0.0163	0.2928	0.2510	0.2910	0.3558	0.5125	5.5935	0.4484	0.4140

Table 13 Computational times of SOGWO and its rivals across CEC-2022 test functions ($D = 20$)

Function	SOGWO	SO	GWO	PSO	ABC	EO	SSA	WOA	SCA	CDO	RBMO	SHIODEG	RFO	SSAKOA
$C1$	1.0134	0.7200	1.0678	4.6585	3.5196	0.0408	0.7485	0.5098	0.8463	1.3856	0.2969	42.3254	1.3936	1.2900
$C2$	1.0361	0.7792	1.0679	5.5562	3.4262	0.0378	0.7445	0.5019	0.8408	1.3696	1.5320	42.2418	1.3799	1.2839
$C3$	1.6298	1.3563	1.6593	5.9301	4.0215	0.0671	1.2896	1.0499	1.4036	1.9225	2.1589	43.4592	1.9240	1.8494
$C4$	1.2012	0.9460	1.2206	5.6884	3.6400	0.0457	0.8981	0.6658	0.9971	1.5311	1.8096	42.6427	1.5500	1.4546
$C5$	1.2361	0.9590	1.2576	5.6785	3.6765	0.0475	0.9277	0.6852	1.0271	1.5878	1.8332	42.5633	1.5565	1.4471
$C6$	1.0809	0.8171	1.1104	5.5664	3.5816	0.0398	0.7778	0.5414	0.8864	1.4076	1.6769	42.2162	1.4153	1.3352
$C7$	1.8661	1.5897	1.8676	6.3740	4.4216	0.0788	1.5457	1.3165	1.6734	2.1675	2.4619	44.1028	2.1822	2.1195
$C8$	2.0749	1.8087	2.0826	6.5687	4.6482	0.0894	1.7830	1.5288	1.8924	2.4101	2.6969	44.3462	2.4250	2.3549
$C9$	1.8575	1.5966	1.8736	6.3107	4.3957	0.0775	1.5466	1.3103	1.6475	2.1878	2.4379	43.6686	2.1683	2.0940
$C10$	1.5916	1.3251	1.6124	6.0539	4.2044	0.0655	1.2864	1.0520	1.4023	1.9552	2.1841	43.2803	1.9170	1.8461
$C11$	2.1592	1.8935	2.1708	6.6726	4.6244	0.0927	1.8576	1.6146	1.9590	2.5041	2.6414	44.3748	2.4844	2.4295
$C12$	2.2951	2.0219	2.3108	6.7707	4.9680	0.0998	1.9906	1.7519	2.1108	2.6078	2.8650	44.6963	2.5859	2.5646

3.3.4 Comparison with the CEC winners

In the initial phase of the experimental studies, the proposed method is tested against the most well-known and up-to-date meta-heuristic algorithms on classic benchmarks and the CEC-2022 test functions to evaluate its performance.

Additionally, this section compares the proposed SOGWO with the top-ranked algorithms, such as EA4eig, NL-SHADE-LBC, NL-SHADE-RSP-MID, and S-LSHADE-DP, that demonstrated outstanding performance on the CEC-2022 competition to thoroughly examine its competitive strength. Experiments in this section are carried out for CEC-2022 test functions under $D = 10$ and $D = 20$ dimensional configurations with 30 independent runs for each algorithm. In contrast to the original CEC-2022 benchmark experiments, a lower and common maximum number of function evaluations is adopted, with 50,000 for $D = 10$ and 200,000 for $D = 20$ for all algorithms. This reduced evaluation budget is selected to provide a common and computationally manageable experimental setting across all competing methods. To ensure a fair comparison, the population size is set to 100 for both dimensionality cases for the proposed SOGWO and all CEC winner algorithms. The outcomes of the comparisons of SOGWO with CEC winner algorithms for $D = 10$ in terms of mean, ErrorM, Std, SEM are displayed in Table 14.

The findings reported in Table 14 suggest that SOGWO yielded superior results compared to the top-ranked algorithms on C1, C4, C5, C7, and C8 out of 12 test functions. It also exhibited competitive performance in the remaining functions, demonstrating low Std and SEM values. A thorough inspection of the mean and overall rank values in Table 14 confirms that the SOGWO is in first place with a mean rank of 1.83. These outcomes show that SOGWO can achieve high-quality solutions to optimization problems. Mean, ErrorM, Std, and SEM values that are produced by executing the results of 30 independent runs of SOGWO and CEC winner algorithms for $D = 20$ in the CEC-2022 test suite are given in Table 15.

The performance results reported in Table 15 indicate that the SOGWO ranked first among CEC winner algorithms, showcasing superior performance in 6 out of 12 test functions. SOGWO ranked second in four of the remaining test functions and third in two others, once again highlighting its competitive strength and ability to produce stable solutions. Even though it does not demonstrate superior performance in certain test functions, it maintains its leading position in the overall ranking with an average rank of 1.67 in the $D = 20$ dimension. These findings underscore that SOGWO possesses a balanced and consistent optimization capability across different types of problem, even when compared to CEC winner algorithms.

Figure 3 displays the rank analysis of SOGWO and winner algorithms on CEC-2022 test suite, stating ranks, total ranks (TR), and final ranks (FR) of the compared algorithms in each test function. The low total rank value in Fig. 3 emphasizes that the method has a robust optimization ability. In light of all this, it can be concluded that the proposed SOGWO has the lowest rank value for both dimensions and therefore exhibits superior performance compared to its peers.

As a result, it has been confirmed that the SOGWO exhibits effective performance in complex and challenging optimization problems not only against existing meta-heuristic algorithms but also against the most powerful optimization approaches.

Table 14 Results compared with top-rank algorithms of CEC-2022 test suite ($D = 10$)

Function	Metric	SOGWO	EA4eig	NL-SHADE-LBC	NL-SHADE-RSP-MID	S-LSHADE-DP
$C1$	Mean	3.000E+02	3.086E+02	3.001E+02	8.332E+03	1.364E+04
	ErrorM	0.000E+00	8.641E+00	7.906E−02	8.032E+03	1.334E+04
	Std	0.000E+00	2.538E+01	1.369E−01	2.386E+03	3.776E+03
	SEM	0.000E+00	4.633E+00	2.499E−02	4.356E+02	6.894E+02
	Rank	1	3	2	4	5
$C2$	Mean	4.060E+02	4.039E+02	4.073E+02	6.753E+02	4.100E+02
	ErrorM	6.011E+00	3.907E+00	7.311E+00	2.753E+02	1.003E+01
	Std	3.632E+00	8.867E+00	2.353E+00	1.125E+02	3.891E+00
	SEM	6.631E−01	1.619E+00	4.296E−01	2.054E+01	7.104E−01
	Rank	2	1	3	5	4
$C3$	Mean	6.000E+02	6.001E+02	6.001E+02	6.400E+02	6.000E+02
	ErrorM	5.290E−04	5.308E−02	6.005E−02	4.003E+01	0.000E+00
	Std	1.222E−03	1.191E−01	4.932E−02	6.783E+00	0.000E+00
	SEM	2.231E−04	2.174E−02	9.004E−03	1.238E+00	0.000E+00
	Rank	2	3	4	5	1
$C4$	Mean	8.031E+02	8.147E+02	8.102E+02	8.459E+02	8.333E+02
	ErrorM	3.118E+00	1.473E+01	1.019E+01	4.589E+01	3.329E+01
	Std	1.472E+00	6.186E+00	4.764E+00	5.878E+00	2.068E+01
	SEM	2.687E−01	1.129E+00	8.697E−01	1.073E+00	3.775E+00
	Rank	1	3	2	5	4
$C5$	Mean	9.000E+02	9.099E+02	9.001E+02	1.297E+03	1.631E+03
	ErrorM	3.583E−03	9.893E+00	1.074E−01	3.967E+02	7.309E+02
	Std	1.651E−02	2.195E+01	1.601E−01	1.309E+02	2.956E+02
	SEM	3.015E−03	4.008E+00	2.923E−02	2.390E+01	5.398E+01
	Rank	1	3	2	4	5
$C6$	Mean	2.703E+03	1.893E+03	1.844E+03	1.138E+07	1.813E+05
	ErrorM	9.026E+02	9.344E+01	4.425E+01	1.137E+07	1.795E+05
	Std	1.374E+03	1.761E+02	3.006E+01	9.167E+06	3.389E+05
	SEM	2.509E+02	3.216E+01	5.488E+00	1.674E+06	6.187E+04
	Rank	3	2	1	5	4
$C7$	Mean	2.007E+03	2.012E+03	2.023E+03	2.085E+03	2.035E+03
	ErrorM	6.956E+00	1.211E+01	2.316E+01	8.471E+01	3.510E+01
	Std	9.441E+00	9.416E+00	5.606E+00	1.422E+01	9.265E+00
	SEM	1.724E+00	1.719E+00	1.023E+00	2.596E+00	1.692E+00
	Rank	1	2	3	5	4
$C8$	Mean	2.215E+03	2.217E+03	2.221E+03	2.240E+03	2.222E+03
	ErrorM	1.534E+01	1.683E+01	2.118E+01	3.995E+01	2.211E+01
	Std	8.522E+00	8.414E+00	6.447E+00	7.450E+00	2.806E+00
	SEM	1.556E+00	1.536E+00	1.177E+00	1.360E+00	5.123E−01
	Rank	1	2	3	5	4

Table 14 (continued)

Function	Metric	SOGWO	EA4eig	NL-SHADE-LBC	NL-SHADE-RSP-MID	S-LSHADE-DP
$C9$	Mean	2.529E+03	2.493E+03	2.529E+03	2.689E+03	2.532E+03
	ErrorM	2.293E+02	1.931E+02	2.293E+02	3.890E+02	2.319E+02
	Std	9.250E−13	7.322E+00	9.250E−13	2.442E+01	2.856E+00
	SEM	1.689E−13	1.337E+00	1.689E−13	4.459E+00	5.215E−01
	Rank	2	1	3	5	4
$C10$	Mean	2.504E+03	2.566E+03	2.508E+03	2.544E+03	2.498E+03
	ErrorM	1.037E+02	1.661E+02	1.079E+02	1.444E+02	9.795E+01
	Std	1.959E+01	5.836E+01	2.860E+01	4.210E+01	1.310E+01
	SEM	3.576E+00	1.065E+01	5.222E+00	7.686E+00	2.391E+00
	Rank	2	5	3	4	1
$C11$	Mean	2.633E+03	2.742E+03	2.615E+03	3.035E+03	2.600E+03
	ErrorM	3.333E+01	1.416E+02	1.509E+01	4.352E+02	1.000E−05
	Std	1.028E+02	1.457E+02	4.588E+01	1.394E+02	5.477E−05
	SEM	1.877E+01	2.660E+01	8.377E+00	2.546E+01	1.000E−05
	Rank	3	4	2	5	1
$C12$	Mean	2.864E+03	2.849E+03	2.863E+03	2.944E+03	2.868E+03
	ErrorM	1.635E+02	1.495E+02	1.630E+02	2.437E+02	1.676E+02
	Std	1.023E+00	2.387E+00	1.250E+00	2.087E+01	1.851E+00
	SEM	1.869E−01	4.358E−01	2.282E−01	3.811E+00	3.380E−01
	Rank	3	1	2	5	4
$w/t/l$		~	8/0/4	8/1/3	12/0/0	9/0/3
Mean Rank		1.83	2.50	2.50	4.75	3.42
Overall Rank		1	2.5	2.5	5	4

3.3.5 Comparative evaluation against state-of-the-art GWO and SO variants

In recent years, numerous improved versions have been proposed to augment the performance of GWO and SO algorithms. To this end, a variety of enhancement strategies, such as adaptive strategies, chaotic maps, opposition-based learning strategy, dimension learning-based hunting mechanism, and hybridization with other metaheuristic algorithms, incorporated into these algorithms to achieve a better exploration–exploitation balance, preserve population diversity, and prevent premature convergence. Therefore, the proposed SOGWO is further evaluated against representative variants, including ESO [47], ISO [62], AGWO [31], GWSSA [39], NEGWO [63], PSOGWO [64], and IGWO [65]. The comparative experiments are performed on the CEC-2022 test functions with 10 and 20 dimensions, and the results are reported in Tables 16 and 17, respectively.

As per results in Table 16, SOGWO outperforms the variant algorithms of GWO and SO for C1, C4, C7, and C10. In addition, SOGWO shares the best results with

Table 15 Results compared with top-rank algorithms of CEC-2022 test suite ($D = 20$)

Function	Metric	SOGWO	EA4eig	NL-SHADE-LBC	NL-SHADE-RSP-MID	S-LSHADE-DP
$C1$	Mean	3.000E+02	1.249E+03	4.156E+02	2.913E+04	4.553E+04
	ErrorM	0.000E+00	9.491E+02	1.156E+02	2.883E+04	4.523E+04
	Std	0.000E+00	1.758E+03	1.293E+02	4.837E+03	7.966E+03
	SEM	0.000E+00	3.210E+02	2.360E+01	8.831E+02	1.454E+03
	Rank	1	3	2	4	5
$C2$	Mean	4.444E+02	4.334E+02	4.478E+02	1.338E+03	4.441E+02
	ErrorM	4.442E+01	3.336E+01	4.776E+01	9.383E+02	4.408E+01
	Std	1.377E+01	2.155E+01	9.079E+00	2.266E+02	1.269E+01
	SEM	2.514E+00	3.935E+00	1.658E+00	4.137E+01	2.317E+00
	Rank	3	1	4	5	2
$C3$	Mean	6.000E+02	6.013E+02	6.003E+02	6.694E+02	6.000E+02
	ErrorM	2.464E−02	1.312E+00	2.538E−01	6.945E+01	0.000E+00
	Std	1.681E−02	2.161E+00	3.203E−01	8.087E+00	0.000E+00
	SEM	3.068E−03	3.946E−01	5.847E−02	1.476E+00	0.000E+00
	Rank	2	4	3	5	1
$C4$	Mean	8.118E+02	8.432E+02	8.276E+02	9.561E+02	9.722E+02
	ErrorM	1.178E+01	4.318E+01	2.756E+01	1.561E+02	1.722E+02
	Std	4.135E+00	1.406E+01	9.375E+00	1.444E+01	3.010E+01
	SEM	7.549E−01	2.568E+00	1.712E+00	2.637E+00	5.495E+00
	Rank	1	3	2	4	5
$C5$	Mean	9.001E+02	1.236E+03	9.019E+02	2.940E+03	6.429E+03
	ErrorM	5.969E−02	3.358E+02	1.945E+00	2.040E+03	5.529E+03
	Std	6.367E−02	2.506E+02	2.506E+00	5.150E+02	1.470E+03
	SEM	1.162E−02	4.576E+01	4.575E−01	9.402E+01	2.683E+02
	Rank	1	3	2	4	5
$C6$	Mean	3.923E+03	4.854E+03	2.166E+03	5.458E+08	3.428E+06
	ErrorM	2.123E+03	3.054E+03	3.660E+02	5.458E+08	3.427E+06
	Std	3.531E+03	4.014E+03	9.406E+02	2.637E+08	2.959E+06
	SEM	6.447E+02	7.329E+02	1.717E+02	4.814E+07	5.402E+05
	Rank	2	3	1	5	4
$C7$	Mean	2.029E+03	2.042E+03	2.041E+03	2.174E+03	2.146E+03
	ErrorM	2.864E+01	4.220E+01	4.088E+01	1.738E+02	1.458E+02
	Std	9.143E+00	1.478E+01	1.084E+01	3.132E+01	3.160E+01
	SEM	1.669E+00	2.699E+00	1.979E+00	5.719E+00	5.769E+00
	Rank	1	3	2	5	4
$C8$	Mean	2.222E+03	2.252E+03	2.226E+03	2.298E+03	2.230E+03
	ErrorM	2.161E+01	5.241E+01	2.619E+01	9.772E+01	2.974E+01
	Std	3.198E+00	5.120E+01	2.328E+00	3.634E+01	3.714E+00
	SEM	5.839E−01	9.347E+00	4.250E−01	6.635E+00	6.781E−01
	Rank	1	4	2	5	3

Table 15 (continued)

Function	Metric	SOGWO	EA4eig	NL-SHADE-LBC	NL-SHADE-RSP-MID	S-LSHADE-DP
*C*9	Mean	2.481E+03	2.471E+03	2.481E+03	2.822E+03	2.481E+03
	ErrorM	1.808E+02	1.715E+02	1.808E+02	5.224E+02	1.812E+02
	Std	3.051E−05	3.001E+00	3.023E−04	7.643E+01	4.193E−01
	SEM	5.571E−06	5.479E−01	5.519E−05	1.395E+01	7.655E−02
	Rank	2	1	3	5	4
*C*10	Mean	2.470E+03	2.565E+03	2.669E+03	3.332E+03	2.491E+03
	ErrorM	6.993E+01	1.653E+02	2.694E+02	9.317E+02	9.063E+01
	Std	6.079E+01	1.192E+02	4.112E+02	9.250E+02	4.726E+01
	SEM	1.110E+01	2.176E+01	7.508E+01	1.689E+02	8.628E+00
	Rank	1	3	4	5	2
*C*11	Mean	2.904E+03	2.919E+03	2.908E+03	7.116E+03	2.720E+03
	ErrorM	3.040E+02	3.188E+02	3.076E+02	4.516E+03	1.200E+02
	Std	1.854E+01	1.064E+02	2.889E+01	4.045E+02	1.495E+02
	SEM	3.385E+00	1.943E+01	5.275E+00	7.386E+01	2.729E+01
	Rank	2	4	3	5	1
*C*12	Mean	2.947E+03	2.900E+03	2.942E+03	3.463E+03	2.960E+03
	ErrorM	2.465E+02	1.998E+02	2.423E+02	7.630E+02	2.605E+02
	Std	6.040E+00	8.063E−01	7.148E+00	9.229E+01	6.196E+00
	SEM	1.103E+00	1.472E−01	1.305E+00	1.685E+01	1.131E+00
	Rank	3	1	2	5	4
$w/t/l$		~	9/0/3	10/0/2	12/0/0	9/0/3
Mean Rank		1.67	2.75	2.50	4.75	3.33
Overall Rank		1	3	2	5	4

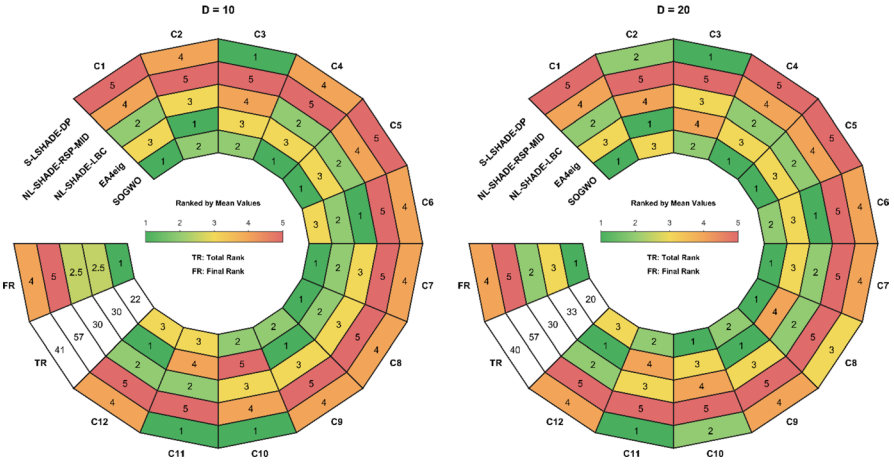


Fig. 3 Illustration of the rank analysis of SOGWO and winner algorithms on CEC-2022 test suite

Table 16 Comparison of optimization results of CEC-2022 test functions ($D = 10$)

Function	Metric	SOGWO	ESO	ISO	AGWO	GWSSA	NEGWO	PSOGWO	IGWO
*C*1	Mean	3.000E+02	3.188E+02	4.609E+02	4.912E+03	1.348E+03	3.000E+02	3.226E+03	3.000E+02
	ErrorM	0.000E+00	1.880E+01	1.609E+02	4.612E+03	1.048E+03	2.098E−02	2.926E+03	1.682E−02
	Std	0.000E+00	8.263E+01	2.768E+02	2.281E+03	1.367E+03	7.826E−02	6.281E+03	1.142E−02
	SEM	0.000E+00	1.509E+01	5.053E+01	4.164E+02	2.496E+02	1.429E−02	1.147E+03	2.084E−03
	Rank	1	4	5	8	6	3	7	2
*C*2	Mean	4.041E+02	4.075E+02	4.026E+02	4.713E+02	5.050E+02	4.179E+02	4.165E+02	4.039E+02
	ErrorM	4.106E+00	7.463E+00	2.631E+00	7.130E+01	1.050E+02	1.791E+01	1.651E+01	3.855E+00
	Std	3.805E+00	1.557E+01	4.073E+00	6.954E+01	9.621E+01	2.636E+01	1.634E+01	3.462E+00
	SEM	6.948E−01	2.842E+00	7.436E−01	1.270E+01	1.757E+01	4.812E+00	2.984E+00	6.320E−01
	Rank	3	4	1	7	8	6	5	2
*C*3	Mean	6.002E+02	6.021E+02	6.050E+02	6.228E+02	6.085E+02	6.011E+02	6.095E+02	6.000E+02
	ErrorM	1.932E−01	2.068E+00	4.981E+00	2.275E+01	8.540E+00	1.122E+00	9.498E+00	9.800E−04
	Std	5.331E−01	5.643E+00	4.909E+00	6.843E+00	4.868E+00	1.771E+00	1.440E+01	4.994E−04
	SEM	9.733E−02	1.030E+00	8.962E−01	1.249E+00	8.887E−01	3.233E−01	2.629E+00	9.117E−05
	Rank	2	4	5	8	6	3	7	1
*C*4	Mean	8.082E+02	8.155E+02	8.147E+02	8.316E+02	8.261E+02	8.206E+02	8.331E+02	8.093E+02
	ErrorM	8.159E+00	1.546E+01	1.474E+01	3.158E+01	2.608E+01	2.063E+01	3.308E+01	9.264E+00
	Std	3.204E+00	4.622E+00	5.180E+00	9.114E+00	5.243E+00	9.631E+00	2.539E+01	5.598E+00
	SEM	5.850E−01	8.439E−01	9.458E−01	1.664E+00	9.572E−01	1.758E+00	4.636E+00	1.022E+00
	Rank	1	4	3	7	6	5	8	2
*C*5	Mean	9.000E+02	9.223E+02	9.522E+02	1.064E+03	1.150E+03	9.051E+02	1.094E+03	9.000E+02
	ErrorM	3.880E−02	2.228E+01	5.216E+01	1.640E+02	2.496E+02	5.084E+00	1.939E+02	1.733E−05
	Std	5.088E−02	5.184E+01	4.965E+01	1.407E+02	1.477E+02	6.457E+00	3.905E+02	3.194E−05
	SEM	9.290E−03	9.465E+00	9.065E+00	2.568E+01	2.696E+01	1.179E+00	7.130E+01	5.832E−06
	Rank	2	4	5	6	8	3	7	1

Table 16 (continued)

Function	Metric	SOGWO	ESO	ISO	AGWO	GWSSA	NEGWO	PSOGWO	IGWO
*C*6	Mean	3.285E+03	3.730E+03	3.107E+03	2.973E+05	5.088E+03	5.320E+03	4.161E+05	4.129E+03
	ErrorM	1.485E+03	1.930E+03	1.307E+03	2.955E+05	3.288E+03	3.520E+03	4.143E+05	2.329E+03
	Std	1.846E+03	2.544E+03	1.910E+03	2.208E+05	2.055E+03	2.255E+03	8.191E+05	1.598E+03
	SEM	3.371E+02	4.644E+02	3.487E+02	4.031E+04	3.752E+02	4.118E+02	1.496E+05	2.917E+02
	Rank	2	3	1	7	5	6	8	4
*C*7	Mean	2.017E+03	2.028E+03	2.029E+03	2.068E+03	2.039E+03	2.032E+03	2.036E+03	2.019E+03
	ErrorM	1.672E+01	2.793E+01	2.871E+01	6.809E+01	3.887E+01	3.159E+01	3.626E+01	1.858E+01
	Std	9.790E+00	1.672E+01	1.075E+01	2.060E+01	2.044E+01	2.518E+01	1.767E+01	9.686E+00
	SEM	1.787E+00	3.053E+00	1.962E+00	3.762E+00	3.731E+00	4.597E+00	3.227E+00	1.768E+00
	Rank	1	3	4	8	7	5	6	2
*C*8	Mean	2.219E+03	2.222E+03	2.223E+03	2.230E+03	2.230E+03	2.231E+03	2.229E+03	2.219E+03
	ErrorM	1.926E+01	2.165E+01	2.278E+01	2.986E+01	3.015E+01	3.107E+01	2.870E+01	1.910E+01
	Std	2.463E+01	4.635E+00	4.503E+00	1.784E+00	9.291E+00	3.149E+01	5.953E+00	9.503E+00
	SEM	4.498E+00	8.461E−01	8.222E−01	3.257E−01	1.696E+00	5.749E+00	1.087E+00	1.735E+00
	Rank	2	3	4	6	7	8	5	1
*C*9	Mean	2.529E+03	2.529E+03	2.530E+03	2.597E+03	2.575E+03	2.529E+03	2.555E+03	2.529E+03
	ErrorM	2.293E+02	2.293E+02	2.295E+02	2.966E+02	2.749E+02	2.293E+02	2.548E+02	2.293E+02
	Std	9.250E−13	4.172E−02	5.209E−01	3.296E+01	5.536E+01	2.131E−02	6.337E+01	9.250E−13
	SEM	1.689E−13	7.616E−03	9.510E−02	6.018E+00	1.011E+01	3.890E−03	1.157E+01	1.689E−13
	Rank	2.5	2.5	5	8	7	2.5	6	2.5

Table 16 (continued)

Function	Metric	SOGWO	ESO	ISO	AGWO	GWSSA	NEGWO	PSOGWO	IGWO
*C*10	Mean	2.502E+03	2.552E+03	2.584E+03	2.593E+03	2.521E+03	2.647E+03	2.588E+03	2.551E+03
	ErrorM	1.020E+02	1.518E+02	1.843E+02	1.930E+02	1.213E+02	2.471E+02	1.880E+02	1.511E+02
	Std	1.404E+00	6.885E+01	6.138E+01	8.752E+01	3.710E+01	1.899E+02	2.195E+02	5.527E+01
	SEM	2.563E−01	1.257E+01	1.121E+01	1.598E+01	6.774E+00	3.466E+01	4.007E+01	1.009E+01
	Rank	1	4	5	7	2	8	6	3
*C*11	Mean	2.658E+03	2.677E+03	2.640E+03	2.931E+03	2.840E+03	2.832E+03	2.846E+03	2.660E+03
	ErrorM	5.840E+01	7.692E+01	4.009E+01	3.309E+02	2.396E+02	2.317E+02	2.456E+02	6.000E+01
	Std	1.100E+02	1.050E+02	1.037E+02	2.283E+02	1.232E+02	1.992E+02	2.549E+02	1.380E+02
	SEM	2.008E+01	1.918E+01	1.894E+01	4.169E+01	2.249E+01	3.636E+01	4.654E+01	2.519E+01
	Rank	2	4	1	8	6	5	7	3
*C*12	Mean	2.866E+03	2.865E+03	2.869E+03	2.889E+03	2.892E+03	2.869E+03	2.862E+03	2.862E+03
	ErrorM	1.663E+02	1.652E+02	1.693E+02	1.886E+02	1.924E+02	1.689E+02	1.622E+02	1.617E+02
	Std	5.863E+00	2.319E+00	3.487E+00	1.582E+01	2.190E+01	1.007E+01	1.638E+00	1.911E+00
	SEM	1.071E+00	4.234E−01	6.367E−01	2.889E+00	3.998E+00	1.839E+00	2.990E−01	3.488E−01
	Rank	4	3	6	7	8	5	2	1
w/*t*/*l*		~	11/1/0	9/0/3	12/0/0	12/0/0	11/1/0	11/0/1	6/1/5
Mean Rank		1.96	3.54	3.75	7.25	6.33	4.96	6.17	2.04
Overall Rank		1	3	4	8	7	5	6	2

Table 17 Comparison of optimization results of CEC-2022 test functions ($D = 20$)

Function	Metric	SOGWO	ESO	ISO	AGWO	GWSSA	NEGWO	PSOGWO	IGWO
$C1$	Mean	3.000E+02	3.715E+02	2.667E+03	1.776E+04	5.680E+03	3.018E+02	1.306E+04	3.059E+02
	ErrorM	0.000E+00	7.154E+01	2.367E+03	1.746E+04	5.380E+03	1.810E+00	1.276E+04	5.866E+00
	Std	0.000E+00	1.164E+02	2.118E+03	5.361E+03	5.849E+03	5.383E+00	1.687E+04	7.799E+00
	SEM	0.000E+00	2.125E+01	3.866E+02	9.788E+02	1.068E+03	9.827E−01	3.080E+03	1.424E+00
	Rank	1	4	5	8	6	2	7	3
$C2$	Mean	4.463E+02	4.518E+02	4.555E+02	6.772E+02	5.198E+02	4.549E+02	5.567E+02	4.480E+02
	ErrorM	4.628E+01	5.184E+01	5.546E+01	2.772E+02	1.198E+02	5.491E+01	1.567E+02	4.799E+01
	Std	1.892E+01	1.010E+01	1.497E+01	8.455E+01	7.921E+01	1.664E+01	2.303E+02	1.275E+01
	SEM	3.454E+00	1.844E+00	2.733E+00	1.544E+01	1.446E+01	3.038E+00	4.205E+01	2.328E+00
	Rank	1	3	5	8	6	4	7	2
$C3$	Mean	6.006E+02	6.145E+02	6.191E+02	6.491E+02	6.155E+02	6.081E+02	6.181E+02	6.000E+02
	ErrorM	5.815E−01	1.453E+01	1.907E+01	4.913E+01	1.547E+01	8.073E+00	1.809E+01	0.000E+00
	Std	6.710E−01	1.224E+01	7.955E+00	9.442E+00	9.891E+00	4.876E+00	2.400E+01	0.000E+00
	SEM	1.225E−01	2.236E+00	1.452E+00	1.724E+00	1.806E+00	8.903E−01	4.382E+00	0.000E+00
	Rank	2	4	7	8	5	3	6	1
$C4$	Mean	8.240E+02	8.557E+02	8.523E+02	9.019E+02	8.844E+02	8.516E+02	8.971E+02	8.255E+02
	ErrorM	2.399E+01	5.568E+01	5.230E+01	1.019E+02	8.440E+01	5.163E+01	9.706E+01	2.548E+01
	Std	9.373E+00	9.912E+00	1.264E+01	1.455E+01	1.445E+01	1.637E+01	7.109E+01	1.763E+01
	SEM	1.711E+00	1.810E+00	2.308E+00	2.657E+00	2.638E+00	2.989E+00	1.298E+01	3.218E+00
	Rank	1	5	4	8	6	3	7	2
$C5$	Mean	9.001E+02	1.509E+03	1.772E+03	2.445E+03	2.194E+03	1.027E+03	2.516E+03	9.000E+02
	ErrorM	1.015E−01	6.088E+02	8.723E+02	1.545E+03	1.294E+03	1.266E+02	1.616E+03	1.333E−06
	Std	1.071E−01	4.326E+02	3.876E+02	4.476E+02	3.509E+02	1.123E+02	2.899E+03	7.303E−06
	SEM	1.955E−02	7.899E+01	7.077E+01	8.173E+01	6.407E+01	2.050E+01	5.293E+02	1.333E−06
	Rank	2	4	5	7	6	3	8	1

Table 17 (continued)

Function	Metric	SOGWO	ESO	ISO	AGWO	GWSSA	NEGWO	PSOGWO	IGWO
*C*6	Mean	6.763E+03	6.169E+04	3.737E+03	1.317E+07	3.402E+06	1.203E+04	3.143E+07	6.127E+03
	ErrorM	4.963E+03	5.989E+04	1.937E+03	1.317E+07	3.400E+06	1.023E+04	3.143E+07	4.327E+03
	Std	5.319E+03	7.198E+04	1.742E+03	1.126E+07	1.220E+07	9.473E+03	1.053E+08	4.983E+03
	SEM	9.710E+02	1.314E+04	3.181E+02	2.057E+06	2.228E+06	1.730E+03	1.923E+07	9.098E+02
	Rank	3	5	1	7	6	4	8	2
*C*7	Mean	2.054E+03	2.086E+03	2.071E+03	2.162E+03	2.106E+03	2.122E+03	2.071E+03	2.029E+03
	ErrorM	5.428E+01	8.612E+01	7.117E+01	1.620E+02	1.061E+02	1.223E+02	7.095E+01	2.886E+01
	Std	1.577E+01	2.884E+01	2.518E+01	6.475E+01	5.264E+01	6.441E+01	4.817E+01	9.778E+00
	SEM	2.880E+00	5.265E+00	4.596E+00	1.182E+01	9.611E+00	1.176E+01	8.795E+00	1.785E+00
	Rank	2	5	4	8	6	7	3	1
*C*8	Mean	2.238E+03	2.232E+03	2.234E+03	2.259E+03	2.289E+03	2.281E+03	2.256E+03	2.228E+03
	ErrorM	3.761E+01	3.160E+01	3.374E+01	5.882E+01	8.939E+01	8.127E+01	5.636E+01	2.842E+01
	Std	4.122E+01	2.197E+01	2.379E+01	4.129E+01	7.367E+01	6.227E+01	5.645E+01	3.746E+00
	SEM	7.526E+00	4.011E+00	4.344E+00	7.538E+00	1.345E+01	1.137E+01	1.031E+01	6.838E−01
	Rank	4	2	3	6	8	7	5	1
*C*9	Mean	2.481E+03	2.481E+03	2.481E+03	2.563E+03	2.655E+03	2.482E+03	2.497E+03	2.481E+03
	ErrorM	1.808E+02	1.809E+02	1.808E+02	2.628E+02	3.554E+02	1.823E+02	1.966E+02	1.808E+02
	Std	3.051E−05	2.442E−01	5.171E−04	2.639E+01	1.273E+02	4.447E+00	2.952E+01	9.250E−13
	SEM	5.571E−06	4.458E−02	9.441E−05	4.817E+00	2.324E+01	8.119E−01	5.390E+00	1.689E−13
	Rank	2	4	2	7	8	5	6	2

Table 17 (continued)

Function	Metric	SOGWO	ESO	ISO	AGWO	GWSSA	NEGWO	PSOGWO	IGWO
*C*10	Mean	3.169E+03	3.212E+03	3.094E+03	4.737E+03	2.602E+03	3.853E+03	3.991E+03	2.552E+03
	ErrorM	7.688E+02	8.117E+02	6.942E+02	2.337E+03	2.021E+02	1.453E+03	1.591E+03	1.524E+02
	Std	5.517E+02	3.620E+02	4.751E+02	1.159E+03	1.513E+02	7.169E+02	1.235E+03	1.312E+02
	SEM	1.007E+02	6.610E+01	8.674E+01	2.115E+02	2.762E+01	1.309E+02	2.255E+02	2.396E+01
	Rank	4	5	3	8	2	6	7	1
*C*11	Mean	2.890E+03	2.926E+03	2.906E+03	4.457E+03	3.721E+03	2.948E+03	3.837E+03	2.920E+03
	ErrorM	2.902E+02	3.263E+02	3.059E+02	1.857E+03	1.121E+03	3.485E+02	1.237E+03	3.200E+02
	Std	8.401E+01	8.571E+01	9.186E+01	5.089E+02	5.184E+02	1.178E+02	1.284E+03	4.068E+01
	SEM	1.534E+01	1.565E+01	1.677E+01	9.292E+01	9.464E+01	2.152E+01	2.345E+02	7.428E+00
	Rank	1	4	2	8	6	5	7	3
*C*12	Mean	2.968E+03	2.972E+03	3.003E+03	3.094E+03	3.095E+03	2.978E+03	2.945E+03	2.939E+03
	ErrorM	2.677E+02	2.721E+02	3.031E+02	3.939E+02	3.948E+02	2.777E+02	2.447E+02	2.389E+02
	Std	1.317E+01	2.229E+01	2.913E+01	9.895E+01	9.528E+01	3.240E+01	4.463E+00	4.207E+00
	SEM	2.405E+00	4.069E+00	5.319E+00	1.807E+01	1.740E+01	5.915E+00	8.149E−01	7.681E−01
	Rank	3	4	6	7	8	5	2	1
$w/t/l$		~	11/0/1	8/1/3	12/0/0	11/0/1	12/0/0	11/0/1	4/1/7
Mean Rank		2.17	4.08	3.92	7.50	6.08	4.50	6.08	1.67
Overall Rank		2	4	3	8	6.5	5	6.5	1

ESO, NEGWO, and IGWO on C9. On the remaining benchmark functions, SOGWO consistently achieves competitive results, highlighting low Std and SEM values. According to the overall ranking results, the proposed algorithm displays the best performance for CEC-2022 ($D = 10$) with the average rank of 1.96 and securing the top position among all variant algorithms.

The results depicted in Table 17 reveal that SOGWO has superior performance on C1, C2, C4, and C11. As in the 10-dimensional experiments, SOGWO yields the same optimal results with ISO and IGWO on C9 function and delivers remarkable performance across the rest of the test suite. Overall ranking results indicate that SOGWO performs second best with a rank value of 2.17, following IGWO for $D = 20$.

Collectively, the findings from the variant comparisons highlight that SOGWO exhibits outstanding and highly competitive performance across different problem dimensions. SOGWO reaches the highest position among the variants with an average ranking value of 1.96 in dimension $D = 10$, and displays a performance that is very akin to the leader with an average ranking value of 2.47 in dimension $D = 20$. Furthermore, the best and shared-best results achieved across different test functions indicate that the proposed hybrid structure can largely maintain solution quality despite increasing problem dimensions.

3.3.6 Overall effectiveness of SOGWO

The capability of the SOGWO in solving global optimization problems is compared with that of cutting-edge algorithms and CEC winners across various performance criteria and dimensions, using standard benchmark functions and CEC-2022 test functions. In addition to these comparisons, this section evaluates the overall effectiveness (OE) of the algorithms in terms of the general quality of the solution and the total performance deviation of the SOGWO method. The overall effectiveness values are calculated for each test function using the fitness values obtained by the methods and the best-known fitness, as shown in Eq. (33).

$$OE = \frac{\sum_{i=1}^{NF} \left| F_i^* - F_i \right|}{NF} \tag{33}$$

where NF refers to the number of test functions, F_i^* and F_i correspond to the best-known fitness for the ith test function and the fitness value achieved by the algorithms, respectively. Table 18 reports the OE values for all test functions of SOGWO and its rivals.

A thorough review of Table 18 indicates that the SOGWO has the smallest OE values for the classic benchmark and CEC-2022 ($D = 20$), while the RBMO algorithm has the lowest OE value for CEC-2022 ($D = 10$). However, when the average OE values are considered, it can clearly be seen that the proposed SOGWO has the lowest OE value and is in leading position based on the average OE value ranking. In contrast, the RBMO algorithm, which performed best on CEC-2022 ($D = 10$), was ranked fourth. It was observed that SOGWO demonstrated remarkable performance compared to the algorithms under consideration,

Table 18 Overall effectiveness comparison for SOGWO and competing algorithms

Test Suite	SOGWO	SO	GWO	PSO	ABC	EO	SSA	WOA	SCA	CDO	RBMO	SHIODEG	RFO	SSAKOA
Standard	1.09E+00	1.16E+00	2.87E+02	2.94E+02	7.14E+05	3.62E+02	2.02E+06	9.68E+02	6.07E+02	3.77E+02	1.82E+02	3.06E+02	6.22E+05	1.71E+02
CEC22 (D=10)	1.77E+02	1.56E+02	5.30E+02	3.83E+02	5.53E+03	1.24E+03	2.02E+03	1.58E+03	1.18E+05	7.68E+07	1.14E+02	6.52E+02	8.11E+02	1.84E+02
CEC22 (D=20)	4.81E+02	7.74E+02	2.03E+05	1.25E+05	1.94E+05	1.62E+03	1.32E+07	1.82E+03	5.67E+06	4.10E+08	9.01E+02	1.37E+06	5.78E+07	7.54E+02
Average	2.20E+02	3.10E+02	6.81E+04	4.20E+04	3.05E+05	1.07E+03	5.08E+06	1.46E+03	1.93E+06	1.62E+08	3.99E+02	4.58E+05	1.95E+07	3.70E+02
Improvement (%)	~	29.0323	99.6769	99.4762	99.9279	79.4393	99.9957	84.9315	99.9886	99.9999	44.8622	99.9520	99.9989	40.5405
Rank	1	2	8	7	9	5	12	6	11	14	4	10	13	3

achieving improvement rates ranging from 29.0323% to 99.9999% relative to all other algorithms. Furthermore, it has been discovered that the hybrid SOGWO achieves performance gains of 29.0323% and 99.6769% compared to the component algorithms SO and GWO, respectively. These key insights highlight that the performance improvement achieved is not solely due to increased computational complexity, but also that SOGWO effectively leverages the advantages of component methods, addresses their shortcomings, and efficiently integrates the search behaviors of the methods.

3.3.7 Combined compromise solution calculation for performance evaluation

In this section, the supremacy of the proposed SOGWO is demonstrated in a multidimensional way, using a combined compromise solution calculation (CoCoSo) technique based multi-criteria decision-making approach rather than traditional evaluations based on singular performance metrics. Instead of focusing on a single performance metric, this approach aims to achieve a balanced and optimal solution by allowing for the evaluation of different performance indicators together. CoCoSo method provides a holistic framework for making decisions when comparing algorithms, by converting all performance metrics into a single score [37]. This method merges two evaluation approaches: the Weighted Sum Method (WSM) and the Weighted Product Method (WPM) [66]. The implementation procedures of the CoCoSo method are outlined below.

Generating an initial decision-making matrix: In this stage, the most fundamental step of the multi-criteria decision-making process involves creating a decision matrix that forms the data infrastructure of the method, using the algorithms and performance criteria to be compared. The decision matrix (Z) is structured as:

$$Z = \begin{bmatrix} z_{11} & z_{12} & \cdots & z_{1n} \\ z_{21} & z_{22} & & z_{2n} \\ \vdots & & \ddots & \vdots \\ z_{m1} & z_{m2} & \cdots & z_{mn} \end{bmatrix}$$

where z_{ij} is performance score of the ith algorithm with respect to criterion j, m is the number of algorithms and n is the number of criteria.

Standardization of the decision matrix: At this point, linear normalizing transformations are used to address inconsistencies caused by criteria with different scales and units in the decision matrix and make them comparable. Normalization is performed in two different ways, based on both benefit and cost criteria, using the following expressions.

For beneficial criterion:

$$r_{ij} = \frac{z_{ij} - \min\left(z_{ij}\right)}{\max\left(z_{ij}\right) - \min\left(z_{ij}\right)} \tag{34}$$

For cost criterion:

$$r_{ij} = \frac{\max\left(z_{ij}\right) - z_{ij}}{\max\left(z_{ij}\right) - \min\left(z_{ij}\right)} \tag{35}$$

where r_{ij} signifies the normalized $\ddagger_{ij}$ decision matrix values.

Computation of performance indexes: Utilizing the WSM, the S_i index reflecting the weighted sum performance of each algorithm is calculated, while the P_i index representing the weighted product performance is obtained using the WPM, as given in Eqs. (36) and (37), respectively.

$$S_i = \sum_{j=1}^{n} w_j \cdot r_{ij} \tag{36}$$

$$P_i = \prod_{j=1}^{n} \left(r_{ij}\right)^{w_j} \tag{37}$$

where w_j represents the importances of the criteria and is referred to as relative weights.

Calculation of appraisal scores: At this phase, three different appraisal scores are calculated based on the S and P values derived from each algorithm. These scores illustrate the algorithms' general performance capabilities. These appraisal scores are computed as following equations:

$$K_{ia} = \frac{P_i + S_i}{\sum\left(P_i + S_i\right)} \tag{38}$$

$$K_{ib} = \frac{S_i}{\min S_i} + \frac{P_i}{\min P_i} \tag{39}$$

$$K_{ic} = \frac{\lambda S_i + (1-\lambda) P_i}{\lambda \max S_i + (1-\lambda) \max P_i} \tag{40}$$

where λ ranges from 0 to 1 and is typically set to 0.5.

Determination of the final ranking: The final rankings of the comparative algorithms are assessed based on aggregation of the appraisal scores, depicted in Eq. (45).

$$K_i = \left(K_{ia} \cdot K_{ib} \cdot K_{ic}\right)^{1/3} + \frac{1}{3}\left(K_{ia} + K_{ib} + K_{ic}\right) \tag{41}$$

The algorithm with the highest K_i value is considered the best algorithm. The results of the CoCoSo method are displayed in Table 19.

The results obtained using the CoCoSo method have once again demonstrated that the SOGWO is more successful than other algorithms with which it was

Table 19 CoCoSo method results and ranking of comparative algorithms

Algorithm	S_i	P_i	K_{ia}	K_{ib}	K_{ic}	K_i	Rank
SOGWO	0.9885	22.9881	0.0762	4.0020	1.0000	2.3657	1
SO	0.9584	22.9511	0.0760	3.9221	0.9972	2.3323	2
GWO	0.8885	22.8262	0.0753	3.7336	0.9891	2.2521	6
PSO	0.8977	22.8756	0.0755	3.7607	0.9915	2.2647	5
ABC	0.7609	22.0480	0.0725	3.3552	0.9513	2.0734	9
EO	0.5916	19.3076	0.0632	2.7453	0.8299	1.7370	13
SSA	0.3874	15.8513	0.0516	2.0000	0.6773	1.3215	14
WOA	0.7998	22.1583	0.0729	3.4625	0.9575	2.1206	8
SCA	0.7079	20.5670	0.0676	3.1251	0.8873	1.9322	11
CDO	0.7308	21.3839	0.0702	3.2355	0.9223	2.0034	10
RBMO	0.9087	22.8928	0.0756	3.7900	0.9927	2.2771	4
SHIODEG	0.8272	22.7334	0.0748	3.5697	0.9827	2.1827	7
RFO	0.5985	22.3511	0.0729	2.9552	0.9572	1.9192	12
SSAKOA	0.9194	22.9060	0.0757	3.8186	0.9937	2.2891	3

compared in terms of performance. SOGWO achieves an S_i value of 0.9885, which proves the outstanding performance of the SOGWO in terms of weighted total performance against other algorithms. Similarly, the P_i value associated with SOGWO is also higher than that of its competitors, indicating that the method performs consistently and reliably across the criteria. SOGWO leads its competitors with a combined appraisal score of 2.3657, highlighting the effectiveness of the proposed method across all evaluated criteria. Since the CoCoSo method considers both weighted sum and weighted multiplication performance when evaluating alternatives, it can be concluded that the SOGWO method is a more reliable and balanced method, taking into account not only average success rates but also the performance balances between the criteria. These analysis results confirm that SOGWO also performs exceptionally well in multi-criteria decision-making processes, demonstrating that the method is a powerful and preferable option for solving complex optimization problems.

3.4 Qualitative analysis

In this section, qualitative analyses are conducted to further reveal the behavior of the SOGWO during the optimization process. These analyses focus on the algorithm's search mechanism in the solution space and its convergence characteristics in reaching the optimum solution. In this context, the behavioral characteristics of the algorithm are evaluated by analyzing the search dynamics and convergence curves. Furthermore, how population diversity is maintained over iterations and how the exploration–exploitation balance evolves during the search process are examined through population diversity and exploration–exploitation behavior analyses, respectively. In addition to all these analyses, this section includes a leader trajectory analysis which examines how the SOGWO algorithm's leadership mechanism guides the

search process. These analyses provide insight into SOGWO's dynamic behavior, not only in terms of solution quality but also in terms of exploring the search space, concentrating on promising regions, and guiding the population.

3.4.1 Search dynamics

This section offers a comprehensive overview of the proposed SOGWO during the optimization procedure, highlighting its ability to navigate complex search landscapes by balancing exploration and exploitation to attain the optimal solution. To characterize the search dynamics of SOGWO, a variety of indicators are analyzed, including search history, trajectory in two dimensions, average fitness, and convergence curves. Figure 4 illustrates the search dynamics of the SOGWO on some benchmark test functions.

The first column provides the 2D visualization of the test functions to emphasize the structural topology of the search space. The second column displays the location history of the search agents, which provides an observation of their progress during the optimization process, where the red dots indicate the best solution achieved by SOGWO. By inspecting Fig. 4, it highlights that SOGWO has a strong ability to reach the optimal solutions by broadly exploring the entire solution space and identifying promising areas.

The third and fourth columns represent the dynamic changes in the trajectories of the first and second dimensions throughout the iterations, respectively. The trajectory analysis reveals that SOGWO focuses on exploration in the initial stages and on exploitation in later stages. Hence, it achieves robust convergence by both shifting from global to local search in a controlled manner and managing exploration and exploitation mechanisms in a balanced way.

The fifth column yields fluctuations and tendencies in fitness values during the optimization process. As illustrated in Fig. 4, the population initially consists of low-quality solutions but evolves over time to produce more stable and high-quality solutions. This demonstrates that SOGWO effectively searches the solution space, thereby enhancing the overall solution quality of the entire population. Consequently, SOGWO gradually reaches a global optimum while preventing premature convergence, exhibiting a smooth transition from exploration to exploitation.

The last column depicts the convergence curve of the best fitness, reflecting changes and improvements in solution quality over the course of the iterations. From Fig. 4, it is evident that the SOGWO exhibits rapid improvement in the early iterations, signifies strong global search capability and fast identification of promising regions. As iterations progress, the curve gradually stabilizes, highlighting a tendency to converge toward an optimal or near-optimal solution. This confirms that SOGWO properly balances exploration and exploitation, enabling a robust optimization process in the solution space.

Overall, a visual analysis of the search dynamics of SOGWO reveals that it effectively guides the search toward promising solutions and avoids local optima. Additionally, it initially emphasizes global search to explore diverse regions of the solution space, while subsequently focusing on local search to improve solution quality.

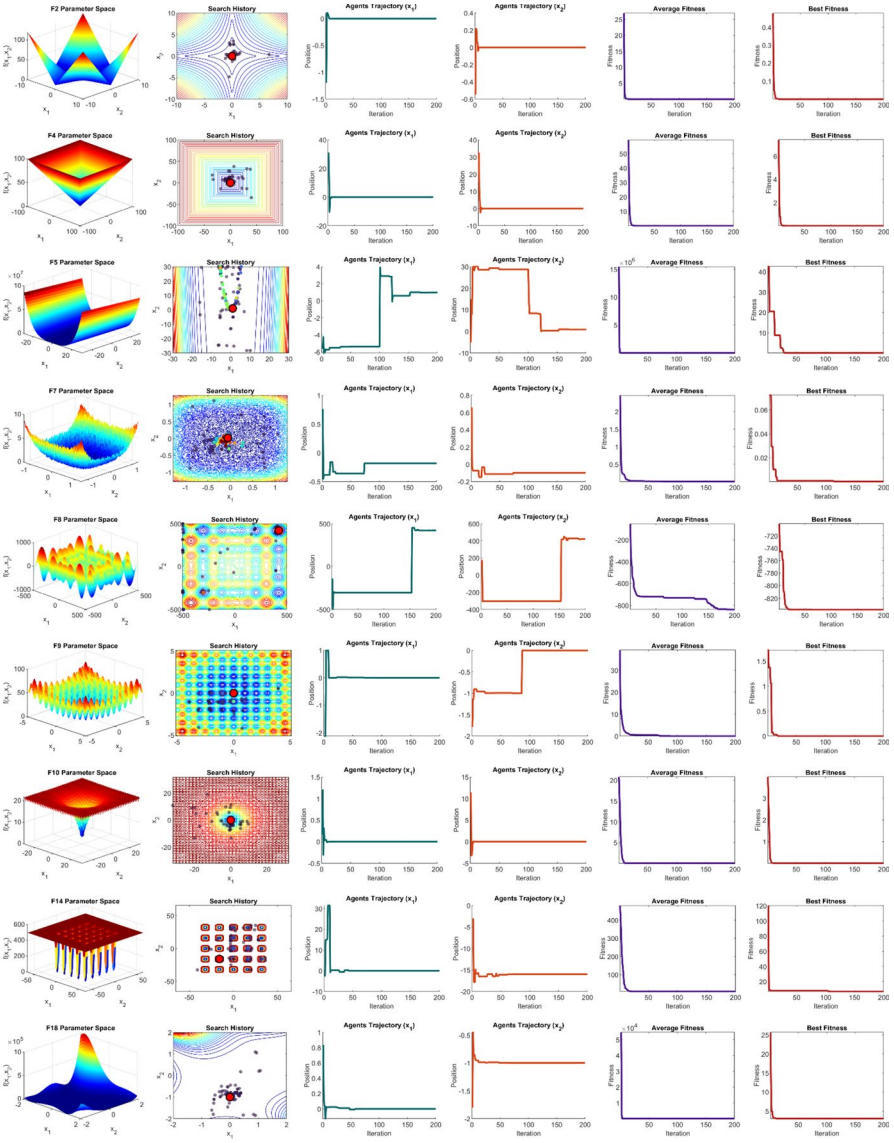


Fig. 4 Search characteristics of SOGWO

3.4.2 Convergence analysis

This section presents convergence curves that demonstrate the effectiveness of the proposed algorithm compared to its competitors. These curves serve as a powerful tool for assessing the performance of meta-heuristic algorithms during the optimization process. By illustrating the change in fitness values over iterations, they provide a visual analysis of the algorithm's convergence speed and stability to the optimal

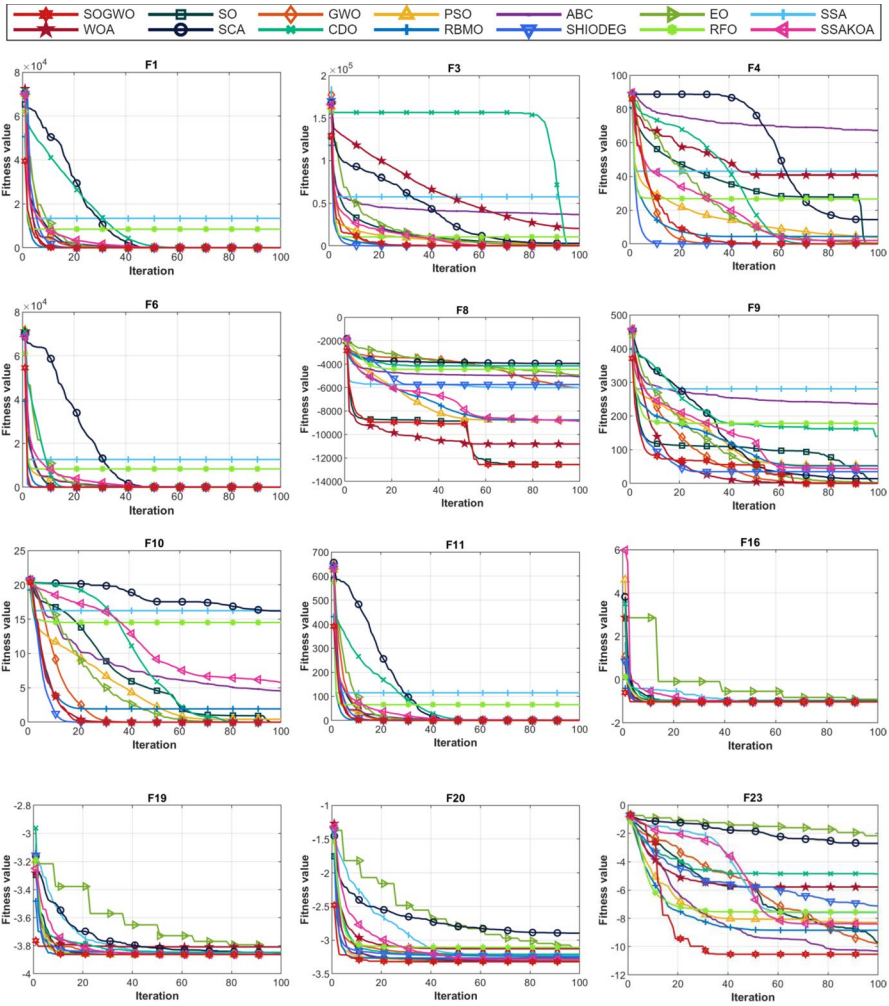


Fig. 5 Convergence curves of standard benchmark functions

solution. Thus, convergence curves play a vital role in evaluating both the efficacy of search mechanisms and improvements of solution quality. The convergence characteristics of SOGWO across its rivals on standard benchmark functions are shown in Fig. 5.

Based on the convergence curves presented in Fig. 5, the SOGWO effectively explores the solution space by displaying a rapid decrease from high fitness values in the initial stages. This demonstrates that the algorithm possesses a strong global search capability. As the iterations progress, the decreasing rate of change of the curve indicates that SOGWO transitions to local search and narrows its focus around the current best solutions. However, in some functions, it has been observed to exhibit a slow and controlled decrease behavior. This allows the algorithm to

prevent premature convergence by spreading across broader areas of the solution space and facilitating a balanced and gradual convergence rather than rapid initial improvement. Thus, the algorithm tends to proceed more cautiously, especially in multimodal or complex problems, thereby avoiding local optima. In other words, the algorithm maintains diversity during the search process while simultaneously conducting the exploitation phase in a balanced manner.

Depending on the structure of the problem, these convergence behaviors are achieved by combining the information-sharing mechanism of the SO algorithm and the hierarchical leadership structure of GWO, improving the search process and enabling it to reach lower fitness values more effectively. Consequently, it can be said that the hybrid structure reduces the risk of premature convergence and offers more robust search behavior by managing both the global and local search processes in a balanced way.

3.4.3 Population diversity analysis

This section focuses on population diversity, one of the measures illustrating search characteristics of candidate solutions in the search space during the optimization process. The rapid decrease in population diversity during the early stages of the search process shows that search agents concentrate around a narrow area, thereby increasing the risk of early convergence to a local optimum and stagnation. Conversely, high population diversity indicates that individuals are spread across a wider area in the search space, exhibiting a more comprehensive exploration capability. This study adopts a dimension-wise diversity measure to quantitatively characterize the spread of candidate solutions across the search space and track population diversity evolution throughout the optimization process, which is defined in Eq. (42).

$$Div(t) = \frac{1}{D}\sum_{j=1}^{D}\frac{1}{N}\sum_{i=1}^{N}\left|\text{median}\left(x_j(t)\right) - x_{ij}(t)\right| \tag{42}$$

where $Div(t)$ refers to the dimension-wise diversity at iteration t, $\text{median}\left(x_j(t)\right)$ is the median value of dimension j for all snakes, $x_{ij}(t)$ denotes the value of dimension j of snake i. N and D are the population size and problem dimension the problem, respectively.

Figure 6 depicts the population diversity trajectories of the SOGWO and its components algorithms on some benchmark functions. The behavior observed in Fig. 6 suggests that GWO preserves population diversity in many functions and explores the search space more comprehensively. In contrast, the rapid decline in SO's population diversity suggests a tendency to concentrate in promising regions during the early stages of the search process. On the other hand, SOGWO exhibits a problem-dependent and dynamic search characteristic. While SOGWO progressively reduces population diversity, facilitating intensified exploitation of promising regions for some functions, it preserves a relatively high level of diversity for a longer period for more challenging functions such as F8, F9, F15, and F20. Furthermore, as with the F21 function, in some functions, diversity increases again

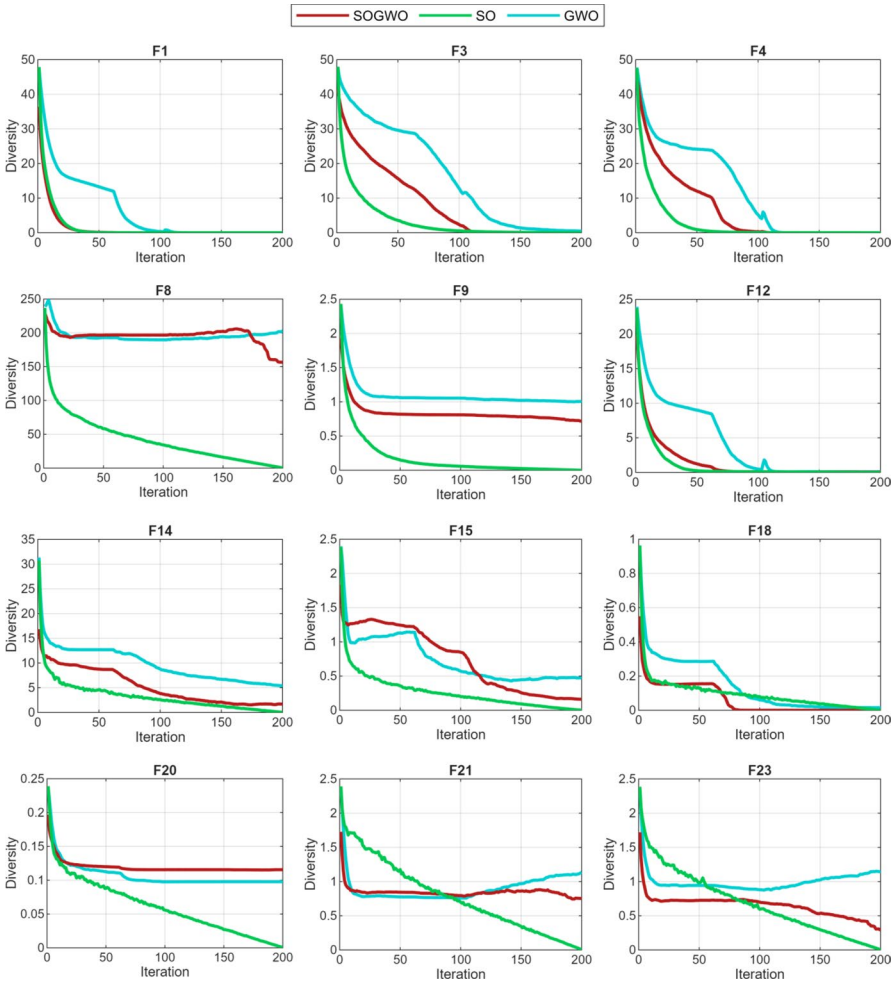


Fig. 6 Population diversity analysis in some test functions

in later iterations; one could argue that SOGWO permits restoring population diversity by directing search agents to different solution regions as needed during the optimization process. This indicates that SOGWO has a dynamic structure; consequently, it can be said that SOGWO establishes a balance between exploration and exploitation that varies depending on the problem.

Overall, population diversity analysis shows that SOGWO can adapt to the problem, going beyond simply combining the exploration capabilities of GWO and the exploitation capabilities of SO. Therefore, this adaptive search behavior allows SOGWO to effectively concentrate in promising areas depending on the problem characteristics, while also enabling the restoration of population diversity when required. Thus, it can be claimed that SOGWO strikes a flexible exploration–exploitation balance.

3.4.4 Exploration and exploitation behavior analysis

In this section, an exploration–exploitation analysis is conducted to evaluate the search behavior of the SOGWO in the solution space. Exploration and exploitation are two key components of the performance of meta-heuristic algorithms. Exploration aims to find the global optimal solution by seeking different regions of the solution space and reflects the algorithm's global search capability. On the other hand, exploitation improves the best solution found by searching around it and represents the local search capability of the algorithm. Therefore, establishing a proper balance between exploration and exploitation ensures that the algorithm avoids local optima and converges to the global optimum. Concerning this, a population diversity-based measure was used to quantitatively evaluate the exploration and exploitation behavior of SOGWO and the exploration and exploitation rates in each iteration are calculated by Eqs. (43) and (44), respectively.

$$Exploration(\%) = \frac{Div(t)}{Div_{max}} \times 100 \tag{43}$$

$$Exploitation(\%) = \frac{Div_{max} - Div(t)}{Div_{max}} \times 100 \tag{44}$$

where $Div(t)$ is the diversity value at iteration t, Div_{max} corresponds to maximum diversity observed during the optimization process.

Figure 7 visualizes the exploration and exploitation abilities of SOGWO in some test functions. The experimental results highlight how the internal dynamics of SOGWO evolve throughout iterative processes, reflecting its adaptive search behavior. While SOGWO exhibits high exploration capabilities by exploring the solution space in the initial iterations on functions F1, F3, F4, F12, and F18, its exploitation ability becomes more dominant as the iterations progress. This demonstrates that SOGWO first scans the entire solution space, then focuses on promising regions to converge to global optimum. The exploration–exploitation ratios for F9, F20, F21, and F23 reflect a more balanced distribution, indicating that SOGWO effectively utilizes both global and local optimization mechanisms simultaneously. It is observed that SOGWO reveals a more pronounced exploration phase during the first half of the iterations in F14 and F15, while it transitions to exploitation in the subsequent iterations. This behavior suggests that the algorithm employes an adaptive search strategy. Moreover, SOGWO demonstrates a significantly higher exploration capability in F8, indicating that SOGWO focuses more on global search depending on the problem structure.

Overall, SOGWO strikes an efficient balance between exploration and exploitation in different search space topology. SOGWO exhibits a structure that is exploration-oriented in the early stages and exploitation-oriented in the later stages in some functions, while it displays a more balanced exploration–exploitation behavior in others. Consequently, SOGWO demonstrates

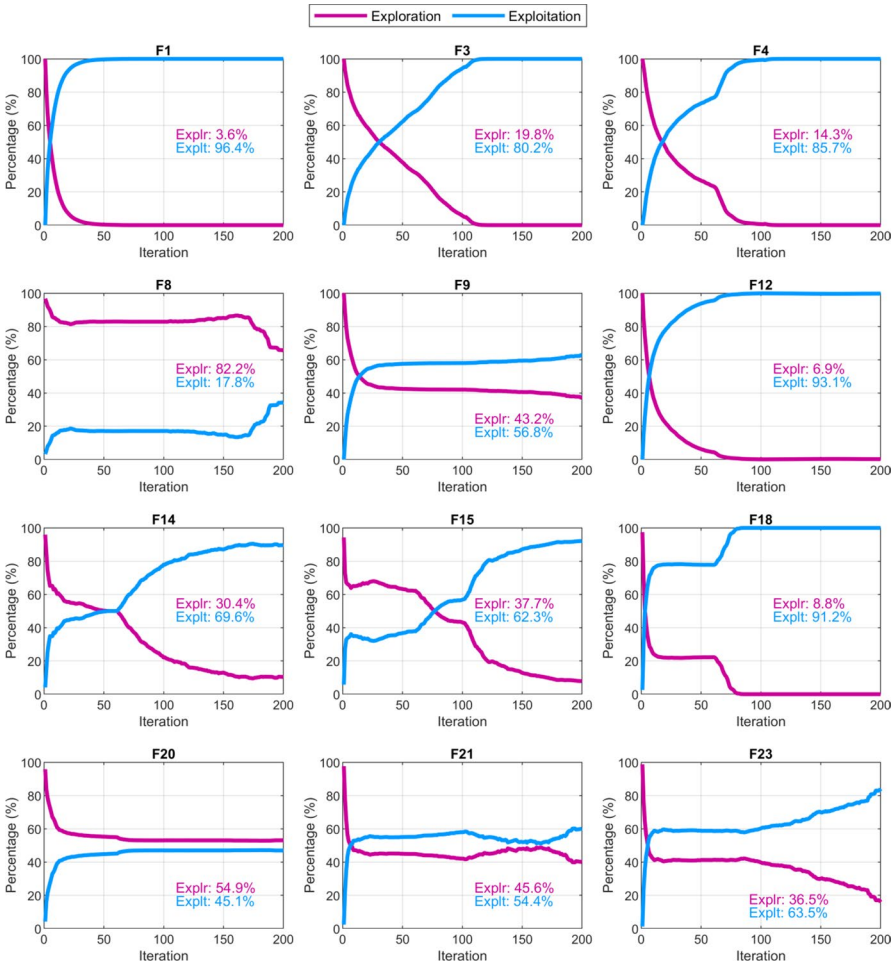


Fig. 7 Exploration and exploitation behavior analysis in some test functions

effective optimization ability by dynamically balancing exploration and exploitation processes depending on the problem structure.

3.4.5 Leader trajectory analysis

In previous sections, the performance of SOGWO is evaluated through extensive experiments on both benchmark and CEC-2022 test functions, and its effectiveness relative to the compared methods is demonstrated. However, these experiments cannot directly reveal how the leader (best) solution evolves in the search space throughout the optimization process. Therefore, this section examines the search behavior of the proposed SOGWO, how frequently it updates the best solution, and the trajectory followed by the leader solution in the search space. Thus, inferences can be

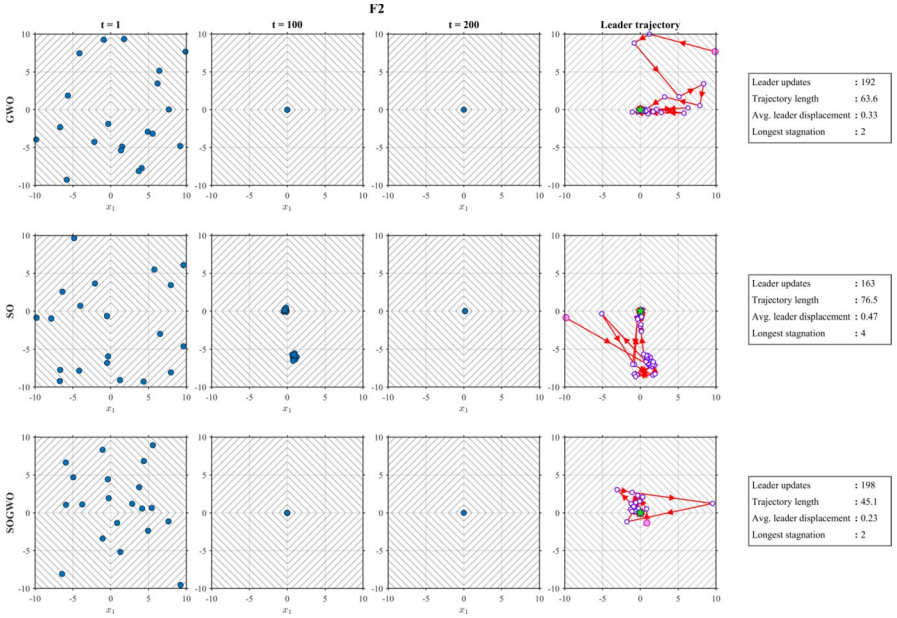


Fig. 8 Leader trajectory analysis of GWO, SO, and the proposed SOGWO on F2

drawn regarding how the leader solution exhibits characteristics in local regions, how leaders guide individuals, how population diversity is ensured, how the leadership mechanism affects periods of stagnation, and how the algorithm strikes a balance between exploration and exploitation. For this purpose, four different metrics reflecting the impact of the leadership mechanism are used: leader updates, leader trajectory length, average leader displacement, and longest stagnation. These criteria provide insight into the algorithm's internal dynamics, which are based on its leadership mechanism. Leader updates refer to the total number of updates the algorithm improves the best solution throughout the optimization process. Updating the leader solution demonstrates that the population dynamically drives search behavior while revealing its ability to discover new promising regions. Leader trajectory length measures the spatial displacement of the leader solution between successive iterations. Minimal movement of the leader indicates that the algorithm tends to converge prematurely and fails to sufficiently explore new search regions, while excessive movement suggests that the leader solution is wandering unnecessarily in promising regions. Average leader displacement assesses the balance between the exploration and exploitation components of the algorithm. A high value indicates aggressive exploration behavior, while a low value suggests controlled progress in promising areas. Longest stagnation evaluates the tendency and persistence of an algorithm towards stagnation during the optimization process. Figures 8,9 and 10 present the leader trajectories of the SO, GWO, and proposed SOGWO, along with the average values of these metrics, for randomly selected functions F2, F8, and F14, respectively.

Upon examining the leader solution movements for F2 function, GWO exhibits an exploration-oriented search behavior by performing wide movements, while SO displays a more irregular search behavior. By contrast, SOGWO more controllably discovers promising regions with a shorter leader trajectory and a lower average displacement value while maintaining a high number of leader updates. Therefore, it reflects a more balanced search behavior, striking a balance between exploration and exploitation. Furthermore, the algorithm continues to generate new solutions without remaining stuck in the same leader solution for extended periods with its low stagnation time.

The F8 function contains numerous local optima and, due to its complex structure, is used to evaluate the ability of methods to avoid local minima. The leader behavior for F8 indicates that GWO tends to converge early, as its stagnation period is longer than that of the other methods. However, SO performs more updates on the leader solution and follows a considerably longer trajectory. On the other hand, SOGWO converged to the global optimum in a more controlled manner while significantly reducing its leader trajectory and stagnation period. These results highlight that GWO's guidance mechanism limits SO's unnecessary search movements and, consequently, that SOGWO exhibits efficient search behavior.

In the F14 function, the fact that SO delivers a long period of stagnation reflects that the leader solution remains in the same region for an extended period. However, GWO executes wide-ranging leader movements and explores the solution space more comprehensively. SOGWO preserves the leader solution at a dynamic level and reduces the stagnation period by balancing the characteristics of the component

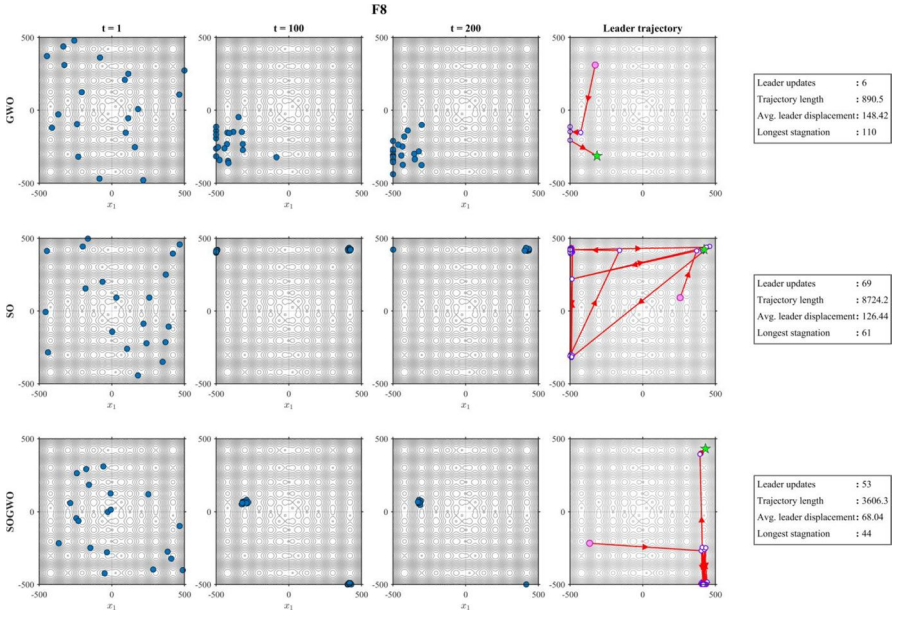


Fig. 9 Leader trajectory analysis of GWO, SO, and the proposed SOGWO on F8

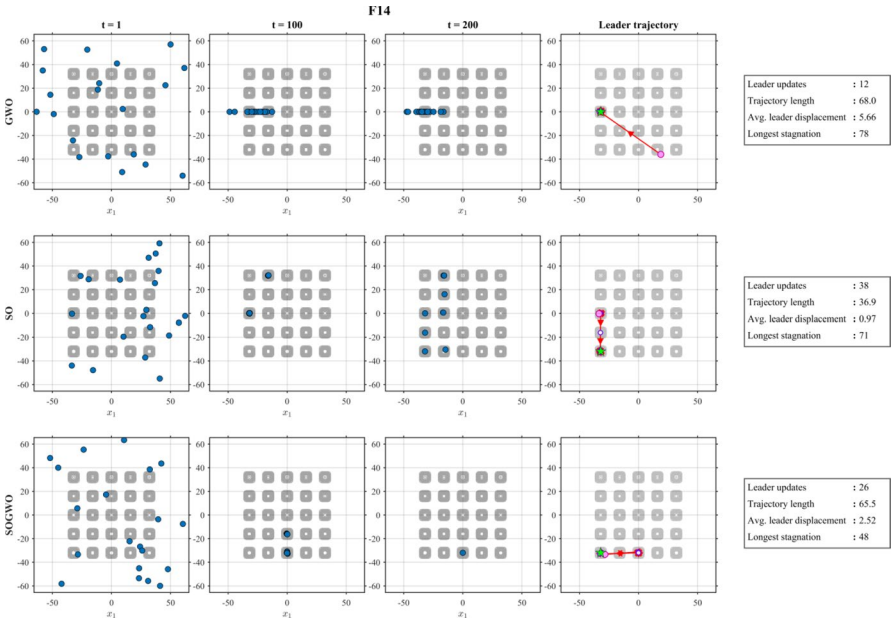


Fig. 10 Leader trajectory analysis of GWO, SO, and the proposed SOGWO on F14

algorithms. This illustrates that the hybrid leadership mechanism not only ensures rapid convergence but also prevents premature convergence.

Overall, the leadership behavior analyses of the proposed SOGWO and its component algorithms indicate that GWO's hierarchical leadership mechanism effectively guides SO's search characteristics. Therefore, it can be said that SOGWO manages a more stable optimization process by reducing unnecessary search movements and stagnation periods across different problem characteristics.

3.5 Statistical analysis

Experimental studies have proven that the proposed method surpasses its competitors. However, the statistical significance of the performance differences between the compared methods has not been examined. To verify whether the observed success was coincidental, this section of the study presents statistical analyses. A two-stage analysis is performed using the Friedman and Wilcoxon signed-rank test, which are non-parametric statistical tests, to prove the effectiveness and stability of the SOGWO and to verify the reliability of the experimental performance results. These analyses are conducted on three categories of test functions: classic benchmark functions and CEC-2022 ($D = [10, 20]$).

Table 20 Friedman test results of SOGWO and its rivals on classic benchmark and CEC-2022 test suites

Suites	Classic Benchmark		CEC-2022 ($D = 10$)		CEC-2022 ($D = 20$)	
Algorithms	Friedman Rank	Final Rank	Friedman Rank	Final Rank	Friedman Rank	Final Rank
SOGWO	2.52	1	2.21	2	2.42	1
SO	4.33	2	5.08	3	4.75	4
GWO	5.39	3	7.08	7	6.75	8
PSO	7.17	6	6.25	5	6.58	7
ABC	9.00	10	7.17	8	6.33	6
EO	9.91	11	6.42	6	4.25	3
SSA	10.09	12	11.58	13	13.42	14
WOA	6.74	5	10.33	11	9.17	10
SCA	10.17	13	8.92	10	8.75	9
CDO	8.26	9	13.17	14	11.92	12
RBMO	7.30	7	5.67	4	5.58	5
SHIODEG	7.52	8	8.50	9	10.08	11
RFO	10.96	14	10.50	12	12.42	13
SSAKOA	5.63	4	2.13	1	2.58	2
χ^2	102.4671		94.5833		112.6476	
p-value	5.5511E−16		1.8430E−14		0.0000	

3.5.1 Friedman test

The Friedman test, a ranking-based technique, is used in the first stage of statistical analysis to compute average rank values for each algorithm to statistically examine the overall efficacy of SOGWO and the comparable algorithms. Table 20 summarizes the results of Friedman analyses performed on different experimental groups.

As can be seen in Table 20, since the Friedman test results yielded $p < 0.05$ across all test suites, it can be concluded that the performance differences observed among the algorithms are statistically significant. Upon examining the rank values of the algorithms, it is observed that the proposed SOGWO ranks first in the classic benchmark and the CEC-2022 ($D = 20$), while it is in second place for CEC-2022 ($D = 10$), indicating that it exhibited competitive behavior.

3.5.2 Wilcoxon signed rank test

After the Friedman test, the Wilcoxon signed rank test is applied in the second stage of statistical analysis to reveal the pairwise performance differences between the compared algorithms. This method considers the differences in performance results obtained by the compared algorithms for each problem. The absolute values of the differences between the algorithms are ranked, and the test statistics and the corresponding p-value are calculated using the sums of positive

Table 21 Wilcoxon signed rank test results of SOGWO and competitive algorithms across classic benchmark functions

SOGWO vs.	SO	GWO	PSO	ABC	EO	SSA	WOA	SCA	CDO	RBMO	SHIODEG	RFO	SSAKOA
R^+	210	251	245	246	276	262	257	263	263	244	264	276	222
R^-	66	25	31	30	0	14	19	13	13	32	12	0	54
n^+	19	20	20	19	23	19	21	21	21	20	21	23	17
n^-	4	3	3	4	0	4	2	2	2	3	2	0	6
ties	0	0	0	0	0	0	0	0	0	0	0	0	0
p-value	2.85E−02	5.88E−04	1.14E−03	1.02E−03	2.70E−05	1.62E−04	2.95E−04	1.44E−04	1.44E−04	1.26E−03	1.27E−04	2.70E−05	1.06E−02
Hypothesis	✔	✔	✔	✔	✔	✔	✔	✔	✔	✔	✔	✔	✔

and negative ranks. If $p < 0.05$, it is concluded that the performance difference between the algorithms is statistically significant. In the tables, the symbol "✓" denotes that the null hypothesis is rejected, meaning that performance differences between the competing algorithm are statistically significant, whereas the symbol "✗" indicates that observed differences are not statistically significant. Table 21 showcases the Wilcoxon signed-rank test results comparing SOGWO to its rivals on classic benchmark functions with 5% significance level.

In Table 21, R^+ and R^- in the Wilcoxon signed-rank test represent the rank sums of the problems where the SOGWO exhibits superiority and failure compared to the competing algorithm, respectively. Additionally, the values n^+, n^-, and ties indicate the number of test functions for which SOGWO achieves better, worse, or equivalent results. The findings in Table 21 reveal that SOGWO achieves superior performance over its rivals at the 95% confidence level for classic benchmark functions. These results affirm that SOGWO's performance advantages over its rivals in experimental studies are not coincidental and that the performance differences are statistically significant. Table 22 reports the Wilcoxon signed-rank test result of competitive algorithms across CEC-2022 ($D = 10$) test suite.

A detailed examination of Table 22 reveals that, although there is no statistically significant difference between SOGWO and the SO and SSAKOA algorithms, there are significant performance differences among the other competitors. When the R^+ and n^+ values of the algorithms are evaluated along with the test results, it is evident that the SOGWO displays superior performance in most test functions. The results indicate that, although the differences between SOGWO and both SO and SSAKOA are not statistically significant, SOGWO exhibits competitive performance against these methods and achieves better results in a considerable number of the test functions. The Wilcoxon signed-rank test results for opposing algorithms on CEC-2022 ($D = 20$) test suite are documented in Table 23.

The Wilcoxon signed-rank test results for the CEC-2022 ($D = 20$) test suite reported in Table 23 suggest that the performance differences between the proposed SOGWO and the ABC, EO, and SSAKOA algorithms in pairwise comparisons are not statistically significant. However, the fact that the R^+ and n^+ values favor SOGWO indicates that the SOGWO produces superior results in a large majority of the test functions. Therefore, although statistical significance is not achieved with the ABC, EO, and SSAKOA algorithms, it can be concluded that SOGWO demonstrates superior performance.

As a complement to the statistical analysis, this section also presents radar chart for CEC-2022 test suite with 10 and 20 dimensions, as illustrated in Fig. 11. In radar charts, the fact that the polygon representing the algorithm is closer to the center indicates successful performance.

An examination of Fig. 11 reveals that, for both $D = 10$ and $D = 20$, the SOGWO exhibits a profile closer to the center compared to its competitors and demonstrates better performance, consistent with the results of the statistical analysis.

Table 22 Wilcoxon signed rank test results of SOGWO and competitive algorithms across CEC-2022 ($D = 10$) test suite

SOGWO vs.	SO	GWO	PSO	ABC	EO	SSA	WOA	SCA	CDO	RBMO	SHIODEG	RFO	SSAKOA
R^+	52	78	74	76	75	78	78	78	78	65	78	67	34
R^-	14	0	4	2	3	0	0	0	0	13	0	11	21
n^+	9	12	10	11	11	12	12	12	12	10	12	11	6
n^-	2	0	2	1	1	0	0	0	0	2	0	1	4
ties	1	0	0	0	0	0	0	0	0	0	0	0	2
p-value	1.02E−01	4.88E−04	3.42E−03	1.46E−03	2.44E−03	4.88E−04	4.88E−04	4.88E−04	4.88E−04	4.25E−02	4.88E−04	2.69E−02	5.57E−01
Hypothesis	✖	✔	✔	✔	✔	✔	✔	✔	✔	✔	✔	✔	✖

Table 23 Wilcoxon signed rank test results of SOGWO and competitive algorithms across CEC-2022 ($D = 20$) test suite

SOGWO vs.	SO	GWO	PSO	ABC	EO	SSA	WOA	SCA	CDO	RBMO	SHIODEG	RFO	SSAKOA
R^+	57	70	78	64	45	78	78	70	78	68	78	78	52
R^-	9	8	0	14	21	0	0	8	0	10	0	0	26
n^+	8	11	12	10	7	12	12	11	12	11	12	12	8
n^-	3	1	0	2	4	0	0	1	0	1	0	0	4
ties	1	0	0	0	1	0	0	0	0	0	0	0	0
p-value	3.22E−02	1.22E−02	4.88E−04	5.22E−02	3.20E−01	4.88E−04	4.88E−04	1.22E−02	4.88E−04	2.10E−02	4.88E−04	4.88E−04	3.39E−01
Hypothesis	✓	✓	✓	✖	✖	✓	✓	✓	✓	✓	✓	✓	✖

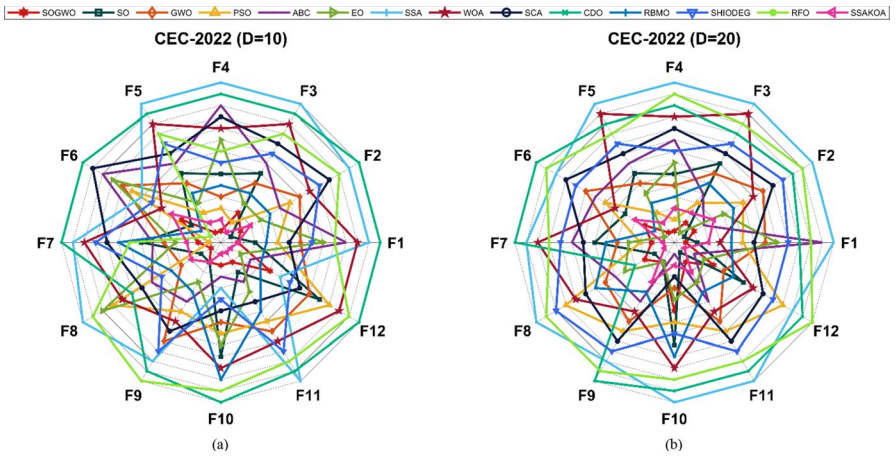


Fig. 11 Radar charts of SOGWO and comparison algorithms on the CEC-2022 ($D = 10, 20$)

3.6 Ablation study

In this section, an ablation study is conducted to evaluate the contribution of the hybrid structure in the proposed SOGWO to optimization performance. To this end, the individual and combined impacts of the basic components of the algorithm are examined, and the original SO, GWO, and proposed SOGWO are compared under the same experimental conditions. In the proposed approach, the GWO position update mechanism is first applied separately to the male and female snake populations, considering the top three solutions within each population. The elite solutions, determined according to the internal dynamics of each population, guide the position update process of search agents. Subsequently, the improved population derived from the elite solutions is incorporated into the position update mechanism of SO, thereby updating the new positions of the female and male snakes. In order to assess the impact of the structure on performance, the SO, GWO, and proposed SOGWO are comparatively analyzed, and the results for some test functions are displayed in Fig. 12.

A visual analysis of Fig. 12 reveals that the proposed SOGWO demonstrates superior optimization performance in comparison to the SO and GWO algorithms. This augmentation is due to the balanced integration of GWO's robust exploration capacity and SO's effective exploitation ability. While GWO explores extensive regions of the search space to increase diversity, SO focuses on promising solutions to contribute to local improvement. Consequently, the enhanced performance of the proposed SOGWO can be attributed not only to the individual effects of the algorithms but also to the pivotal role played by the integrated use of the exploration and exploitation components.

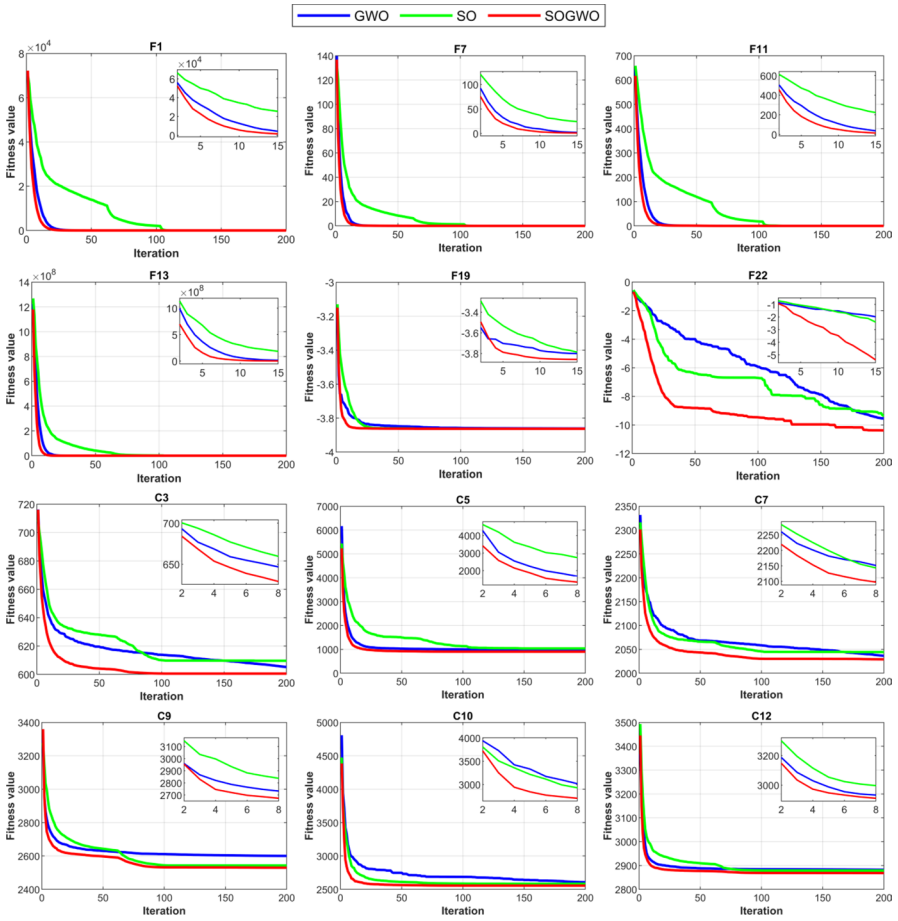


Fig. 12 Impact analysis of SOGWO

3.7 Sensitivity analysis

In this study, a hybrid SOGWO is developed by merging the strong characteristics of the SO and GWO algorithms. In experimental studies, the control parameter values of the SO algorithm, which forms the basis of the hybrid algorithm, are used as recommended in the original paper. However, this section presents a comprehensive sensitivity analysis to examine the search characteristics of the proposed hybrid structure in different parameters and to evaluate the suitability of the original parameters within the SOGWO. Accordingly, the threshold values of the parameters Q and *Temp*, which are critically important in the decision mechanism of the algorithm, are assessed on classical benchmark functions. To this end, the threshold values for parameters Q and *Temp* are defined as $T_1 = \{0.25, 0.30, 0.35, 0.40, 0.45\}$ and $T_2 = \{0.40, 0.50, 0.60, 0.70, 0.80, 0.90\}$, respectively. To guarantee a fair

Table 24 Ranking results for the threshold values of the parameters *Temp* and Q

T_2	T_1				
	0.25	0.30	0.35	0.40	0.45
0.40	13.3913	15.6304	12.7391	16.3696	18.2826
0.50	10.3478	12.8261	11.7391	16.5435	18.8696
0.60	9.9565	14.0652	17.7174	17.5652	20.3261
0.70	12.7609	16.1087	13.8913	14.8913	19.4348
0.80	14.7174	15.9783	16.0435	17.2391	19.4130
0.90	14.6087	12.5652	15.9783	14.6522	20.3478

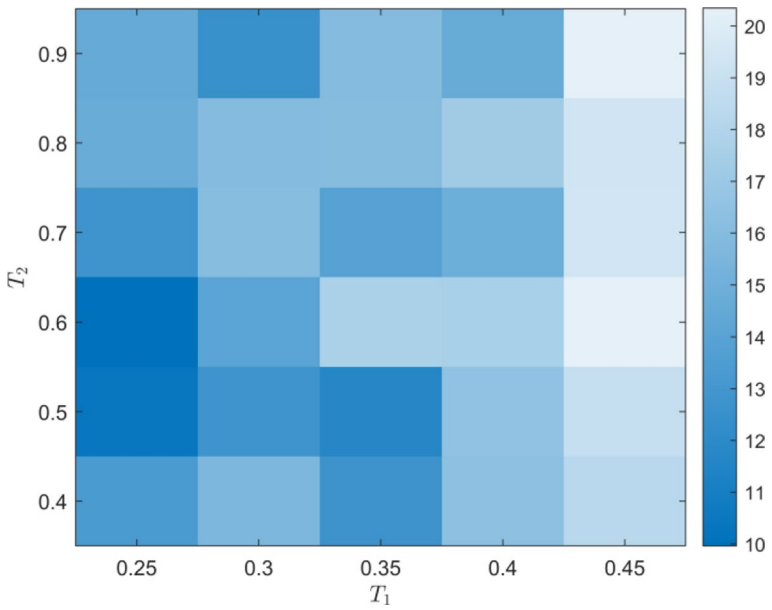


Fig. 13 Heatmap of average ranks across parameter combinations of SOGWO

comparison, SOGWO is run independently 30 times on 23 test functions for a total of 30 different combinations. Table 24 illustrates the ranking results for different threshold values of the Q and *Temp*.

Upon examining the results in Table 24, the best parameter combination is obtained as $T_1 = 0.25$ and $T_2 = 0.6\,0$. Thus, it is observed that the optimal parameter combination for the hybrid method is identical to the parameter values in the original SO. This outcome indicates that, despite the hybridization process, the internal structure of SO is preserved. Furthermore, the fact that the SOGWO achieves high performance with the original parameter values demonstrates that this is due to the leadership mechanism of GWO. This indicates that the hybrid structure enhances the algorithm's search capacity and enables more comprehensive exploration and exploitation within the solution space.

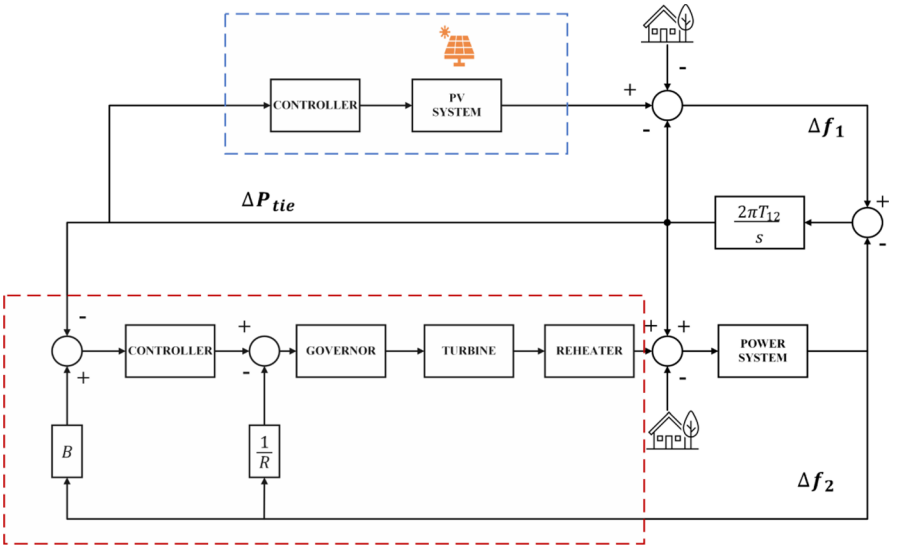


Fig. 14 Transfer function model of studied power system

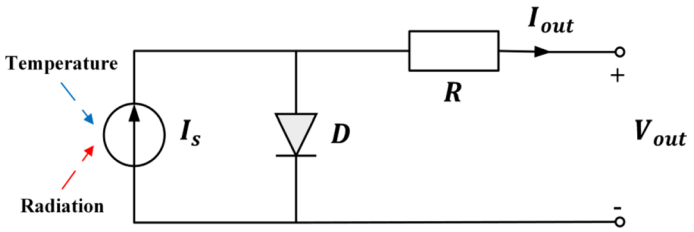


Fig. 15 PV cell model

The distribution of the rank values from the sensitivity analysis is also exhibited as a heatmap in Fig. 13 to thoroughly examine the impact of the parameters. Heatmap results show that parameter combinations are concentrated in certain regions and have the lowest rank values in those regions.

4 PV-thermal power system model

As a test system, a two-area interconnected power system was modeled in the MATLAB/SIMULINK software to evaluate the effectiveness of the proposed controller and the developed hybrid optimization technique. Area-1 in the power system consists of a PV system, while area-2 is reheat thermal power system. The transfer function model of the two-area power system is given in Fig. 14. In the figure, Δf_1 and Δf_2 represent the frequency change for area-1 and area-2, and ΔP_{tie} is the oscillation in the tie-line power change between the connected areas.

The PV system in the studied power system acts as area-1 and is interconnected with area-2. As shown in Fig. 15, the PV cell model consists of a diode and a current source connected in parallel and a resistance in series with them. Here, the current source is a variable depending on radiation which is expressed as the intensity of the sunlight and temperature. Therefore, the output voltage and generated power of a solar panel vary throughout the day. Maximum power point tracking (MPPT) is one of the methods used to maximize the power that can be obtained from PV systems. In addition, the voltage value generated can be adjusted to the desired values with the help of converters. Considering all these, the mathematical model of the PV system including components such as MPPT, converter, and filter is expressed as follows.

$$G_{PV}(s) = \frac{a + bs}{s^2 + cs + d} = \frac{-18s + 900}{s^2 + 100s + 50} \tag{45}$$

The thermal system in area-2 consists of four different components: governor, turbine, reheater and power system. All components are considered linear and represented by first-order transfer functions for simplicity when constructing the transfer function model of the thermal system. The transfer functions of these components are given in the equations below for the governor, turbine, reheater and power system, respectively. In these equations, K_i is the gain value for each system component, and τ_i is the time constant of these components.

$$G_G(s) = \frac{K_G}{1 + s\tau_G} \tag{46}$$

$$G_T(s) = \frac{K_T}{1 + s\tau_T} \tag{47}$$

$$G_R(s) = \frac{1 + sK_R\tau_R}{1 + s\tau_R} \tag{48}$$

$$G_{PS}(s) = \frac{K_{PS}}{1 + s\tau_{PS}} \tag{49}$$

The ACE value for area-2 is expressed by the following equation. In the equation, B is the frequency bias parameter.

$$ACE = B\Delta f_2 + \Delta P_{tie} \tag{50}$$

5 Optimization problem

The PI controller consists of two parameters, proportional gain (K_P) and integral gain (K_I), as shown in Fig. 16. The transfer function of this controller is expressed by Eq. (51). As can be seen from Eq. (51), four different parameters, two in each

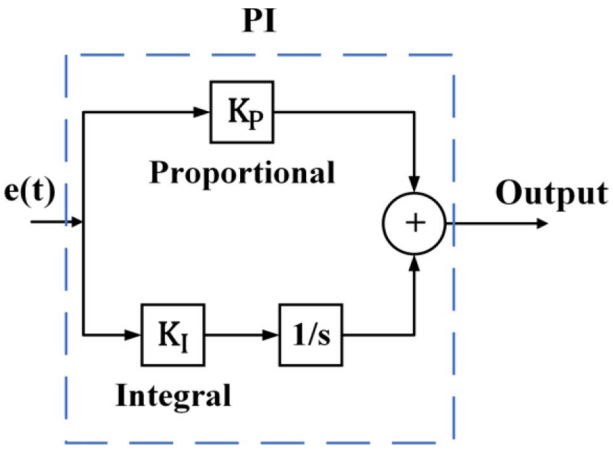


Fig. 16 PI controller

area, need to be optimized for LFC in a two-area power system. For this, the desired control system features and constraints must be taken into account. The main purpose of the LFC operation is to damp the fluctuations in the system frequency and the power change between the control areas, due to load demand or different disturbances, to the nominal values as soon as possible. To achieve this goal, values such as maximum overshoot (*MO*), minimum overshoot (*MU*) and settling time (t_s) must be improved.

$$G_C(s) = K_{Pi} + \frac{K_{Ii}}{s}, i = 2 \tag{51}$$

LFC issue is an optimization problem. In an optimization problem, the goal is to find solutions that minimize the objective function used. Therefore, in this study, integral of time-multiplied absolute error (*ITAE*) is applied as objective function (*OF*) to provide minimum *MO* / *MU* / t_s performance values. ITAE was selected to ensure a fair and consistent comparison with the other studies considered in this work and is expressed by the following equation.

$$OF = ITAE = \int_0^{t_{sim}} t\left(\left|\Delta f_1\right| + \left|\Delta f_2\right| + \left|\Delta P_{tie}\right|\right)dt \tag{52}$$

While solving the LFC problem, the following constraints are taken for the PI controller parameters. In order to make a fairer comparison with other studies, the lower limit was taken as -2, the upper limit was taken as 2 in this study as well.

$$K_{Pi}^{min} \le K_{Pi} \le K_{Pi}^{max}$$
$$K_{Ii}^{min} \le K_{Ii} \le K_{Ii}^{max}$$

The transfer function model of the system shown in Fig. 14 was modeled in the MATLAB/SIMULINK program. Additionally, SOGWO codes are written in m.file

Table 25 Optimized controller parameters

Technique	K_{P1}	K_{I1}	K_{P2}	K_{I2}
SOGWO: PI	−0.4114	−0.3504	−2	−0.2733
SCHO: PI	−0.4758	−0.0931	−2	−0.9339
GTO: PI	−0.5235	−0.0973	−2	−0.9238
SSA: PI	−0.7715	−0.0483	−1.0837	−0.8929

script. Written codes and the transfer function model are integrated in order to calculate the fitness of the candidate solutions; thus, PI controller parameters can be adjusted optimally. Initially, the parameters K_{P1}, K_{I1}, K_{P2}, and K_{I2} are determined randomly. Then these values are sent to the SIMULINK model, and the corresponding Δf_1, Δf_2, and ΔP_{tie} values are calculated. Using Eq. (52), a fitness value is assigned for each parameter, and the next iteration is passed. This cycle continues until a certain stopping criterion is met.

6 Simulation studies and results

In the proposed SOGWO, the number of iterations and the number of populations were taken as 50, and the simulation studies were investigated under five different scenarios. In the first scenario, the system response was analyzed under a 0.1 pu load disturbance applied simultaneously to both areas at the beginning of the simulation. Since power systems may experience load variations of different magnitudes, the second scenario considered a varying load profile in area-2 ranging from −0.02 pu to 0.03 pu. In the third scenario, the impact of solar irradiation was examined. Subsequently, the system behavior was evaluated in the presence of nonlinearities. Finally, a parameter sensitivity analysis was carried out. The obtained results of the proposed algorithm were compared with the results of Sinh Cosh Optimizer (SCHO) [4], Gorilla Troops Optimizer (GTO) [67], Salp Swarm Algorithm (SSA) [68], Whale Optimization Algorithm (WOA) [69], Shuffled Frog Learning Algorithm (SFLA) [70], and Firefly Algorithm (FA) [1] in the literature.

System parameters were set as $K_{PS} = 120Hz/pu.MW$, $\tau_{PS} = 20s$, $\tau_R = 10s$, $\tau_G = 0.08s$, $\tau_T = 0.3s$, $K_R = 0.33Hz/pu.MW$, $2\pi T_{12} = 0.54pu.MW/Hz$, $B = 0.8pu.MW/Hz$, $R = 2.5Hz/pu.MW$, as in the comparison studies [1, 70, 71]. The optimal controller gains obtained as a result of the simulation studies are given in Table 25.

The negative gain values reported in the table are a consequence of the adopted sign convention for the error signal and PI control law. They do not indicate positive feedback; the overall control loop maintains negative feedback.

6.1 Scenario-I: 10% load change in both areas

In order to examine the effectiveness of the proposed SOGWO-PI controller, it is necessary to examine the load changes occurring in both areas. For this reason, the

Table 26 System performance numerical results for scenario-I

Controller	t_s(s)			$MO(Hz)$		$MO(pu.MW)$	$MU(Hz)$		$MU(pu.MW)$
	Δf_1	Δf_2	ΔP_{tie}	Δf_1	Δf_2	ΔP_{tie}	Δf_1	Δf_2	ΔP_{tie}
SOGWO: PI	2.268	2.633	0	0	0.00398	0.0243	− 0.1639	− 0.225	− 0.0224
SCHO: PI	1.6231	2.4612	1.9986	0.0209	0.0459	0.0228	− 0.1569	− 0.2217	− 0.0296
GTO: PI	1.5515	2.4046	1.1134	0.0218	0.0489	0.0408	− 0.1382	− 0.1863	− 0.0191
SSA: PI	1.9059	2.6428	2.3188	0.0611	0.0699	0.0325	− 0.2327	− 0.2576	− 0.0379
WOA: PI	2.1045	5.7759	4.3108	0.0974	0.1017	0.0377	− 0.2196	− 0.2670	− 0.0479
SFLA: PI	5.2736	10.2835	8.5521	0.2101	0.2186	0.0453	− 0.2881	− 0.2738	− 0.0647
FA: PI	4.8609	5.6082	2.5018	0.1565	0.1376	0.0364	− 0.3063	− 0.2757	− 0.0505

system performance was evaluated for the load change of $0.1pu$ in both area-1 and area-2 in the 0th second of the simulation. The system responses obtained as a result of the simulation are given in Table 26 and Fig. 17 for the frequency change in area-1, frequency change in area-2, and tie-line power change, respectively. In addition, the numerical values obtained from the figures are given in Table 26. It can be seen from the figures and the table that the proposed SOGWO tuned PI controller provides less overshoot and shorter settling time. For the settling time calculations, tolerance limits of ± 0.1 Hz were applied to Δf_1 and Δf_2, whereas a tolerance limit of ± 0.025 MW was considered for ΔP_{tie}.

6.2 Scenario-II: Random load change in area-2

Different values of load changes may occur in power systems. For this reason, the LFC process should be carried out taking these situations into account. For this purpose, system performance was analyzed in case of load demand varying between $-0.02pu$ and $0.03pu$ in area-2. In this case, the system responses are given in Fig. 18 for frequency change in area-1, frequency change in area-2, and tie-line power change, respectively. As can be seen from the figures, the SOGWO: PI controller makes zero oscillations that occur in frequency and tie-line power changes in a short time at different load changes.

6.3 Scenario-III: Solar irradiation effect

In this section of the study, the effect of solar irradiation on the performance of the proposed SOGWO: PI controller was investigated. Since the power generated by PV systems varies throughout the day depending on solar irradiation and temperature conditions, it is important to evaluate the system performance under such varying operating conditions. In this context, the system behavior was analyzed considering the PV power variation shown in Fig. 19 for Area-1 and a variable load demand applied to

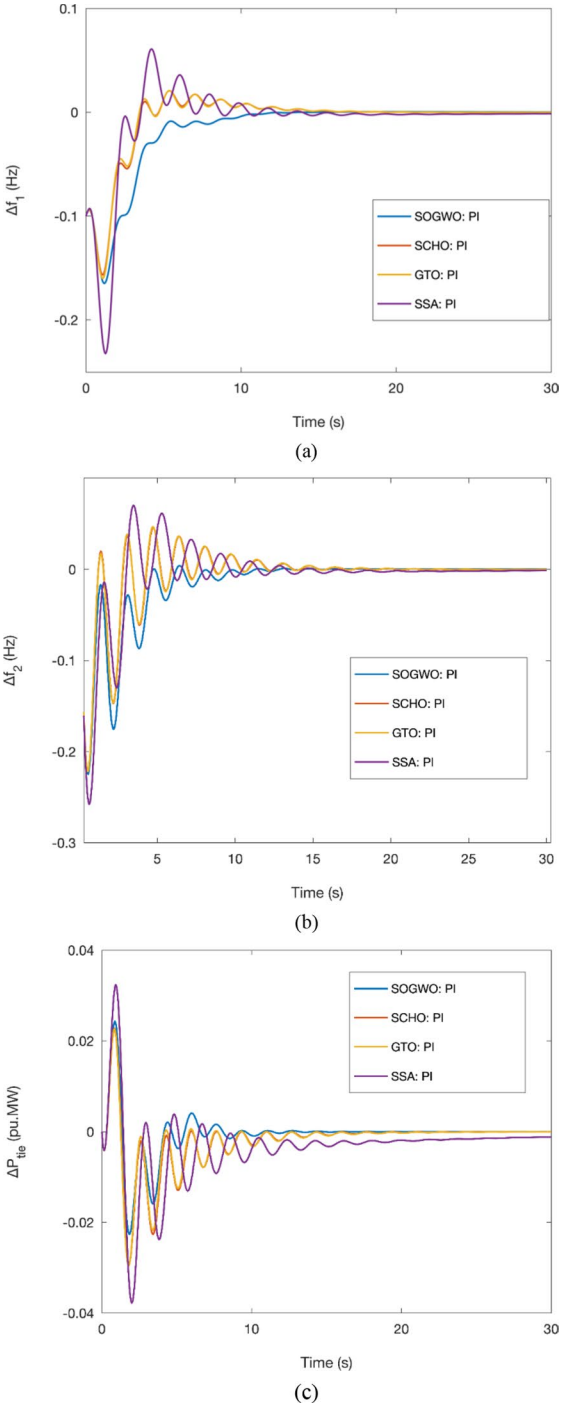


Fig. 17 The system responses for scenario-I **a** Δf_1 **b** Δf_2 **c** ΔP_{tie}

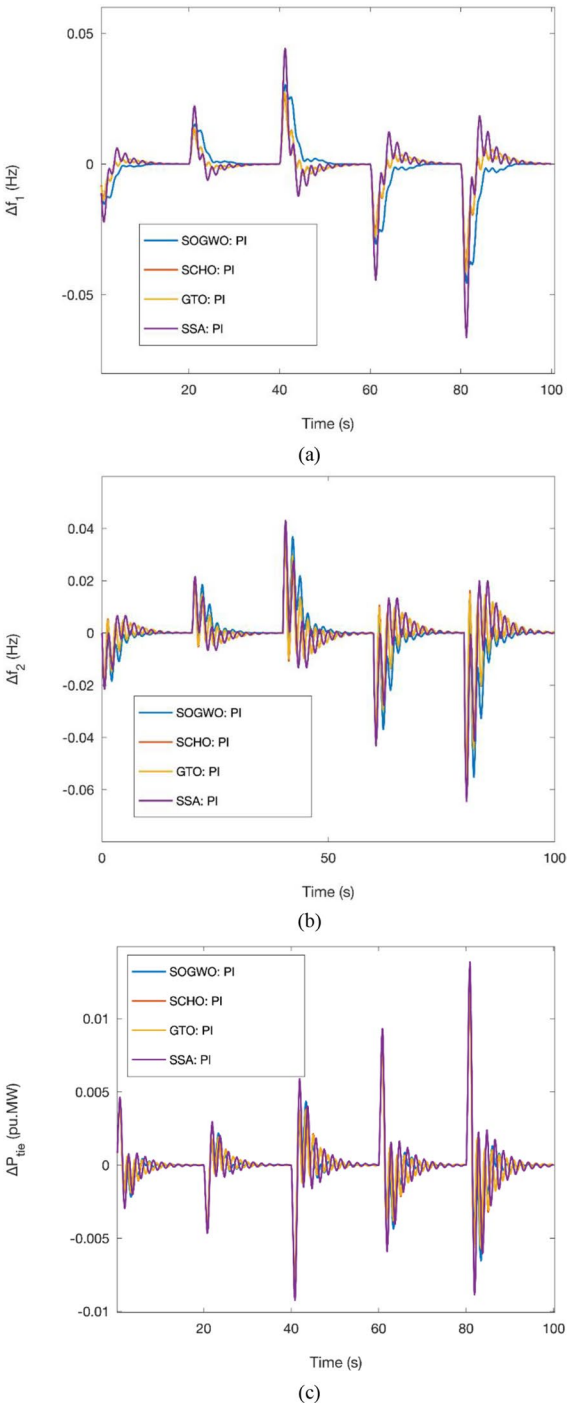


Fig. 18 The system responses for scenario-II **a** Δf_1 **b** Δf_2 **c** ΔP_{tie}

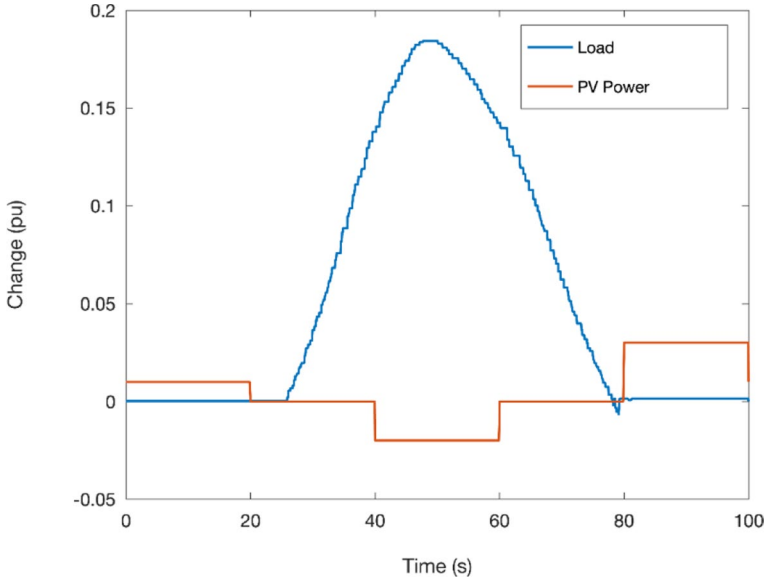


Fig. 19 PV power and load change

area-2. The corresponding system responses under varying PV power and load demand conditions are presented in Fig. 20.

As can be observed from Fig. 20, the oscillations in the system frequencies and tie-line power deviation increase during periods of high PV power generation. Nevertheless, these oscillations are maintained within small limits owing to the proposed SOGWO: PI controller.

6.4 Scenario-IV: Boiler dynamics (BD) effect

To achieve a more realistic analysis, nonlinearities such as boiler dynamics (BD) should also be taken into consideration in the system model. The transfer functions of the components included in the BD block diagram are presented in the following equations, while the corresponding block diagram of the BD is shown in Fig. 21.

Boiler storage:

$$G_{\mathrm{BS}}(s) = \frac{1}{C_{\mathrm{B}} s} \tag{53}$$

Fuel system:

$$G_{FS}(s) = \frac{e^{-T_D s}}{T_F s + 1} \tag{54}$$

Pressure control:

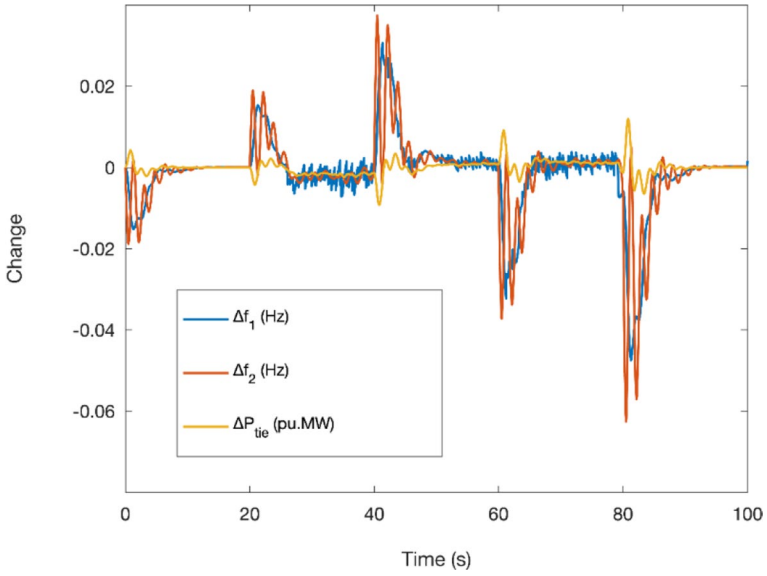


Fig. 20 The system responses for scenario-III

$$G_{PC}(s) = \frac{K_{IB}T_{IB}s^2 + K_{IB}\left(T_{RB} + T_{IB}\right)s + K_{IB}}{0.1T_{RB}s^2 + s} \tag{55}$$

where K_1, K_2, K_3 are the system parameters, T_D is the fuel ignition system delay time, T_F is the fuel system time constant, C_B is the boiler storage time constant, T_{RB} is the lead–lag compensator time constant, K_{IB} is the boiler integrator gain, and T_{IB} is the proportional–integral ratio of the gains [67].

The system responses in the presence of BD are illustrated in Fig. 22. As can be observed from the figure, the proposed SOGWO: PI controller effectively suppresses the effects of BD within a short period of time.

6.5 Scenario-V: Parameter analysis

In this section, a parameter variation test was carried out to demonstrate the robustness and effectiveness of the proposed SOGWO: PI controller under varying system parameters. In this test, it was assumed that the time constants of system components such as the governor, turbine, reheater, and power system varied by $\pm 25\%$. These variations represent practical operating conditions where system parameters may change as a result of aging, maintenance activities, or environmental influences. Figure 23 illustrates the changes in the oscillations of the frequency deviations in each area and the tie-line power deviation resulting from the variations in system parameters. As can be seen from the figure, although the overshoot values of the oscillations change with variations in the time constants of the system parameters, these changes remain within acceptable limits and are damped out in a short time.

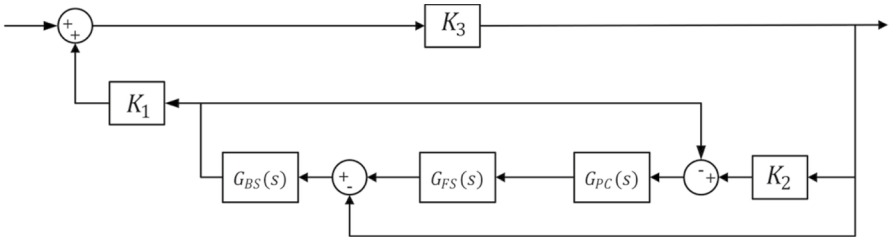


Fig. 21 The block diagram of the BD

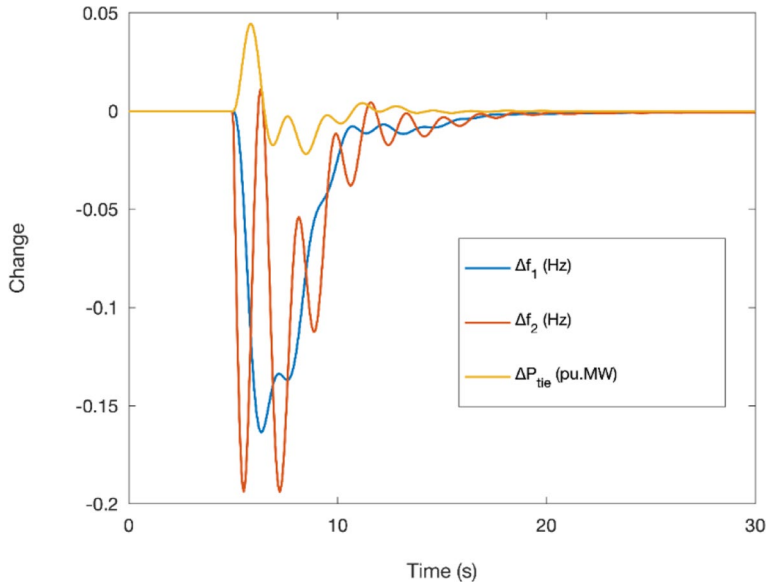
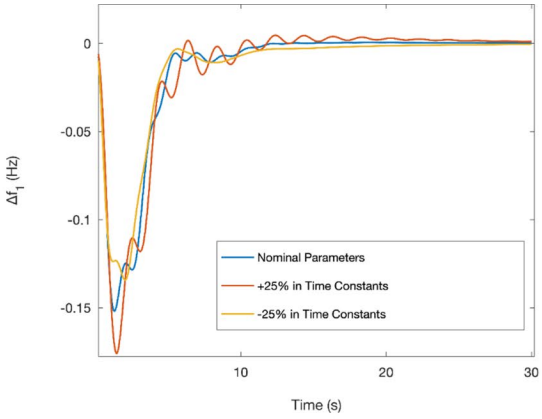


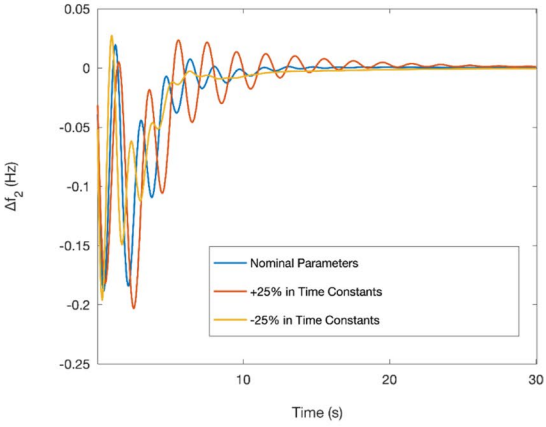
Fig. 22 The system responses for scenario-IV **a** Δf_1 **b** Δf_2 **c** ΔP_{tie}

7 Conclusion

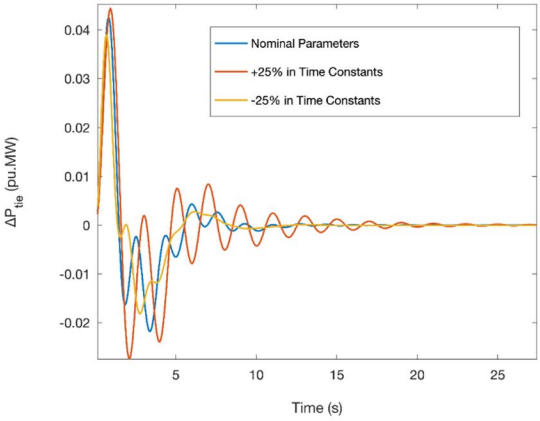
In this study, a hybrid algorithm named SOGWO, which is by combining the male–female social mechanism of the snake optimizer (SO) and the leader-focused search strategy of the grey wolf optimizer (GWO), has been developed. In the proposed SOGWO, the selection of separate alpha, beta, and delta leaders for both male and female snake populations increase the number of elite solutions guiding the search process. This approach increases population diversity and reduces the risk of premature convergence by distributing search agents among multiple promising regions rather than focusing all agents on a single leader. This characteristic of the SOGWO provides it with a multi-centered guiding mechanism that enables the simultaneous exploration of different regions of the solution space and helps it manage a balanced optimization process. In the first phase of the experiment, the



(a)



(b)



(c)

Fig. 23 The system responses for scenario-V **a** Δf_1 **b** Δf_2 **c** ΔP_{tie}

proposed hybrid algorithm has been tested on unimodal, multimodal, fixed-dimension multimodal benchmark functions, and CEC-2022 test functions to demonstrate its capabilities against the popular and high-performing algorithms. The findings from experimental studies highlight that the developed hybrid SOGWO is in a leadership position among its counterparts in optimization problems with different characteristics and challenge levels. The fact that the SOGWO maintains its leading position despite test functions with different characteristics indicates that the method possesses a balanced exploration–exploitation mechanism across a wide range of optimizations and exhibits effective and consistent performance. Additionally, to evaluate the effectiveness of the SOGWO against powerful optimization algorithms, further comparisons are conducted with the EA4eig, NL-SHADE-LBC, NL-SHADE-RSP-MID, and S-LSHADE-DP algorithms, which achieved top rankings in the CEC-2022 competition. The outcomes demonstrate that SOGWO possesses high-quality optimization capabilities even when compared to winner algorithms. Furthermore, quantitative evaluations performed using overall effectiveness and CoCoSo analyses made it possible to examine the success of the algorithms within a multidimensional framework without reducing it to a single ranking criterion and are revealed additional findings supporting the superior performance of the proposed method. The experimental evaluations are not limited to quantitative analyses; qualitative analyses are also carried out to showcase the convergence and search behaviors of the algorithms. The results are verified by nonparametric statistical tests that confirm the statistical significance of the observed performance differences. The comprehensive analysis framework implemented in this study shows that the performance of SOGWO is not by chance. This increases the reliability of the findings about the potential of the algorithm and indicates that SOGWO's efficiency in searching is the reason for its success. In the second step, the proposed SOGWO was applied to the load frequency control (LFC) problem in two-area power systems to demonstrate the effectiveness of the SOGWO. The results were compared with methods such as SCHO, GTO, SSA, WOA, SFLA, and FA. From the simulation results, it is seen that the proposed SOGWO has remarkable performance for various scenarios. To sum up, it can be pointed out that the proposed SOGWO can be an alternative optimization algorithm and considered as effective solutions for problems in engineering and other fields.

Author contribution Eda Özkul: Conceptualization, Methodology, Software, Writing—Original Draft, Visualization, Supervision. Özge Tezel: Conceptualization, Methodology, Software, Writing—Review and Editing, Visualization, Validation. Özay Can: Conceptualization, Methodology, Writing—Original Draft, Visualization, Validation.

Funding This research did not receive any specific grant from funding agencies in the public, commercial, or not-for-profit sectors.

Data availability No datasets were generated or analysed during the current study.

Declarations

Conflicts of interest The authors declare that they have no conflict of interest.

Ethical approval Not applicable.

Consent to participate Not applicable.

Consent for publication Not applicable.

References

1. Abd-Elazim SM, Ali ES (2018) Load frequency controller design of a two-area system composing of PV grid and thermal generator via firefly algorithm. Neural Comput Appl 30:607–616. https://doi.org/10.1007/s00521-016-2668-y
2. Ekinci S, Can Ö, Ayas MŞ et al (2024) Automatic generation control of a hybrid PV-reheat thermal power system using RIME algorithm. IEEE Access 12:26919–26930. https://doi.org/10.1109/ACCESS.2024.3367011
3. Obma J, Audomsi S, Ardhan K et al (2025) Strategic chess algorithm-based PI controller optimization for load frequency control in two-area hybrid photovoltaic–thermal power systems. Int J Robot Control Syst 5:1156–1171. https://doi.org/10.31763/ijrcs.v5i2.1844
4. Ekinci S, Izci D, Bajaj M, Blazek V (2025) Novel application of sinh cosh optimizer for robust controller design in hybrid photovoltaic-thermal power systems. Sci Rep 15:2825. https://doi.org/10.1038/s41598-025-86597-5
5. Ekinci S, Izci D, Turkeri C et al (2025) Frequency regulation of two-area thermal and photovoltaic power system via flood algorithm. Results Control Optim 18:100539. https://doi.org/10.1016/j.rico.2025.100539
6. Yilmaz MF, Andiç C, Öztürk A (2026) Load Frequency Control of a PV-Thermal Power System with Integrated EV Battery Using the INFO Algorithm. Tehnički vjesnik 33:885–895. https://doi.org/10.17559/TV-20250516002670
7. Ramjug-Ballgobin R, Ramlukon C (2021) A hybrid metaheuristic optimisation technique for load frequency control. SN Appl Sci 3:547. https://doi.org/10.1007/s42452-021-04482-y
8. Agwa AM (2020) Equilibrium optimization algorithm for automatic generation control of interconnected power systems. Prz Elektrotech 96:143–148. https://doi.org/10.15199/48.2020.09.30
9. Padhy S, Panda S (2021) Application of a simplified Grey Wolf optimization technique for adaptive fuzzy PID controller design for frequency regulation of a distributed power generation system. Prot Control Mod Power Syst. https://doi.org/10.1186/s41601-021-00180-4
10. Gupta DK, Soni AK, Jha AV et al (2021) Hybrid Gravitational–Firefly Algorithm-Based load frequency control for hydrothermal two-area system. Mathematics (Basel) 9:712. https://doi.org/10.3390/math9070712
11. Kalyan CHNS, Rao GS (2021) Impact of communication time delays on combined LFC and AVR of a multi-area hybrid system with IPFC-RFBs coordinated control strategy. Prot Control Mod Power Syst 6:7. https://doi.org/10.1186/s41601-021-00185-z
12. Abubakr H, Hussein MM, Mohamed TH (2020) Frequency stabilization of two area power system interconnected by AC/DC links using Jaya algorithm. Int J Adv Sci Technol 29:548–559
13. Sharma G, Krishnan N, Arya Y, Panwar A (2021) Impact of ultracapacitor and redox flow battery with JAYA optimization for frequency stabilization in linked photovoltaic-thermal system. Int Trans Electr Energy Syst 31:e12883. https://doi.org/10.1002/2050-7038.12883
14. Sahu PC, Prusty RC, Sahoo BK (2020) Modified sine cosine algorithm-based fuzzy-aided PID controller for automatic generation control of multiarea power systems. Soft Comput 24:12919–12936. https://doi.org/10.1007/s00500-020-04716-y
15. Latif A, Hussain SMS, Das DC, Ustun TS (2021) Optimization of two-stage IPD-(1+I) controllers for frequency regulation of sustainable energy based hybrid microgrid network. Electronics 10:919. https://doi.org/10.3390/electronics10080919

16. Kheshti M, Ding L, Askarian-Abyaneh H et al (2021) Improving frequency regulation of wind-integrated multi-area systems using LFA-fuzzy PID control. Int Trans Electr Energy Syst 31:e12802. https://doi.org/10.1002/2050-7038.12802
17. Safi SJ, Tezcan SS, Eke I, Farhad Z (2018) Gravitational search algorithm (GSA) based PID controller design for two area multi-source power system load frequency control (LFC). Gazi Univ J Sci 31:139–153
18. Latif A, Hussain SMS, Das DC, Ustun TS (2021) Design and implementation of maiden dual-level controller for ameliorating frequency control in a hybrid microgrid. Energies 14:2418. https://doi.org/10.3390/en14092418
19. Sharma M, Prakash S, Saxena S, Dhundhara S (2021) Optimal fractional-order tilted-integral-derivative controller for frequency stabilization in hybrid power system using salp swarm algorithm. Electr Power Compon Syst 48:1912–1931. https://doi.org/10.1080/15325008.2021.1906792
20. Ramachandran R, Satheesh Kumar J, Madasamy B, Veerasamy V (2021) A hybrid MFO-GHNN tuned self-adaptive FOPID controller for ALFC of renewable energy integrated hybrid power system. IET Renew Power Gener 15:1582–1595. https://doi.org/10.1049/rpg2.12134
21. Mohanty D, Panda S (2020) Frequency control of hybrid power system by sine fu nction adapted improved whale optimisation technique. Int J Ambient Energy 43:3518–3535. https://doi.org/10.1080/01430750.2020.1839550
22. Babu NR, Saikia LC, Bhagat SK, Saha A (2021) Maiden application of hybrid crow-search algorithm with particle swarm optimization in LFC studies. In: Bansal P, Tushir M, Balas VE, Srivastava R (eds) Proceedings of International Conference on Artificial Intelligence and Applications. Springer, Singapore, pp 427–439
23. Babu NR, Saikia LC, Bhagat SK et al (2021) LFC of a Solar Thermal Integrated Thermal System Considering CSO Optimized TI-DN Controller. In: Das B, Patgiri R, Bandyopadhyay S, Balas VE (eds) Modeling, Simulation and Optimization. Springer, Singapore, pp 323–334
24. Yakout AH, Kotb H, Hasanien HM, Aboras KM (2021) Optimal fuzzy PIDF load frequency controller for hybrid microgrid system using marine predator algorithm. IEEE Access 9:54220–54232. https://doi.org/10.1109/ACCESS.2021.3070076
25. Jalali N, Razmi H, Doagou-Mojarrad H (2020) Optimized fuzzy self-tuning PID controller design based on Tribe-DE optimization algorithm and rule weight adjustment method for load frequency control of interconnected multi-area power systems. Appl Soft Comput 93:106424. https://doi.org/10.1016/j.asoc.2020.106424
26. Wolpert DH, Macready WG (1997) No free lunch theorems for optimization. IEEE Trans Evol Comput 1:67–82. https://doi.org/10.1109/4235.585893
27. Raidl GR, Puchinger J, Blum C (2019) Metaheuristic hybrids. In: Gendreau M, Potvin J-Y (eds) Handbook of metaheuristics. Springer International Publishing, Cham, pp 385–417
28. Gaidhane PJ, Nigam MJ (2018) A hybrid grey wolf optimizer and artificial bee colony algorithm for enhancing the performance of complex systems. J Comput Sci 27:284–302. https://doi.org/10.1016/j.jocs.2018.06.008
29. Jafari M, Salajegheh E, Salajegheh J (2019) An efficient hybrid of elephant herding optimization and cultural algorithm for optimal design of trusses. Eng Comput 35:781–801. https://doi.org/10.1007/s00366-018-0631-5
30. Teng Z, Lv J, Guo L (2019) An improved hybrid grey wolf optimization algorithm. Soft Comput 23:6617–6631. https://doi.org/10.1007/s00500-018-3310-y
31. Ma C, Huang H, Fan Q et al (2022) Grey wolf optimizer based on Aquila exploration method. Expert Syst Appl 205:117629. https://doi.org/10.1016/j.eswa.2022.117629
32. Çetinbaş İ, Tamyurek B, Demirtaş M (2023) Parameter extraction of photovoltaic cells and modules by hybrid white shark optimizer and artificial rabbits optimization. Energy Convers Manag 296:117621. https://doi.org/10.1016/j.enconman.2023.117621
33. Tu B, Wang F, Huo Y, Wang X (2023) A hybrid algorithm of grey wolf optimizer and harris hawks optimization for solving global optimization problems with improved convergence performance. Sci Rep 13:22909. https://doi.org/10.1038/s41598-023-49754-2
34. Zhang H, Zhang Y, Niu Y et al (2024) A Grey wolf optimizer combined with artificial fish swarm algorithm for engineering design problems. Ain Shams Eng J 15:102797. https://doi.org/10.1016/j.asej.2024.102797

35. Biswas S, Maiti B, Singh G et al (2025) A novel hybrid optimizer based on coati optimization algorithm and differential evolution for global optimization and constrained engineering problems. Int J Comput Intell Syst 18:157. https://doi.org/10.1007/s44196-025-00855-y
36. Al Afghani Edsa S, Sunat K (2025) Enhancing chernobyl disaster optimization: a novel hybridization approach with modified grey wolf optimizer for solving complex optimization problems. Clust Comput 28:159. https://doi.org/10.1007/s10586-024-04816-6
37. Singh G, Biswas S, Ezugwu AE-S et al (2025) Enhanced global optimization using a novel hybrid sine cosine-gazelle algorithm with Brownian motion and Lévy flight mechanisms. Int J Comput Intell Syst 18:108. https://doi.org/10.1007/s44196-025-00823-6
38. Alawadi S, Fakhouri HN, Alkhabbas F et al (2026) SHIODEG: a hybrid success-history intelligent optimization algorithm for engineering design problems. J Supercomput 82:282. https://doi.org/10.1007/s11227-026-08398-5
39. Ferradji MA, Seghir R (2026) A novel metaheuristic global optimisation method based on grey wolf optimiser and salp swarm algorithm. J Exp Theor Artif Intell 38:15–51. https://doi.org/10.1080/0952813X.2025.2515578
40. Yameen MZ, Junejo AK, Lu Z et al (2025) Hybrid GOA and PSO optimization for load frequency control in renewable multi source dual area power systems. Sci Rep 15:17549. https://doi.org/10.1038/s41598-025-01481-6
41. Odelu P, Shiva CK, Sen S et al (2026) Hybrid Optimization for Robust Frequency Regulation in Shipboard Microgrids with Renewable Sources, Energy Storage, and Controllable Loads. Optim Control Appl Methods 47:312–336. https://doi.org/10.1002/oca.70061
42. Abdulaziz A, Flah A, Dashtdar M et al (2025) AI-enhanced load frequency control in multi-area power systems via a self-tuning PIDF with ANN-based NMPC and hybrid cat-pikas optimization. Results Eng 28:107462. https://doi.org/10.1016/j.rineng.2025.107462
43. Prusty C, Rout B, Chirantan S (2026) Optimizing model predictive control for frequency stabilization in marine microgrids using hybrid optimization algorithms. J Dyn Syst Meas Control 148:041011. https://doi.org/10.1115/1.4070882
44. Hashim FA, Hussien AG (2022) Snake optimizer: a novel meta-heuristic optimization algorithm. Knowl-Based Syst 242:108320. https://doi.org/10.1016/j.knosys.2022.108320
45. Sholeh MN, Sari UC (2026) A systematic review of recent advances in snake optimizer algorithm. J Comb Optim 51:22. https://doi.org/10.1007/s10878-026-01403-w
46. Al-Shourbaji I, Kachare PH, Alshathri S et al (2022) An efficient parallel reptile search algorithm and snake optimizer approach for feature selection. Mathematics (Basel) 10:2351. https://doi.org/10.3390/math10132351
47. Yao L, Yuan P, Tsai C-Y et al (2023) ESO: an enhanced snake optimizer for real-world engineering problems. Expert Syst Appl 230:120594. https://doi.org/10.1016/j.eswa.2023.120594
48. Samiayya D, Radhika S, Chandrasekar A (2023) An optimal model for enhancing network lifetime and cluster head selection using hybrid snake whale optimization. Peer-to-Peer Netw Appl 16:1959–1974. https://doi.org/10.1007/s12083-023-01487-9
49. Zheng W, Ai Y, Zhang W (2024) Improved snake optimizer using Sobol sequential nonlinear factors and different learning strategies and its applications. Mathematics (Basel) 12:1708. https://doi.org/10.3390/math12111708
50. Yang Y, Liu Y, Yan P et al (2025) An improved snake optimization algorithm based on hybrid strategy. J Supercomput 81:771. https://doi.org/10.1007/s11227-025-07258-y
51. Mirjalili S, Mirjalili SM, Lewis A (2014) Grey wolf optimizer. Adv Eng Softw 69:46–61. https://doi.org/10.1016/j.advengsoft.2013.12.007
52. Eberhart R, Kennedy J (1995) A new optimizer using particle swarm theory. In: MHS'95. Proceedings of the Sixth International Symposium on Micro Machine and Human Science. pp 39–43
53. Karaboga D, Basturk B (2007) A powerful and efficient algorithm for numerical function optimization: artificial bee colony (ABC) algorithm. J Glob Optim 39:459–471. https://doi.org/10.1007/s10898-007-9149-x
54. Faramarzi A, Heidarinejad M, Stephens B, Mirjalili S (2020) Equilibrium optimizer: A novel optimization algorithm. Knowl-Based Syst 191:105190. https://doi.org/10.1016/j.knosys.2019.105190
55. Mirjalili S, Gandomi AH, Mirjalili SZ et al (2017) Salp swarm algorithm: a bio-inspired optimizer for engineering design problems. Adv Eng Softw 114:163–191. https://doi.org/10.1016/j.advengsoft.2017.07.002

56. Mirjalili S, Lewis A (2016) The whale optimization algorithm. Adv Eng Softw 95:51–67. https://doi.org/10.1016/j.advengsoft.2016.01.008
57. Mirjalili S (2016) SCA: a sine cosine algorithm for solving optimization problems. Knowl-Based Syst 96:120–133. https://doi.org/10.1016/j.knosys.2015.12.022
58. Shehadeh HA (2023) Chernobyl disaster optimizer (CDO): a novel meta-heuristic method for global optimization. Neural Comput Appl 35:10733–10749. https://doi.org/10.1007/s00521-023-08261-1
59. Fu S, Li K, Huang H et al (2024) Red-billed blue magpie optimizer: a novel metaheuristic algorithm for 2D/3D UAV path planning and engineering design problems. Artif Intell Rev 57:134. https://doi.org/10.1007/s10462-024-10716-3
60. Braik M, Al-Hiary H (2025) Rüppell's fox optimizer: a novel meta-heuristic approach for solving global optimization problems. Clust Comput 28:292. https://doi.org/10.1007/s10586-024-04950-1
61. Güven AF (2025) A novel hybrid Salp Swarm Kepler optimization for optimal sizing and energy management of renewable microgrids with EV integration. Energy 334:137696. https://doi.org/10.1016/j.energy.2025.137696
62. Zhu Y, Huang H, Wei J et al (2025) ISO: an improved snake optimizer with multi-strategy enhancement for engineering optimization. Expert Syst Appl 281:127660. https://doi.org/10.1016/j.eswa.2025.127660
63. Bakria D, Beladel A, Korich B et al (2025) A novel enhanced Grey Wolf Optimizer for global optimization problems: application to photovoltaic parameter extraction. Energy Rep 14:2782–2796. https://doi.org/10.1016/j.egyr.2025.09.027
64. Al-kubragyi SSA, Ali II, Alwazni HSMA (2024) Solving the multi-objective economic-emission load dispatch optimization problem using hybrid GWO-PSO algorithm. Int J Intell Eng Syst 17:738–750. https://doi.org/10.22266/ijies2024.0831.56
65. Nadimi-Shahraki MH, Taghian S, Mirjalili S (2021) An improved grey wolf optimizer for solving engineering problems. Expert Syst Appl 166:113917. https://doi.org/10.1016/j.eswa.2020.113917
66. Yazdani M, Zarate P, Kazimieras Zavadskas E, Turskis Z (2018) A combined compromise solution (CoCoSo) method for multi-criteria decision-making problems. Manag Decis 57:2501–2519. https://doi.org/10.1108/MD-05-2017-0458
67. Can O, Ayas MS (2024) Gorilla troops optimization-based load frequency control in PV-thermal power system. Neural Comput Appl 36:4179–4193. https://doi.org/10.1007/s00521-023-09273-7
68. Çelik E, Öztürk N, Houssein EH (2022) Influence of energy storage device on load frequency control of an interconnected dual-area thermal and solar photovoltaic power system. Neural Comput Appl 34:20083–20099. https://doi.org/10.1007/s00521-022-07558-x
69. Khadanga RK, Kumar A, Panda S (2020) A novel modified whale optimization algorithm for load frequency controller design of a two-area power system composing of PV grid and thermal generator. Neural Comput Appl 32:8205–8216. https://doi.org/10.1007/s00521-019-04321-7
70. Khadanga RK, Kumar A, Panda S (2020) A hybrid shuffled frog-leaping and pattern search algorithm for load frequency controller design of a two-area system composing of PV grid and thermal generator. Int J Numer Model Electron Netw Devices Fields 33:e2694. https://doi.org/10.1002/jnm.2694
71. Dahiya P, Saha AK (2022) Frequency regulation of interconnected power system using Black Widow Optimization. IEEE Access 10:25219–25236. https://doi.org/10.1109/ACCESS.2022.3155201

Publisher's Note Springer Nature remains neutral with regard to jurisdictional claims in published maps and institutional affiliations.

Springer Nature or its licensor (e.g. a society or other partner) holds exclusive rights to this article under a publishing agreement with the author(s) or other rightsholder(s); author self-archiving of the accepted manuscript version of this article is solely governed by the terms of such publishing agreement and applicable law.

Authors and Affiliations

Eda Özkul[1] · Özge Tezel[1] · Özay Can[2]

✉ Özge Tezel
ozgetezel@ktu.edu.tr

Eda Özkul
edaozkul@ktu.edu.tr

Özay Can
ozay.can@erdogan.edu.tr

[1] Department of Computer Science, Karadeniz Technical University, 61080 Trabzon, Türkiye

[2] Department of Electronic and Automation, Recep Tayyip Erdoğan University, 53100 Rize, Türkiye